PATENT COOPERATION TREATY

PCT

INTERNATIONAL PRELIMINARY EXAMINATION REPORT

(PCT Article 36 and Rule 70)

Applicant's or agent's file reference IOPL-007PC	**FOR FURTHER ACTION**	See Notification of Transmittal of International Preliminary Examination Report (Form PCT/IPEA/416)
International application No. PCT/US99/17338	International filing date *(day/month/year)* 30 JULY 1999	Priority date *(day/month/year)* 30 JULY 1998
International Patent Classification (IPC) or national classification and IPC IPC(7): H05B 3/26 and US Cl.: 250/504R, 493.1, 495.1		
Applicant ION OPTICS, INC.		

1. This international preliminary examination report has been prepared by this International Preliminary Examining Authority and is transmitted to the applicant according to Article 36.

2. This REPORT consists of a total of 4 sheets.

   [✓] This report is also accompanied by ANNEXES, i.e., sheets of the description, claims and/or drawings which have been amended and are the basis for this report and/or sheets containing rectifications made before this Authority. (see Rule 70.16 and Section 607 of the Administrative Instructions under the PCT).

   These annexes consist of a total of 101 sheets.

3. This report contains indications relating to the following items:

   - I [X] Basis of the report
   - II [ ] Priority
   - III [ ] Non-establishment of report with regard to novelty, inventive step or industrial applicability
   - IV [ ] Lack of unity of invention
   - V [X] Reasoned statement under Article 35(2) with regard to novelty, inventive step or industrial applicability; citations and explanations supporting such statement
   - VI [ ] Certain documents cited
   - VII [ ] Certain defects in the international application
   - VIII [ ] Certain observations on the international application

Date of submission of the demand	Date of completion of this report
29 FEBRUARY 2000	10 JUNE 2000
Name and mailing address of the IPEA/US Commissioner of Patents and Trademarks Box PCT Washington, D.C. 20231 Facsimile No. (703) 305-3230	Authorized officer KIET T. NGUYEN Telephone No. (703) 308-4855

Form PCT/IPEA/409 (cover sheet) (July 1998)*

INTERNATIONAL PRELIMINARY EXAMINATION REPORT

International application No.
PCT/US99/17338

I. Basis of the report

1. With regard to the **elements** of the international application:*

☐ the international application as originally filed

☒ the description:
pages (See Attached) , as originally filed
pages , filed with the demand
pages , filed with the letter of

☒ the claims:
pages (See Attached) , as originally filed
pages , as amended (together with any statement) under Article 19
pages , filed with the demand
pages , filed with the letter of

☒ the drawings:
pages (See Attached) , as originally filed
pages , filed with the demand
pages , filed with the letter of

☒ the sequence listing part of the description:
pages (See Attached) , as originally filed
pages , filed with the demand
pages , filed with the letter of

2. With regard to the **language**, all the elements marked above were available or furnished to this Authority in the language in which the international application was filed, unless otherwise indicated under this item.
These elements were available or furnished to this Authority in the following language which is:

☐ the language of a translation furnished for the purposes of international search (under Rule 23.1(b)).

☐ the language of publication of the international application (under Rule 48.3(b)).

☐ the language of the translation furnished for the purposes of international preliminary examination (under Rules 55.2 and/or 55.3).

3. With regard to any **nucleotide and/or amino acid sequence** disclosed in the international application, the international preliminary examination was carried out on the basis of the sequence listing:

☐ contained in the international application in printed form.

☐ filed together with the international application in computer readable form.

☐ furnished subsequently to this Authority in written form.

☐ furnished subsequently to this Authority in computer readable form.

☐ The statement that the subsequently furnished written sequence listing does not go beyond the disclosure in the international application as filed has been furnished.

☐ The statement that the information recorded in computer readable form is identical to the writen sequence listing has been furnished.

4. ☒ The amendments have resulted in the cancellation of:

☒ the description, pages NONE

☒ the claims, Nos. NONE

☒ the drawings, sheets/~~fig~~ NONE

5. ☒ This report has been drawn as if (some of) the amendments had not been made, since they have been considered to go beyond the disclosure as filed, as indicated in the Supplemental Box (Rule 70.2(c)).**

** Replacement sheets which have been furnished to the receiving Office in response to an invitation under Article 14 are referred to in this report as "originally filed" and are not annexed to this report since they do not contain amendments (Rules 70.16 and 70.17).*

***Any replacement sheet containing such amendments must be referred to under item 1 and annexed to this report.*

Supplemental Box
(To be used when the space in any of the preceding boxes is not sufficient)

Continuation of: Boxes I - VIII

I. BASIS OF REPORT:

This report has been drawn on the basis of the description,
page(s) 1-8 & 11-30, as originally filed.
page(s) 9-10 & 31-126/3, filed with the demand.
and additional amendments:
NONE

This report has been drawn on the basis of the claims,
page(s) NONE, as originally filed.
page(s) NONE, as amended under Article 19.
page(s) 126/1, filed with the demand.
and additional amendments:
NONE

This report has been drawn on the basis of the drawings,
page(s) NONE, as originally filed.
page(s) 126/2-126/3, filed with the demand.
and additional amendments:
NONE

This report has been drawn on the basis of the sequence listing part of the description:
page(s) NONE, as originally filed.
pages(s) NONE, filed with the demand.
and additional amendments:
NONE

5. (Some) amendments are considered to go beyond the disclosure as filed:
NONE

INTERNATIONAL PRELIMINARY EXAMINATION REPORT

International application No.
PCT/US99/17338

V. Reasoned statement under Article 35(2) with regard to novelty, inventive step or industrial applicability; citations and explanations supporting such statement

1. statement

Novelty (N)	Claims	1-28	YES
	Claims	NONE	NO
Inventive Step (IS)	Claims	1-28	YES
	Claims	NONE	NO
Industrial Applicability (IA)	Claims	1-28	YES
	Claims	NONE	NO

2. citations and explanations (Rule 70.7)

Claims 1-28 meet the criteria set out in PCT Article 33(2)-(4), because the prior art does not teach or fairly suggest a narrow band incoherent radiation emitter detector which includes a planar filament emission/detection element having a emission detection width dl/l less than about 0.1, wherein l is the wavelength of a radiation as recited in claims 1, 15, 23 and 28.

---------- NEW CITATIONS ----------

NONE

FIG. 1A shows an IR source in accordance with the invention;

FIG. 1B shows the beam shape of the IR source of FIG. 1;

FIG. 1C shows a graphical comparison of drive power of the IR source of FIG. 1 and a standard source;

FIGS. 1D, 2 and 3A show alternative IR sources in accordance with the invention;

FIGS 3B, 3C and 3D show exemplary filament emitters in accordance with the invention;

FIG. 4 shows another IR source in accordance with the invention;

FIGS. 5 and 6 show additional exemplary emitters;

FIG. 7 shows the spectral irradiance as a function of wavelength for a textured metal foil filament of the invention;

FIGS. 7A(a) and 7A(b) show exemplary mask patterns for an IR source according to the invention;

FIGS 7A(c), 7B and 7C show the emission spectra of IR sources of the invention;

FIGS. 7D(a) and 7D(b) show emission wavelength versus etched cavity size and versus cavity-to cavity spacing, respectively;

FIGS. 8A (1 of 3), 8A (2 of 3), and 8A (3 of 3) and FIGS. 8B(a)-8B(c) show a window-frame construction technique for forming individual emitter elements according to the invention;

FIGS 9A and 9B show conversion efficiency gains using lithographic feature design and fabrication according to the invention;

FIG. 10 shows an exemplary IR hydrocarbon leak sensor in accordance with the invention;

FIGS. 11A and 11B show an exemplary IR gas sensor engine in accordance with the invention;

FIGS. 11C-11I show other exemplary devices using separate radiation sources and detectors in accordance with the invention;

FIG. 13 shows in schematic form, a test configuration for the invention;

FIG. 14A shows an exemplary nondispersive test bed using the invention;

FIG. 14B shows in block diagram form, an exemplary signal processing for date reduction for the test bed of FIG. 14A;

FIG. 15 shows a calibration spectrum for a hyperspectral imaging system of the invention;

FIGS. 17A and 17B show an exemplary resolution test pattern and a resolution tester respectively for the invention;

FIGS. 18 and 18B show an exemplary system of the invention;

FIG. 19A shows an exemplary reference source according to the invention in a filter wheel slot; and

FIG. 19B shows exemplary signal sources adjacent to a metric.

PATENT COOPERATION TREATY

PCT

INTERNATIONAL PRELIMINARY EXAMINATION REPORT

(PCT Article 36 and Rule 70)

Applicant's or agent's file reference IOPL-007PC	**FOR FURTHER ACTION**	See Notification of Transmittal of International Preliminary Examination Report (Form PCT/IPEA/416)
International application No. PCT/US99/17338	International filing date *(day/month/year)* 30 JULY 1999	Priority date *(day/month/year)* 30 JULY 1998
International Patent Classification (IPC) or national classification and IPC IPC(7): H05B 3/26 and US Cl.: 250/504R, 493.1, 495.1		
Applicant ION OPTICS, INC.		

1. This international preliminary examination report has been prepared by this International Preliminary Examining Authority and is transmitted to the applicant according to Article 36.

2. This REPORT consists of a total of 4 sheets.

   ☑ This report is also accompanied by ANNEXES, i.e., sheets of the description, claims and/or drawings which have been amended and are the basis for this report and/or sheets containing rectifications made before this Authority. (see Rule 70.16 and Section 607 of the Administrative Instructions under the PCT).

   These annexes consist of a total of 106 sheets.

3. This report contains indications relating to the following items:

   - I [X] Basis of the report
   - II [ ] Priority
   - III [ ] Non-establishment of report with regard to novelty, inventive step or industrial applicability
   - IV [ ] Lack of unity of invention
   - V [X] Reasoned statement under Article 35(2) with regard to novelty, inventive step or industrial applicability; citations and explanations supporting such statement
   - VI [ ] Certain documents cited
   - VII [ ] Certain defects in the international application
   - VIII [ ] Certain observations on the international application

Date of submission of the demand	Date of completion of this report
29 FEBRUARY 2000	10 JUNE 2000
Name and mailing address of the IPEA/US Commissioner of Patents and Trademarks Box PCT Washington, D.C. 20231 Facsimile No. (703) 305-3230	Authorized officer KIET T. NGUYEN Telephone No. (703) 308-4855

Form PCT/IPEA/409 (cover sheet) (July 1998)*

INTERNATIONAL PRELIMINARY EXAMINATION REPORT

International application No.
PCT/US99/17338

I. Basis of the report

1. With regard to the elements of the international application:*

☐ the international application as originally filed

☒ the description:
pages (See Attached) , as originally filed
pages _____ , filed with the demand
pages _____ , filed with the letter of _____

☒ the claims:
pages (See Attached) , as originally filed
pages _____ , as amended (together with any statement) under Article 19
pages _____ , filed with the demand
pages _____ , filed with the letter of _____

☒ the drawings:
pages (See Attached) , as originally filed
pages _____ , filed with the demand
pages _____ , filed with the letter of _____

☒ the sequence listing part of the description:
pages (See Attached) , as originally filed
pages _____ , filed with the demand
pages _____ , filed with the letter of _____

2. With regard to the **language**, all the elements marked above were available or furnished to this Authority in the language in which the international application was filed, unless otherwise indicated under this item.
These elements were available or furnished to this Authority in the following language _____ which is:

☐ the language of a translation furnished for the purposes of international search (under Rule 23.1(b)).

☐ the language of publication of the international application (under Rule 48.3(b)).

☐ the language of the translation furnished for the purposes of international preliminary examination (under Rules 55.2 and/or 55.3).

3. With regard to any **nucleotide and/or amino acid sequence** disclosed in the international application, the international preliminary examination was carried out on the basis of the sequence listing:

☐ contained in the international application in printed form.

☐ filed together with the international application in computer readable form.

☐ furnished subsequently to this Authority in written form.

☐ furnished subsequently to this Authority in computer readable form.

☐ The statement that the subsequently furnished written sequence listing does not go beyond the disclosure in the international application as filed has been furnished.

☐ The statement that the information recorded in computer readable form is identical to the writen sequence listing has been furnished.

4. ☒ The amendments have resulted in the cancellation of:

☒ the description, pages NONE

☒ the claims, Nos. NONE

☒ the drawings, sheets/~~fig~~ NONE

5. ☒ This report has been drawn as if (some of) the amendments had not been made, since they have been considered to go beyond the disclosure as filed, as indicated in the Supplemental Box (Rule 70.2(c)).**

** Replacement sheets which have been furnished to the receiving Office in response to an invitation under Article 14 are referred to in this report as "originally filed" and are not annexed to this report since they do not contain amendments (Rules 70.16 and 70.17).*

***Any replacement sheet containing such amendments must be referred to under item 1 and annexed to this report.*

Supplemental Box
(To be used when the space in any of the preceding boxes is not sufficient)

Continuation of: Boxes I - VIII

I. BASIS OF REPORT:

This report has been drawn on the basis of the description,
page(s) 1-8 & 11-30, as originally filed.
page(s) 9-10 & 31-126/1, filed with the demand.
and additional amendments:
NONE

This report has been drawn on the basis of the claims,
page(s) NONE, as originally filed.
page(s) NONE, as amended under Article 19.
page(s) 126/1, filed with the demand.
and additional amendments:
NONE

This report has been drawn on the basis of the drawings,
page(s) NONE, as originally filed.
page(s) 126/2-126/3, filed with the demand.
and additional amendments:
NONE

This report has been drawn on the basis of the sequence listing part of the description:
page(s) NONE, as originally filed.
pages(s) NONE, filed with the demand.
and additional amendments:
NONE

5. (Some) amendments are considered to go beyond the disclosure as filed:
NONE

INTERNATIONAL PRELIMINARY EXAMINATION REPORT

International application No.
PCT/US99/17338

V. Reasoned statement under Article 35(2) with regard to novelty, inventive step r industrial applicability; citations and explanations supporting such statement

1. statement

Novelty (N)	Claims	1-28	YES
	Claims	NONE	NO
Inventive Step (IS)	Claims	1-28	YES
	Claims	NONE	NO
Industrial Applicability (IA)	Claims	1-28	YES
	Claims	NONE	NO

2. citations and explanations (Rule 70.7)

Claims 1-28 meet the criteria set out in PCT Article 33(2)-(4), because the prior art does not teach or fairly suggest a narrow band incoherent radiation emitter detector which includes a planar filament emission/detection element having a emission detection width dl/1 less than about 0.1, wherein l is the wavelength of a radiation as recited in claims 1, 15, 23 and 28.

NEW CITATIONS

NONE

FIG. 1A shows an IR source in accordance with the invention;

FIG. 1B shows the beam shape of the IR source of FIG. 1;

FIG. 1C shows a graphical comparison of drive power of the IR source of FIG. 1 and a standard source;

FIGS. 1D, 2 and 3A show alternative IR sources in accordance with the invention;

FIGS 3B, 3C and 3D show exemplary filament emitters in accordance with the invention;

FIG. 4 shows another IR source in accordance with the invention;

FIGS. 5 and 6 show additional exemplary emitters;

FIG. 7 shows the spectral irradiance as a function of wavelength for a textured metal foil filament of the invention;

FIGS. 7A(a) and 7A(b) show exemplary mask patterns for an IR source according to the invention;

FIGS 7A(c), 7B and 7C show the emission spectra of IR sources of the invention;

FIGS. 7D(a) and 7D(b) show emission wavelength versus etched cavity size and versus cavity-to cavity spacing, respectively;

FIGS. 8A (1 of 3), 8A (2 of 3), and 8A (3 of 3) and FIGS. 8B(a)-8B(c) show a window-frame construction technique for forming individual emitter elements according to the invention;

FIGS 9A and 9B show conversion efficiency gains using lithographic feature design and fabrication according to the invention;

FIG. 10 shows an exemplary IR hydrocarbon leak sensor in accordance with the invention;

FIGS. 11A and 11B show an exemplary IR gas sensor engine in accordance with the invention;

FIGS. 11C-11I show other exemplary devices using separate radiation sources and detectors in accordance with the invention;

FIG. 13 shows in schematic form, a test configuration for the invention;

FIG. 14A shows an exemplary nondispersive test bed using the invention;

FIG. 14B shows in block diagram form, an exemplary signal processing for date reduction for the test bed of FIG. 14A;

FIG. 15 shows a calibration spectrum for a hyperspectral imaging system of the invention;

FIGS. 17A and 17B show an exemplary resolution test pattern and a resolution tester respectively for the invention;

FIGS. 18 and 18B show an exemplary system of the invention;

FIG. 19A shows an exemplary reference source according to the invention in a filter wheel slot; and

FIG. 19B shows exemplary signal sources adjacent to a metric.

ATENT COOPERATION TR. .Y

From the INTERNATIONAL BUREAU

PCT

NOTIFICATION OF ELECTION

(PCT Rule 61.2)

To:

Assistant Commissioner for Patents
United States Patent and Trademark Office
Box PCT
Washington, D.C.20231
ETATS-UNIS D'AMERIQUE

in its capacity as elected Office

Date of mailing (day/month/year) 15 June 2000 (15.06.00)	
International application No. PCT/US99/17338	**Applicant's or agent's file reference** 56326-021 (IOPL-007P
International filing date (day/month/year) 30 July 1999 (30.07.99)	**Priority date** (day/month/year) 30 July 1998 (30.07.98)
Applicant JOHNSON, Edward, A. et al	

1. The designated Office is hereby notified of its election made:

[X] in the demand filed with the International Preliminary Examining Authority on:

29 February 2000 (29.02.00)

[ ] in a notice effecting later election filed with the International Bureau on:

2. The election [X] was

[ ] was not

made before the expiration of 19 months from the priority date or, where Rule 32 applies, within the time limit under Rule 32.2(b).

The International Bureau of WIPO **34, chemin des Colombettes** **1211 Geneva 20, Switzerland**	Authorized officer Pascal Piriou
Facsimile No.: (41-22) 740.14.35	Telephone No.: (41-22) 338.83.38

PCT WORLD INTELLECTUAL PROPERTY ORGANIZATION
International Bureau

INTERNATIONAL APPLICATION PUBLISHED UNDER THE PATENT COOPERATION TREATY (PCT)

(51) International Patent Classification 6 : G02B 6/293, G01N 21/35

A1

(11) International Publication Number: WO 99/53350

(43) International Publication Date: 21 October 1999 (21.10.99)

(21) International Application Number: PCT/US99/07781

(22) International Filing Date: 9 April 1999 (09.04.99)

(30) Priority Data:
09/058,488 10 April 1998 (10.04.98) US

(71) Applicant: ION OPTICS, INC. [US/US]; Suite 144, 411 Waverly Oaks Road, Waltham, MA 02454 (US).

(72) Inventors: DALY, James, T.; 35 Patty's Road, Mansfield, MA 02408 (US). BODKIN, Andrew; 37 Forest Street, Needham, MA 02192 (US). GRODEN, Michael, J.; 62 Rattlesnake Hill Road, Auburn, NH 03032 (US). JOHNSON, Edward, A.; 38 Old Stagecoach Road, Bedford, MA 01730 (US).

(74) Agents: LAPPIN, Mark, G. et al.; Lappin & Kusmer LLP, 200 State Street, Boston, MA 02109 (US).

(81) Designated States: European patent (AT, BE, CH, CY, DE, DK, ES, FI, FR, GB, GR, IE, IT, LU, MC, NL, PT, SE).

Published
With international search report.

(54) Title: MONOLITHIC INFRARED SPECTROMETER APPARATUS AND METHODS

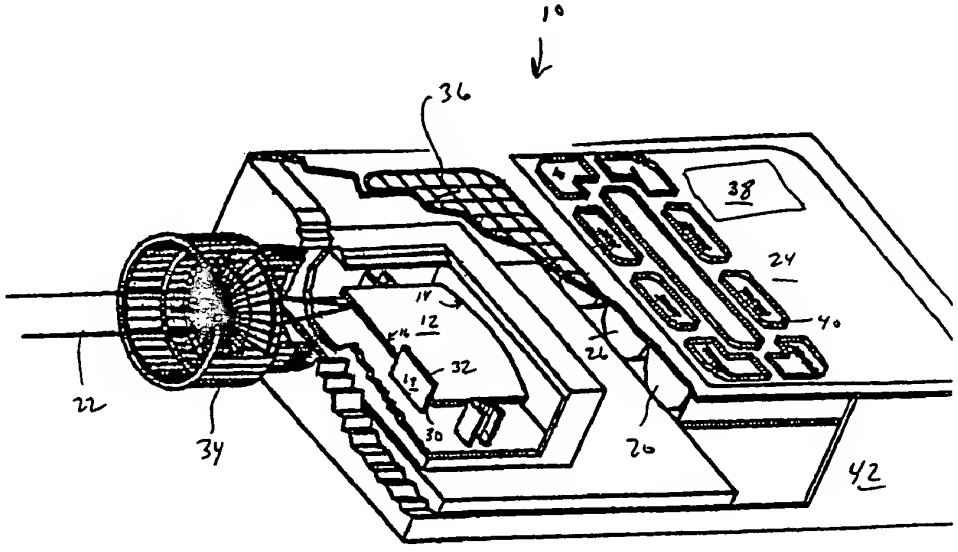

(57) Abstract

A monolithic spectrometer system providing vibration immunity and thermal stability, designed for infrared gas detection and chemical identification in the field or on the loading dock. One embodiment of the invention includes a spectrometer system (10) with the following elements: a silicon block waveguide (12); a cylindrical mirror (14); a diffraction grating (16); and a linear detector array (18). Electronics (20) can couple to the array (18) so as to collect electronic data representative of the spectral characteristics of the light (22) entering the system (10). Control of the system (10) is obtained through user interface (24). A battery (26) can be used to power the system (10).

MONOLITHIC INFRARED SPECTROMETER APPARATUS AND METHODS

Background

Conventional Ebert and Czerny-Turner type spectrometers and spectrographs are known in the art and have been common optical instruments for most of this century. These instruments use free-space optical elements - mirrors, reflective gratings, and slits - to disperse incident light into component wavelengths. Recently, there has been some experimental work using waveguides made of plastic or silicon dioxide, rather than air, to transmit the light from one optical element to the next.

Mst infrared spectrometers and spectrographs of the prior art use cooled infrared detectors as well as separately-aligned optical elements. Cooling the detectors requires added bulk and heavy equipment, such as closed cycle refrigerators, cryogenic liquid, and thermoelectric coolers with large power supplies. Maintaining optical alignment is also a challenge if the instrument is to be subjected to environmental stresses.

Infrared spectroscopy for chemical analysis has typically used laboratory grade spectrometers, spectrographs, or Fourier Transform Infrared (FTIR) instruments. These instruments can be as small as a cigar box and as large as a table top. They generally consist of entrance and exit slits, reflective mirrors and a reflective diffraction grating made of glass which

may or may not be rotated to scan the wavelengths of interest. The FTIR, for example, generally uses a Michelson interferometer with a moving mirror in one interferometer leg and a fixed wavelength reference such as a laser to scan the wavelengths. In addition there is a host of external equipment, including power supplies, scan motors and associated control electronics, and of course a cooled infrared detector. For example, an infrared chemical analysis instrument developed by Foster-Miller uses an FTIR about the size of a breadbox with a liquid nitrogen-cooled mercury cadmium telluride (HgCdTe) detector.

There are a few spectrometers, in the prior art, that attempt to remedy the above-described problems of size, weight, complexity and power consumption. Zeiss manufactures a Monolithic Miniature-Spectrometer, or MMS 1, and distributes the MMS 1 through Hellma International, Inc., of Forest Hills, NY. The MMS 1 uses a conventional silicon photodiode array and a cylinder of glass with an integral imaging grating. However, its operation is limited by the photodiode and the spectral limitations of the glass relative to ultraviolet (UV) and visible wavelengths. The detector is also positioned away from the waveguide, presenting certain optical alignment difficulties, particularly under environmental stresses.

Another instrument has been demonstrated by researchers at Kernforschungszentrum Karlsruhe GmbH (U.S. representative American Laubscher Corp., Farmingdale, NY). It uses a waveguide and grating fabricated in a multi-layer photoresist of polymethyl methacrylate (PMMA) to couple the output of an optical fiber to a linear detector array or array of fibers. This instrument is designed for demultiplexing applications. As above, because of the choice of materials, operation of this device is limited to visible and near-IR wavelengths of 600nm to 1300nm. Specifically, fabrication of the waveguide and grating is done by a process called LIGA (which stands for the German words for Lithography, Galvanoformung and Abformung)

which uses a three-layer photoresist and deep-etch X-ray lithography.

Yet another instrument has been developed by researchers at Oak Ridge National Laboratory. It is a microspectrometer based on a modified Czerny-Turner configuration and machined from a block of PMMA also known as Acrylic or Plexiglas. It has a bandwidth of about 1μm centered at 980nm and uses an externally mounted linear photodiode array.

None of these prior art spectrometers permit fully monolithic operation and spectral sensitivity from 1.1μm - 12μm, or further, and with uncooled detectors.

It is, accordingly, an object of the invention to provide apparatus that solves or reduces the above-described problems in the prior art.

Another object of the invention is to provide a hand-held, monolithic, rugged IR spectrometer.

A further object of the invention is to provide methods of manufacturing uncooled IR spectrographs.

Yet another object of the invention is to provide a process of isolating chemical species over a large infrared band with a monolithicaily-constructed IR spectrometer.

These and other objects will become apparent in the description which follows.

Summary of the Invention

The spectrograph of the invention overcomes many of the problems in the prior art by using uncooled detectors, e.g., microbolometers, which eliminate the need for associated cooling

equipment. Other detectors such as PbSe or PbS are also suitable. In addition, the spectrograph of the invention is monolithically constructed with a single piece of silicon, which eliminates the need for alignment and which makes the device inherently rugged and light weight. The use of standard silicon microelectronics technology also makes the invention low-cost, as compared to the prior art. By way of example, these costs can be orders of magnitude lower than the conventional spectrographs, i.e., hundreds of dollars instead of tens of thousands of dollars.

In one aspect, the invention includes a solid optical grade waveguide (similar to a slab of glass) coupled to a line array of detectors. Light from a source (e.g., earth emissions transmitted through gases) is focussed at a first surface of the waveguide, reflected from an internal mirror to a diffractive surface, which diffracts the light to a second reflector which focusses the light onto the array at a second surface of the waveguide. Accordingly, because of refraction, an f/1 light bundle entering the waveguide is translated to about an f/2 bundle within the waveguide, making it easier to cope with wavefronts therein.

In one aspect, the waveguide is silicon to transmit IR light; and the detector array is one of microbolometers, PbSe, PbS, or other IR sensitive detectors.

In another aspect, the waveguide is transmissive to visible light and the detectors are CCD elements.

In yet another aspect, the waveguide is ZnSe and the detectors are "dual band" so that visible and IR light energy are simultaneously captured at the detectors. For example, each pixel of the dual band detector can include a microbolometer and a CCD element.

The invention has several advantages over the prior art. First, it monolithically integrates

all parts of the spectrometer, including the detector, thereby making the instrument compact, rugged and alignment-free. Further, by fabricating the entire device on one piece of silicon, using silicon micromachining technology, we take advantage of the thirty years of silicon process development, and the emergence of silicon as a commodity item, to enable the fabrication of the instrument at a very low cost.

Other capabilities, features and advantages of a spectrometer constructed according to the invention include: (a) the ability to sense and identify chemicals i n a variety of applications and environments, (b) the ability to determine chemical concentrations, (c) operation with low-cost, low power, and long-term unattended operation or calibration, (d) uncooled operation, without expensive and unwieldy cooled detector elements, and (e) a rugged, alignment-free instrument.

The invention is next described further in connection with preferred embodiments, and it will become apparent that various additions, subtractions, and modifications can be made by those skilled in the art without departing from the scope of the invention.

Brief Description of the Drawings

Figure 1 shows a perspective view of a spectrometer system of the invention;

Figure 2 illustrates optical bench features of the waveguide, optical path, and detector of the system of Figure 1; and

Figure 3 shows a schematic layout of the optical trace of the system of Figure 1.

Detailed Description of the Drawings

As shown in Figure 1, one embodiment of the invention includes a spectrometer system 10 with the following elements: a silicon block waveguide 12, a cylindrical mirror 14 (e.g., gold-coated), a diffraction grating 16 (preferably gold-coated), and a linear detector array 18 (e.g., a microbolometer or microthermopile array). Electronics 20 can couple to the array 14 so as to collect electronic data representative of the spectral characteristics of the light 22 entering the system 10. Control of the system 10 is obtained through user interface 24. A battery 26 can be used to power the system 10.

The system of Figures 1 and 2 can further include detector preamps 30, a multiplexer 32, input focusing lenses 34, a microprocessor 36, an LCD display 38, keys 40 on the interface 24, and a protective housing 42.

Generally, these elements have the following function, as further described in the attached appendices and in the related provisional application.

1. Silicon block waveguide 12.

The silicon slab waveguide is the transmitting medium for the light before and after it is dispersed by the grating. Because it is a high index of refraction material (n=3.4), compared to the surrounding environment (n-1), light will be reflected from the polished top, bottom and sides of the waveguide without loss. The silicon block also acts as a fixed dimension frame upon which the grating, mirror, and detector array are fabricated thereby making the instrument compact, rugged, and alignment-free.

2. Reflective flat mirror 14.

The reflective flat mirror folds the path of the injected light so as to achieve a fiber-to-grating vs. grating-to-detector distance ratio of 2:1 or more. This is important if the input light comes from an infrared fiber with a typical core diameter of ²00~m yet we are focusing the light onto a detector array with 50~m wide pixels. To focus the light effectively with only one concave surface, fiber-to-grating vs. grating-to-detector distance ratio is directly proportional to the ratio of entrance and exit spot sizes.

3. Reflective diffraction grating 16.

The concave grating disperses the light into its component wavelengths (shown in Figure 3 as light path 40) and focuses it onto the detector plane18. In a normal grating with uniform line spacing, each wavelength has a different focal length. Therefore, the focal points for the various wavelengths will lie along the circumference of a circle that includes the gratin,. This circle is called the Rowland circle and is well-known by those skilled in the art of optics. However chirping the grating, i.e., varying the line spacing, flattens out the focal points for the various wavelengths almost completely.

4. Detector plane 19''.

The detector plane 19'' (Figure 3) is where the linear detector array 18 is located and the point at which the grating 16 focuses all wavelengths.

5. Linear detector array 18.

The linear detector array 18 converts the dispersed photons into electrical signals for each

wavelength.

8. Anti-reflection coating(s).

Anti-reflection coatings should be used on either or both the input plane and the detector array plane. By suppressing reflection at the interface bekveen high index of refraction silicon and the ambient environment, we ensure that the maximum number of photons are available for detection.

The invention can be used in applications where infrared analysis for chemical identification and concentration measurement is desired, especially in applications which require low cost, expendable sensors; low power sensors; or uncooled sensors. Particular applications may include detection and measurement of hazardous and pollutant gases, polluted water, chemical analysis of core samples, rocket plumes, smokestacks, biologic and chemical warfare agents, etc.

Appendix A shows and describes other features, embodiments, aspects and advantages of the invention.

The invention thus attains the objects set forth above, among those apparent from preceding description. Since certain changes may be made in the above apparatus and methods without departing from the scope of the invention, it is intended that all matter contained in the above description or shown in the accompanying drawing be interpreted as illustrative and not in a limiting sense.

It is also to be understood that the following claims are to cover all generic and specific features of the invention described herein, and all statements of the scope of the invention which,

APPENDIX A

TO

Monolithic Infrared Spectrometer Apparatus and Methods

By: James T. Daley, Andrew Bodkin, Michael Groden and Edward Johnson

Filed: April 10, 1998

TABLE OF CONTENTS

ABSTRACT

The next missions to Mars are targeted toward collecting surface samples and returning a representative subset of them to Earth. It is important that instrumentation placed n the surface be capable of rapidly differentiating the range of composition and aggregation of surface samples available, of characterizing the regimes from which they are collected, and of classifying the samples collected for later sample return. We propose to develop further and to validate an existing breadboard spectrometer that meets these characterization requirements. The resulting 3-12 μm instrument will be tiny, rugged, inexpensive to replicate, and will require very few resources, leaving significant system resources to support a range of complimentary instruments.

The proposed spectrometer is small, lightweight, low power, and can classify rocks on a large range of spatial scales. An integrated infrared illuminator will allow operation as a reflectance instrument for close inspection of small areas of rock or soil. Alternatively, larger areas can be analyzed from a distance. The signal-to-noise ratio will range from 200 to 4800, depending on the wavelength and mode of operation.

The existing breadboard instrument combines three key technologies: 1) a compact silicon waveguide spectrometer developed by Ion Optics, Inc., 2) high performance, broadband, uncooled thermopile detector linear arrays developed at JPL, and 3) a custom thermopile readout chip developed by Black Forest Engineering. Further improvements in all three areas, combined with compact packaging, will result in a small, rugged instrument having sufficient sensitivity to characterize rock and soil mineralogy and allow sample selection for subsequent return to Earth. The engineering model produced in this effort will be, with minor modifications, ready for flight qualification.

A strong Education/Public Outreach effort will make information about this program available to the public over the internet as well as provide opportunities for participation by minority college students.

1. RESEARCH OBJECTIVES

A. Science Objectives

It is the objective of this proposal to create a miniature instrument capable of classifying rocks, soils, and the surrounding terrain. We will accomplish this throu,h modest modifications to an existing solid state spectrograph.

The next missions to Mars are targeted toward collecting surface samples and returning a representative subset of them to Earth. It is important that instrumentation placed on the surface be capable of differentiating the range of types of surface samples available, and characterizing the types of samples collected for later sample return. It is important that a range of in situ measurement techniques be used so that the strengths of each technique can be used to complement the strengths of others. For example, an x-ray diffraction measurement gives very precise estimates of the mineralogy, but is not ideally suited for examining large areas, many samples, or elemental composition. Alpha backscatter provides an excellent measurement of elemental composition. Infrared spectroscopy is suited for indicating the mineralogy of large areas and the large-scale variance of mineralogy in rocks, but can only provide precise measurements of composition and/or precise classification of mineral types in favorable mineral mixtures. Combining the techniques, however, provides a very powerful in-situ tool set ideal for selecting the few very precious samples returned to Earth. To allow several in situ measurement techniques on the same platform, it is necessary that each technique utilize a minimum amount of resources with respect to cost, mass, energy, volume, and data rate. We propose here a micro infrared spectrometer that meets these criteria.

Mars is known to have large ancient volcanic areas, polar regions having layered terrain and surrounded by permafrost, and extensive areas which are consistent with water or ice erosion. There is evidence for layering in rocks, ancient lacustrine environments, and active aeolian features (such as sand dunes). Most rock surfaces seem to have a substantial coating of desert varnish, though a range of rock coloration (including white) has been detected. The generally red appearance of the surface has been attributed to oxidized iron. The soil has an abnormally high CO_2 content, the result of exposure to a CO_2 environment, moisture, and solar radiation.

Samples that might provide evidence of life may be found in regions that were once water-rich, for example ancient lake beds. The strongest indication of such an environment would be the

detection of evaporite d posits, rich in sulfates and carbonates, or confirmation of lacustrine sedimentary deposits, or the presence of highly altered materials (such as clays).

For volcanic regimes, the greatest interest lies in differentiating between basalt compositions, particularly with respect to silicon, iron, calcium and magnesium content. This information can be used to locate different sources, determine the degree of differentiation of magmas, and can be used to validate models equating flow form to magmatic viscosity.

Detection of metamorphic minerals would provide significant information on local tectonic activity on Mars. The location and size of ice deposits is also of extreme interest. Measurement of Mars dust is important for understanding Mars, and for implementing sample return and manned landing missions to Mars. Critical parameters include variation in composition, soil density, and variations in particle size.

Infrared spectroscopy provides a method for readily distinguishing between classes of rocks and mapping variations in mineralogy within rocks. This technique is most effective when used in association with techniques that provide definitive composition and mineralogy for individual grains in rocks. Depending on the wavelength region, infrared spectroscopy can provide estimates of the SiO_2 content, the degree of hydration of minerals, and can distinguish between various clays and evaporites. Infrared measurements also can provide very quantitative information in favorable circumstances, such a when a Christiansen peak is present. The technique is also suitable for estimating particle size both from scattering properties and from thermal emission measurements. Reflectance measurements penetrate to a few wavelengths of light, so are most diagnostic for freshly exposed surfaces. Thermal inertia measurements penetrate to the depth of the diurnal thermal wave.

Choice of the wavelength region to observe depends on the diagnostic features for expected minerals, on the observation conditions, and on the choice of detectors. The spectra in Fig. 1 (from the Aster catalog) illustrate that the spectral region this instrument spans is suited for discriminating between a wide range of geological samples which may be postulated for Mars. Note that the spectra in Fig. 1 are in reflectance units, and that some of the ordinal axes have been scaled differently. Fig. 1 shows, for instance, significant differences which can be used to differentiate (left to right, top to bottom) slate, horneblend schist, enstatite , andesite, clay, basalt, goethite, anorthosite, anorthite, gypsum, apatite, and halite - a range of evaporites, sedimentary and igneous minerals. These spectra are just illustrative, since the issue of which minerals can be distinguished in the presence of weathering is too complex to address here.

Requirements on the spectral ange, spectral resolution, and signal-to-noise requirements for a spectrometer can be estimated from Fig. 1 (the figures are scaled). There is always a push for higher resolution and sensitivity, but it is clearly possible to distinguish between a wide variety of minerals, and, to a lesser extent, the composition within classes of minerals at a modest resolution of about 0.1 micron. Similarly, a signal-to-noise ratio of 30 is sufficient to discriminate between mineral classes in most cases. The proposed solid state spectrograph has a spectral resolution ranging from 0.05 to 0.1 microns, and signal-to-noise ratios ranging from 200 to 4800.

Our miniature solid state spectrograph has several modes of operation. These include 1) a self-illuminated contact mode, suitable for classifying grains in rocks as small as 1x0.1 mm 2) a distant mode suited for characterizing large rock and locations by measuring spectra integrated over areas up to 1-2 meters in diameter.

Reflectance and emissivity measurements sample surfaces to a depth which is at best a few wavelengths of the light being measured. The measurements are best performed on fresh rock or soil surfaces, such as those exposed by trenching, scraping, or drilling. The interpretation of measurements made in this wavelength region are complicated by the crossover between reflected and emitted light (for Mars surface temperatures). There are a multitude of ways to address this issue for ground measurements including measuring samples at different temperatures (different times of day), measuring samples in shadow (though scattered light complicates this), and by measuring radiation from a sample with and without illumination.

Infrared measurements can be made quickly, using few resources, and are ideally suited for determination of the crystal field and the type of molecules contributing to an absorption. Quantitative measurements of elemental composition are better obtained using other techniques. The small size and cost of the proposed infrared spectrograph leave sufficient mass, power, space and budget to include complementary techniques.

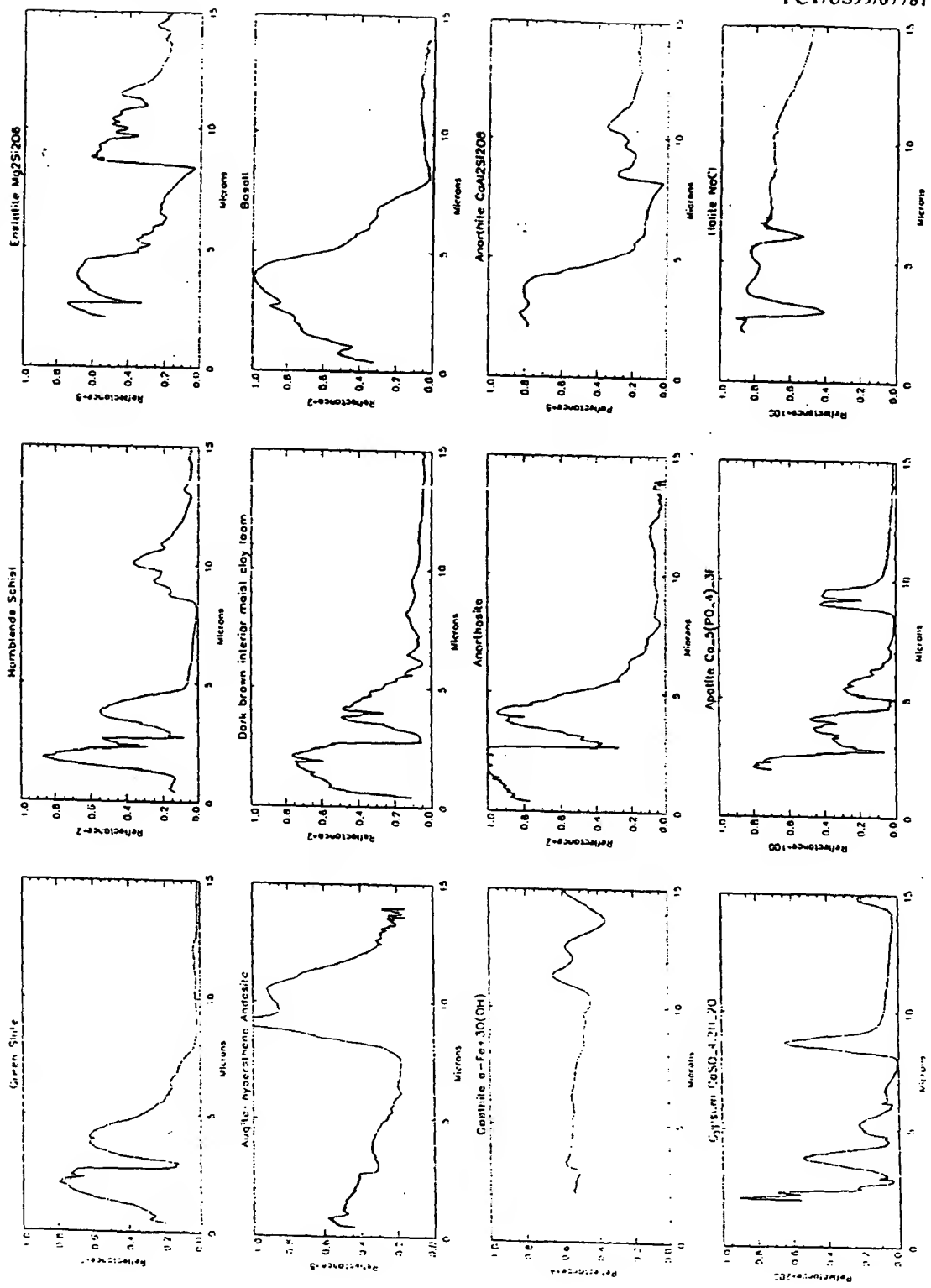

Figure 1. Spectra of a variety of minerals related to petrographic types.

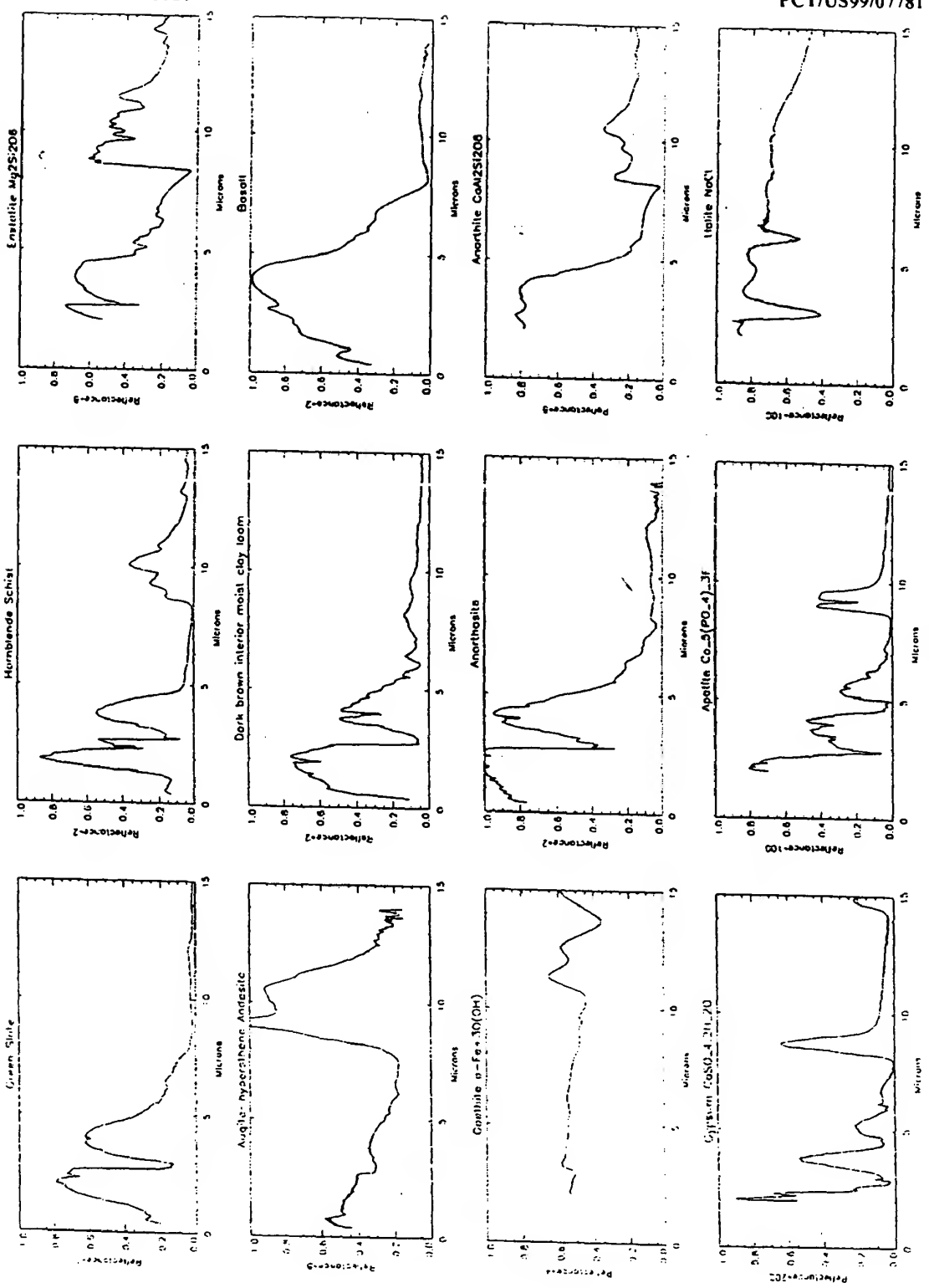

Figure 1. Spectra of a variety of minerals related to petrographic types.

A 3

44

B. Engineering Objectives

We will further develop and validate an existing breadboard spectrometer. The instrument will be compact, lightweight, and low power and will cover the spectral range 3-12 μm. The complete unit will be roughly 4 cm by 3 cm by 2 cm in size, weigh roughly 100 g, and consume about 200 mW of power. The spectral resolution will be 0.05 μm in the 3-6 μm range, and 0.1 μm in the 6-12 μm range. The device can operate as a reflectance instrument (contact mode) for close inspection of small areas of rock or soil, with a signal-to-noise ratio ranging from 600 to 4800. Alternatively, the spectrometer can operate in survey mode, passively measuring rock and soil spectra in both the solar reflectance and thermal emission spectral regions. In survey mode it will look from a distance at a large area and will have a signal-to-noise ratio ranging from 200 to over 1000.

An existing breadboard instrument, shown in Fig. 2, combines three key technologies: 1) a compact silicon waveguide spectrometer developed by Ion Optics, Inc., 2) high performance, broadband, uncooled thermopile detector linear arrays developed at JPL, and 3) a custom thermopile readout chip developed by Black Forest Engineering. A spectrum taken with the silicon waveguide is shown in Fig. 3. Further improvements in all three areas, combined with compact packaging, will result in a small, rugged instrument with sensitivity sufficient to characterize and select samples for subsequent return to Earth. The engineering model produced in this effort will be, with minor modifications, ready for flight qualification.

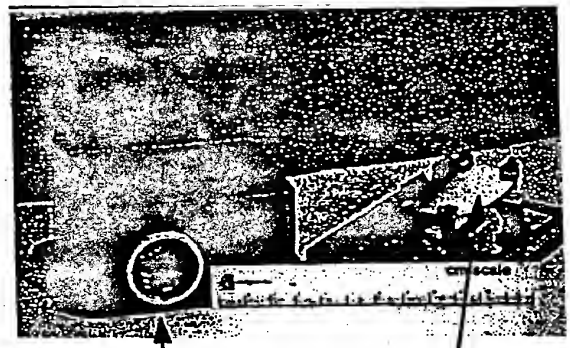

Fig. 2. Silicon waveguide spectrometer and housing developed by Ion Optics with NASA SBIR funding.

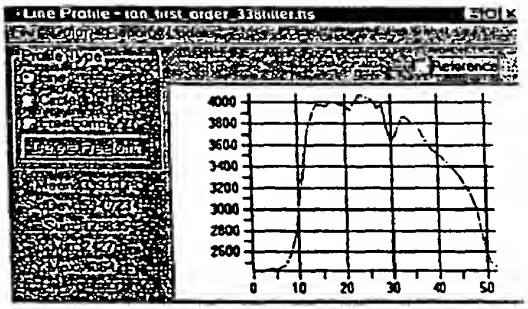

Fig. 3 Uncalibrated spectrum from prototype silicon waveguide. Radiation from the source passes through air and a 3.38 μm cut-on filter. The midpoint of the filter is at channel 11. Channel 30 shows a CO_2 absorption at 4.26 μm.

The existing breadboard instrument, which operates in the 3-5.5 μm range, is shown schematically in Fig. 4. It was developed by Ion Optics with funding from NASA SBIR phase II contract NAS7-1389. At the heart of this breadboard is a D-shaped silicon waveguide 1 mm thick and roughly 5 cm by 3 cm across. The unit uses a conventional Ebert layout, with the optical elements on the edges of the silicon waveguide. Infrared radiation is focused by an external lens onto an entrance slit defined by gold coatings on the silicon edge. Radiation traverses the silicon to a curved mirror on the opposite face, then the light is dispersed by an ion milled diffraction grating and focused by a second concave mirror. After exiting the silicon waveguide on the flat edge, the spectrum is detected by a linear array of thermopile infrared detectors. Each component of the spectrometer: the slab waveguide, the fold mirror, and the reflective diffraction grating, is made of silicon and fabricated into a seamless, permanently aligned unit with no moving parts.

A4

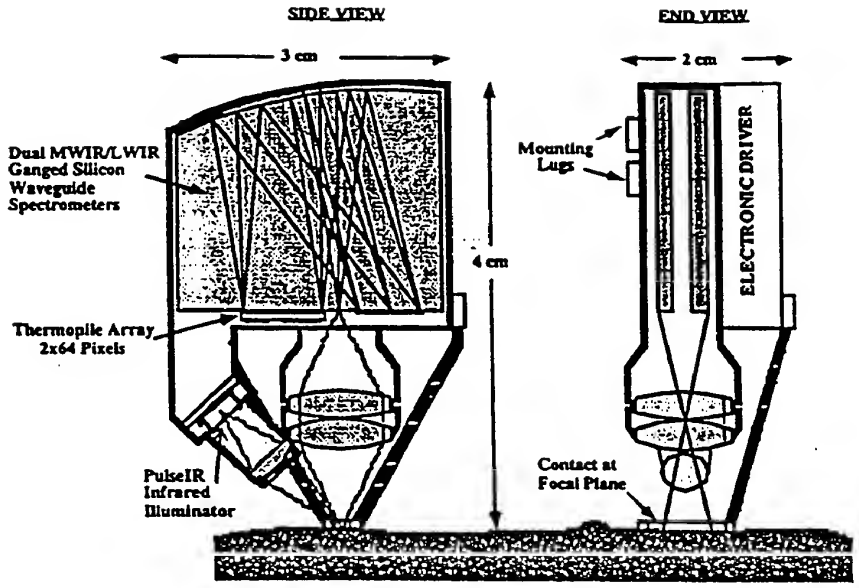

Figure 5. Proposed instrument configuration shows infrared radiator with lens integrated into the instrument package. Two silicon waveguides, with a bilinear thermopile array, cover the spectral range 3-12 μm. The package will be smaller and more robust, with lower power consumption than the existing breadboard spectrometer.

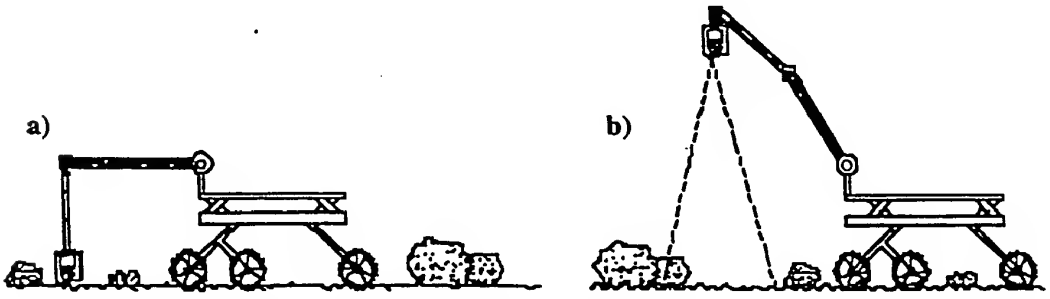

Figure 6. Modes of spectrometer operation. In contact spectrometer mode (a) the rover arm presses the spectrometer against a rock or section of soil. The sample is illuminated, and the reflected spectrum is recorded. The 3-6 μm and 6-12 μm spectrometer waveguides see different rectangular areas on the sample roughly 1.5 mm apart. Each rectangular area is about 1.0 mm long and 0.1 mm wide, matching the spectrometer entrance slit. In survey mode (b) the spectrometer is pointed down or away from the rover, passively sensing reflected solar and thermally emitted radiation. Survey mode analyzes large areas and can help to select interesting areas for further analysis.

The spectrometer can be configured in other ways. The lens can be positioned to provide a fixed focus at longer distances, say 1 meter away. Then the spectrometer will be operated in survey mode while looking at fairly small areas of rock or soil. Because of its compact size, this spectrometer can also be configured to fit down a bore hole to analyze composition at various depths, thus eliminating the problem of removing and analyzing intact core samples.

A 6

2. DESCRIPTION OF EXISTING BREADBOARD INSTRUMENT

A prototype silicon waveguide spectrometer has been developed by Ion Optics, Inc. with phase II funding from NASA/JPL SBIR NAS7-1389. This waveguide has been integrated with 1) a thermopile array developed at JPL and funded by NASA Code S UPN 632-20, and 2) a readout chip developed by Black Forest Engineering as a subcontract to NASA SBIR phase II contract NAS7-1899. Test results for each component are described below.

A. Silicon Waveguide

Fig. 2 shows the D shaped silicon waveguide mounted in a prototype spectrometer housing. This waveguide, with its f/1 input lens, was tested independently of the thermopile detector array by mounting an infrared imaging camera at its output port. Initial tests with a broadband source were very promising. The zero order diffraction spot is roughly the size of the 80 μm input slit, showing that the imaging components of the spectrometer are optimized. Very little stray light is seen between the zero order spot and the first order diffraction spectrum. Comparison of total light in the first order spectrum to the zero order spot yields a 47% grating efficiency. An uncalibrated spectrum is shown in Fig. 3. Radiation from the source passes through air and a 3.38 μm cut-on filter. The midpoint of the filter can be seen at channel 11; channel 30 shows a CO_2 absorption at 4.26 μm. Thus the spectral dispersion is 0.46 μm per pixel, as predicted. The total throughput of the silicon waveguide with input lens is estimated to be 15%.

B. Detector Array

Thermopiles are broadband, uncooled infrared detectors in the same class as bolometers and pyroelectric detectors. A thermopile consists of several series-connected thermocouples running from the substrate to a thermally isolated infrared absorbing structure. Incident infrared radiation creates a temperature difference between the absorber and the substrate, which is measured as a voltage across the thermocouples. Thermopiles offer a simplicity of system requirements that make them ideal for some applications; they typically operate over a broad temperature range and are insensitive to drifts in substrate temperature, requiring no temperature stabilization. They are passive devices, generating a voltage output without bias. They do not require a chopper. Thus, for some applications thermopile detectors can be supported by more simple, lower power, more reliable systems than either bolometers, pyroelectric or ferroelectric detectors. If thermopiles are read out with high input impedance amplifiers they exhibit negligible *1/f* noise since there is no current flow. They typically have high linearity over many orders of magnitude in incident infrared power.

A NASA funded development effort at JPL (Code S UPN 632-20) has produced 64 element linear arrays of thermopile detectors on silicon substrates. These detectors are 1.5 mm long with a pixel pitch of 75 μm, matching the geometry of the current Ion Optics spectrometer. Each micromachined detector consists of a 0.6 μm thick suspended-silicon-nitride membrane with 11 thermocouples composed of Bi-Te and Bi-Sb-Te. A schematic diagram of a single pixel is shown in Fig. 7, while a photograph of the complete array is given in Fig. 8. At room temperature these devices exhibit D* values of 1.4×10^9 $cmHz^{1/2}/W$ over the full range of wavelengths proposed for this instrument (3-12 μm), significantly better than that reported for other thermopile arrays. Detector responsivity is typically 1100 V/W at dc, and response times are 100 ms. Detector noise has been measured at frequencies as low as 20 mHz, and the only noise source is Johnson noise from the 40 kΩ detector resistance. Responsivity and response time have been measured as a function of temperature from room temperature down to 100 K. The total change in these quantities over this temperature range is roughly 20%, indicating that the detectors perform well over the entire range of Martian temperatures.

A 7

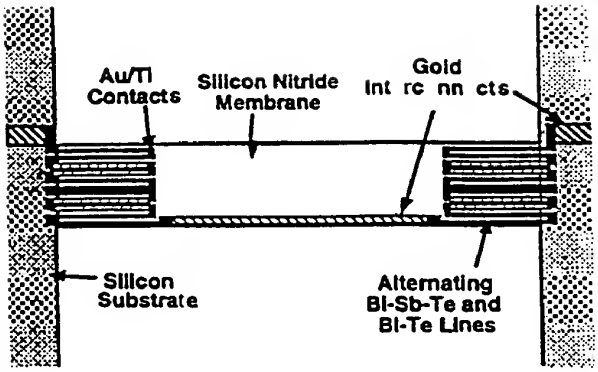

Figure 7. Schematic diagram of a single thermopile detector pixel. The detector is a 0.6 μm thick membrane composed of silicon nitride and metal lines and connected to the substrate at the left and right side of the figure. Infrared radiation heats the thermally isolated membrane. The temperature difference between the membrane and substrate generates a voltage in the 11 series connected Bi-Te / Bi-Sb-Te thermocouples.

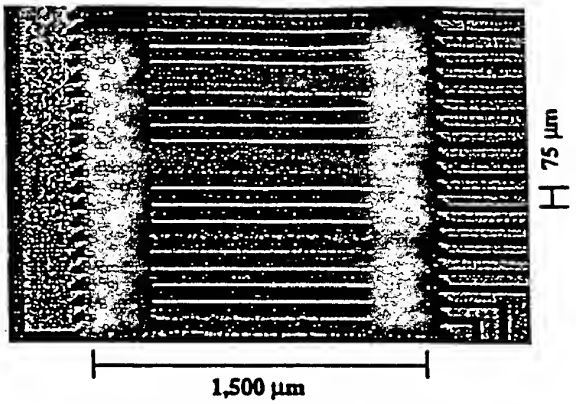

Figure 8. Photograph of a section of 64 element thermopile detector array fabricated at JPL. Each pixel is 1500 μm long, with a pixel pitch of 75 μm.

C. Detector Readout Electronics

To take full advantage of the thermopile array D* values, the signal readout must have a low noise figure for the given detector resistance and at the slowest measurement frequency of interest. In other words, the total input-referred noise after amplification must be only slightly higher than the detector Johnson noise. Typically this goal is difficult to achieve at low frequency for low resistance detectors.

In the current spectrometer, the thermopile array is read out with a custom integrated circuit chip designed by Steve Galeema of Black Forest Engineering. This sixty four channel device includes a preamplifier and filter for each channel, a multiplexer and a 12 bit A/D converter. Power draw is 55 mW. The input uses a chopping scheme to dramatically reduce low frequency noise and drift. The output is easily interfaced with a commercial processor chip. Black Forest's chip was originally designed for use with a thermopile array having a detector resistance of 1300 Ω. Initial tests indicate that the completed chips increase the noise of a 1300 Ω source by a factor of two over the range 0.1-10 Hz. This performance is excellent for a CMOS circuit with such a low source impedance. In the current spectrometer, this readout chip is mated to the 40 kΩ JPL detectors. The mismatch between detector and readout resistance causes some degradation in the system noise performance.

D. Radiation Source

Ion Optics' core product is the *pulsIR*® radiator, shown in Fig. 9. Ion Optics supplies infrared radiator components, first demonstrated in a 1994 DOE SBIR program, for the commercial gas sensor OEM industry. By the end of 1998, Ion Optics *pulsIR*® is expected to be in nearly 10% of all non-dispersive infrared gas sensors built in the United States. The key to the operation of the *pulsIR*® radiator is an extremely thin metal ribbon with a proprietary surface treatment to improve the conversion efficiency of radiator thermal energy to in-band radiation. The *pulsIR*® sources, with efficient, low thermal mass radiators and appropriate infrared windows (or windowless) convert significantly more electrical energy into useful, in band radiation than standard tungsten filament bulbs.

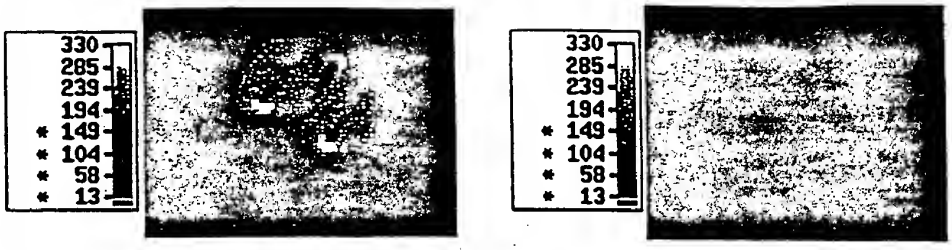

Figure 9. Thermal images of a *puls*IR® source with power applied and 300 ms after power is turned off.

3. WORK PLAN

A. Silicon Waveguide Development

This task will be performed by Ion Optics, Inc.

The objectives of this task are to substantially increase performance of the existing MWIR waveguide, and to make a similar waveguide in the 6-12 μm range. A simultaneous improvement in the resolution and signal-to-noise performance of the existing spectrograph can be made by making the silicon waveguide less than one-half its present size. These improvements can be achieved with a Littrow mount for the grating, folding the spectrometer optical path on itself and significantly reducing the size of the silicon waveguide (Fig. 10). This design disposes of unwanted diffraction orders; dumps for unwanted diffraction orders occupy much of the flat facet space in the breadboard spectrometer. The shorter optical path in the Littrow mount design results in smaller losses due to absorption of light in the silicon and its escape from silicon faces. Lessons learned during fabrication of the current waveguide will lead to a more efficient grating with fewer stray reflections. Combining a Littrow mount design with an improved grating fabrication process is expected to result in a factor of three improvement in both throughput and stray light rejection.

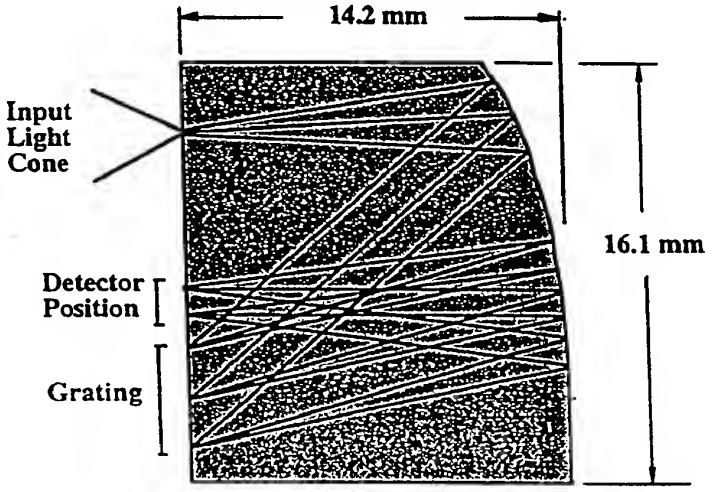

Figure 10. Preliminary modeling of a Littrow mount design of the grating. Optical models indicate the size of the silicon waveguide can be substantially reduced. This innovation is the key to the proposed level of miniaturization and performance enhancement

The design and fabrication of the 6-12 μm grating will benefit from NASA SBIR phase I funding recently awarded to Ion Optics, substantially reducing cost to this proposal of developing the two waveguides.

B. Detector Array Development

This task will be performed at JPL.

To measure spectra from the 3-6 μm and 6-12 μm waveguides simultaneously, the current linear thermopile detector array will have to be redesigned and fabricated as a bi-linear array with the appropriate geometry for the proposed instrument. In addition, we will strive to achieve a factor of two improvement in D* through three changes in the fabrication process.

1) First, properties of the Bi-Te and Be-Sb-Te thermoelectric films can be improved. Film composition can be optimized by changing the sputter target composition in an iterative fashion. Depositing the films on warm (100° C) substrates may improve the thermoelectric properties without overheating the photoresist used in lift-off. Optimization of the post-fabrication annealing procedure may also improve material properties.
2) Thickness of the silicon nitride membrane will be reduced from its current value of 6300 Å to about 4500 Å, decreasing thermal conduction paths to the substrate and improving responsivity and D* values. Response time will not increase because heat capacity is also reduced.
3) The device absorptivity will be increased from its current value of 50-60%. In the 3-6 μm range, this improvement can be achieved by depositing a reflecting layer of platinum on the underside of the membrane and a platinum layer with about 377 Ω/square on the top of the membrane. These metal layers, combined with the 4500 Å silicon nitride layer between them, form an optical cavity with high absorption in the 3-6 μm range. To increase absorption in both the MWIR and LWIR ranges, a gold or carbon black may be used. Alternatively, a metallized surface in close proximity behind the array will increase absorption by allowing some of the lost light to reflect back onto the detectors.

C. Readout Electronics Development

This task will be subcontracted to Black Forest Engineering.

To optimize system signal-to-noise ratio, it is critical to implement a readout that does not significantly add to detector noise. In the current system, noise performance suffers in two ways, first, the readout doubles the noise of the 1300 Ω source resistance, second, the 40 kΩ JPL detector resistance differs from that used in the readout design. The second issue could easily be resolved by redesigning the JPL detectors such that their resistance is optimal for the current readout circuitry. However, there is a potentially large advantage in redesigning the readout instead. Redesigning the readout for the higher source impedance of the JPL detectors should result in a lower noise figure and lower power draw. Typically CMOS amplifiers achieve better noise figures as source impedance is increased; the lower power draw results from lower current needed in the input transistors for higher resistance sources.

Black Forest Engineering will design and test the readout circuits as a subcontract. Fabrication will be performed on multiproject wafers at a commercial foundry.

D. Spectrometer Integration

This task will be performed by Ion Optics, Inc.

Thermopile detectors require vacuum for maximum sensitivity. Therefore, a hermetic package with an infrared window will be designed and fabricated to hold the silicon waveguides, detector array, and readout. The cover will be laser welded under vacuum. A surrounding dust-resistant case will enclose this package in addition to the radiation source, lenses and electronics. Within the dust-resistant case will be a commercial digital signal processor (DSP) chip and associated electronics for controlling the array readout chip. Packaging components will be designed with eventual flight qualification in mind.

The output from the miniature solid state spectrometer will probably consist of an asynchronous serial interface conforming to the EIA-RS-232 standard. The data format is still to be determined, but the RS-232 standard allows the electrical interface between the instrument and its host to be specified independent of the data format. It will consist of a half-duplex, bi-directional, two wire interface. Power consumption can be minimized by reducing the data rate and terminating the lines with high impedance loads.

The ultimate field test is to mount the resulting spectrometer engineering model on the arm of a rover and collect field data remotely. The most likely vehicle for such a demonstration is the JPL FIDO rover, which replaces the Rocky 7 rover. A small interface box will be constructed to supply power to the instrument and allow it to communicate with the rover via a serial RS232/422 bus. In addition, a mounting bracket will be made to provide a mechanical interface between

spectrometer and rover. The spectrometer's power requirements are well within the rover's capability. Alternatively, if a different field test platform is available, an appropriate interface will be supplied.

E. Laboratory and Field Testing

This task will be performed both by JPL and Ion Optics, Inc. Prior to system integration, each component will be tested in the laboratory. The following performance parameters will be measured:

1) Silicon waveguide (all parameters characterized as a function of wavelength)
   - Grating efficiency
   - Spectral resolution
   - Throughput with f/1 input lens
   - Optical cross talk
2) Thermopile detector array
   - Resistance
   - Responsivity versus wavelength
   - D* versus wavelength
   - Temperature dependence of responsivity
   - Response time
3) Thermopile readout chip
   - Power draw
   - Noise versus frequency for source resistance of thermopile detectors
   - System D* for thermopile array plus readout chip

The complete system will be carefully characterized and calibrated in the laboratory. The instrument response function and signal-to-noise performance will be characterized with blackbody sources in vacuum. Wavelength characterization and calibration will utilize a second spectrometer to provide monochromatic light as well as calibration standards (such as indene and polystyrene) to verify band positions. Stability of the calibration will be tested over the range of temperature conditions expected on Mars (200-300K).

Prior to testing on the rover, instrument performance will be validated on mineral and petrologic suites consistent with candidate surface materials expected on Mars. These samples will be measured in Mars-like conditions (CO_2 atmosphere, night and day temperature range) in the laboratory with artificial illumination. They will also be measured in ambient earth conditions with natural illumination. Furthermore, the instrument will be demonstrated in a variety of field sites which have good exposure of a range of petrographic types (such as evaporites, basalts, carbonates). In order to ensure that the instrument is available for rover integration, two or more spectrometers will be fabricated, permitting laboratory characterization and calibration to continue while one spectrometer is used in rover field tests. Making multiple copies of the instrument is expected to be straightforward.

4. EXPECTED RESULTS

A. Performance Goals

The program's performance goals are (a) detector-readout assemblies with a system D* value of 2×10^9 cmHz$^{1/2}$/W and (b) a total spectrometer throughput of 65% with an f/1 input lens. Section 2 describes performance of the existing instrument, while section 3 describes the tasks required to reach these much more aggressive performance goals.

B. Noise Equivalent Radiance

In order to calculate the instrument signal-to-noise ratios for various conditions, we first calculate noise equivalent radiance on the target within a spectral band equivalent to one detector (0.05 μm for 3-6 μm and 0.1 μm for 6-12 μm). With a detector area of 75 μm by 1.5 mm, and a system D* for the detectors plus readout of 2×10^9 cmHz$^{1/2}$/W, the noise equivalent in-band power at the detectors, normalized to frequency bandwidth, is 1.68×10^{-11} W/Hz$^{1/2}$. Assuming an integration time of 10 seconds, noise equivalent in-band power at the detectors is 5.30×10^{-12} W. With a 65% throughput for the input lens and silicon waveguide, the noise equivalent in-band input power to the spectrometer is 8.16×10^{-12} W. Two f/1 optics will image the target onto the slit with no magnification. Thus the target size is the same as the slit (75 μm by 1 mm), and the lens acceptance cone is 0.84 steradians, resulting in a noise equivalent in-band radiance from the target of 1.29×10^{-4} W/(cm^{2}ster).

A 11

AMENDED SHEET

C. Survey Mode Signal-to-Noise Ratio

Using the resulting value for noise equivalent in-band radiance at the target, one can predict signal-to-noise ratios for survey mode. Survey mode is illustrated in Fig. 6b, while the projected signal-to-noise ratios for this mode of operation are shown in Fig. 11. Normally incident sunlight is assumed. For reflected radiation, the target is assumed to have unit reflectivity, while for emitted radiation, unit emissivity is assumed. While these two assumptions are inconsistent, the resulting signal-to-noise values allow one to easily determine sensitivities to given changes in surface emissivity/reflectivity. Over most of the wavelength range, even for a cold surface, the signal-to-noise ratio is more than adequate for mineralogical surveys (signal-to-noise requirements are described in section 1A). Higher signal-to-noise ratios can be obtained at the expense of spectral resolution by adding signals from groups of consecutive pixels. Increasing the integration time is another technique for increasing the signal-to-noise ratio.

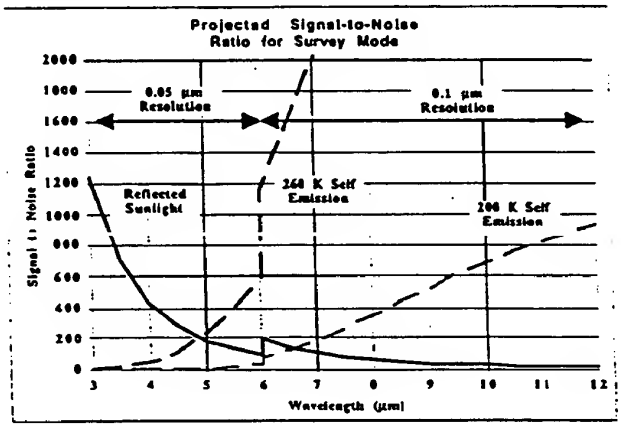

Figure 11. Projected signal-to-noise ratios for survey mode, showing sensitivity to reflected sunlight and thermal emission for typical day and night Mars temperatures. Integration time is 10 s.

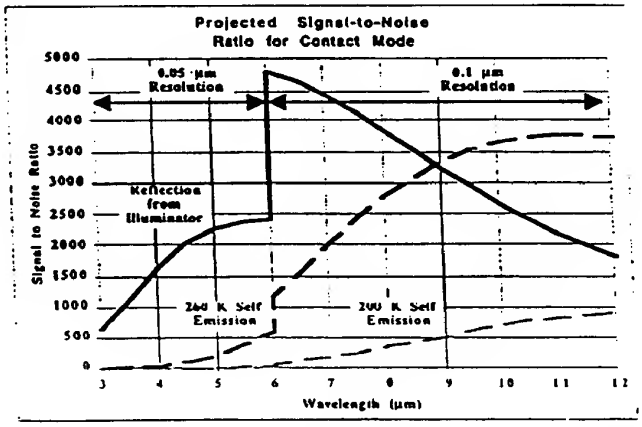

Fig. 12. Projected signal-to-noise ratios for contact mode (Figs. 5 and 6a) with a source electrical power of 60 mW. Integration time is 10 s. The signal-to-noise ratios for thermally emitted radiation are also shown for comparison.

D. Contact Mode Signal-to-Noise Ratio

To calculate signal-to-noise ratios in contact mode (Figs. 5 and 6a), a measure of the reflected illuminator radiance on the target is needed. The illuminator is a filament source produced by Ion Optics, which can be made with high emissivity over the entire wavelength range. Assuming 60 mW of electrical power to the illuminator, 60% efficiency in conversion from electrical power to

AMENDED SHEET

filament heat, and a filament emissivity of 0.9, the filament temperature will be 500 K. The 2 mm by 5 mm filament is imaged onto the target with no magnification by an f/1 lens with 90% transmission. Combining these numbers with the noise equivalent in-band radiance on target calculated above (1.29×10^{-5} W/(cm^{2}ster)), results in the signal-to-noise ratios shown in Fig. 12. In this mode of operation the signal-to-noise ratio far exceeds the level required to meet the mission science goals (described in section 1A). A higher input power to the source or a longer integration time can increase these values significantly.

An upper limit to the instrument mass can be easily calculated. The predicted volume is 24 cm^3. If we assume that the entire volume is aluminum, at 2.7 g/cm^3, the total mass will be about 65 g. A solid Kovar block, with a density of about 8 g/cm^3, would weigh about 192 g. Since much of the volume is occupied empty space, the mass will be significantly less than these values.

The power budget for this instrument is:

reflectance source	60 mW
thermopile readout chips	100 mW
commercial DSP chip for controlling readout chip	50 mW
Total power	210 mW

5. RELEVANCE OF PROPOSED WORK TO NASA

Sample collection for future sample return is a major focus of the Mars 2003 mission. These samples are slated for return on the Mars 2005 mission. This spectrometer is explicitly designed to provide rapid classification of samples together with the areas from which they are obtained. The instrument is also designed to be inexpensive to duplicate and easy to accommodate on successive missions, so that samples collected on each mission can be readily compared.

The search for evidence of life on Mars is a second significant goal of the missions to Mars. It has been postulated that the best places to search for evidence of life are in areas that were once water rich. This instrument operates in a wavelength region that is suited for detecting evidence of lacustrine environments, including evaporites, clays, and carbonates. It can also detect organic molecules, should they be present.

Understanding the environment on Mars for future manned missions is another major NASA goal. Thermal emission and scattering measurements are suited for characterizing soil size properties down to 2-3 microns. This spectrometer is capable of detecting a wide range of mineralogic and organic biohazards, as well as surface ice deposits, should they be present.

Characterizing the mineralogy and geology of Mars is important for understanding the processes that have shaped Mars. This instrument can be used to differentiate between the mineralogy characteristic of igneous, metamorphic, and sedimentary regimes. The silica content of basalts can be estimated and used to validate viscosities estimated from the morphology of flows. Soil types and aggregations, as well as CO_3 content of the soil can be estimated using a combination of scattering, thermal, and spectral techniques. Soil layers can be measured (using all three techniques) in trenches carved by a rover arm and in modest size boreholes.

In short, the many applications of this miniature spectrograph are relevant for a large number of NASA's objectives for missions to Mars. Many of the measurements that can be performed with this instrument are of fundamental importance for understanding Mars. In addition, these measurements can provide confirmation and redundancy for measurements performed by other instruments that may have higher specificity and risk. This instrument is particularly ideal because it is rugged enough to survive a range of landing techniques and consumes a small fraction of the resources available to a rover.

6. SCHEDULE AND COST

We propose a three year effort costing $919.5k. The schedule is designed to maximize the possibility of having an instrument ready for the Mars '03 launch. Before the Mars '03 proposal deadline, improvements in the three key spectrometer components - silicon waveguide, thermopile array, and readout chip - will be complete and test results will be available. Thus the risk of placing this instrument on the Mars '03 rover or lander will be low. Integration, laboratory and field tests will be performed before the Mars '05 proposal deadline.

The requested funding is $365.9k for FY '98, $356.5k for FY '99, and $197.1k for FY '00. The approximate cost breakdown for each task is: silicon waveguide development - $310k, detector

1. Introduction

In this successful phase 2 SBIR program with JPL, Ion Optics, Inc. is developing a tiny, integrated infrared reflection probe. This device will provide fundamental chemical composition and density information which is important in satellite-based exo-biology and ecological studies. Perhaps the most striking application of this instrument is to extract composition information from soil and rock samples, which is critical to the search for evidence of planetary life on the Mars Pathfinder 2003 mission. The phase 2 SBIR program will produce working prototype instruments, as an intermediate step towards developing and demonstrating a fully miniaturized, extremely low power flight instrument for the Mars 2003 mission.

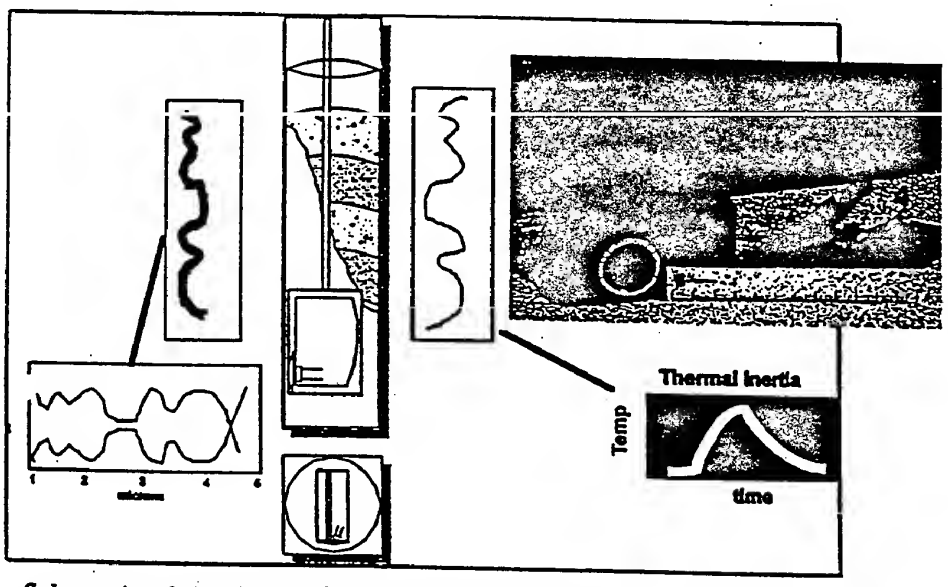

Figure 1 *Schematic of tiny infrared micro-probe arrangement for subsurface exploration on Mars. The miniature solid-state spectrograph and pulsed infrared source allows spectroscopic measurement of spectral lines of specific contaminants as well as local measurements of thermal inertia and soil density. Phase II prototype (inset) is now undergoing final integration and test for delivery in the first quarter of 1998.*

The ultimate purpose of this project is to develop and demonstrate an infrared spectrometer suitable for integration in packages for both Mars Lander and Mars Rover. This instrument is intended to be sufficiently rugged to survive hard landings, small enough to fit in boreholes, light enough to have little impact on the mass budget of landed packages, inexpensive enough to permit a diverse set of instruments on a landed package, and to have sufficient resolution and performance to identify the mineralogy of rocks and soils, to help select a suitable range of materials for sample return and to search for evidence historic environments which may have been capable of supporting life.

B2

Infrared spectral information is critical to understanding Martian geology and evidence of conditions for life. Infrared spectrometers are particularly suitable for rapidly characterizing differences in mineralogy of a large number of rocks and extensive areas of soil. They are most powerful, in the in-situ environment, when used in combination with instruments which can unequivocally (though at a slower pace) identify elemental compositions and crystal structures. IR spectrometers are also very useful for micro-thermometry and micro-calorimetry (powerful techniques for differentiating rocks) because a color temperature can be obtained. In the search for environments which may have supported life on Mars, the infrared region from 1 to 10 microns is particularly useful for detecting evidence of past aqueous environments. This is due to the multitude of bands in this wavelength region related to clays, evaporites, and carbonates.

2. Technical Accomplishments

Most of the effort this month has focused on the fabrication of the silicon waveguides. In particular, we have had to work closely with the vendor etching the grating in order to work through design and processing issues. We have now received the etched gratings and the waveguides are being AR and gold coated. In parallel with this activity we continue to work on the signal processing software and electronics. We have slowed the effort on the neural network software pending collection of test data from the unit under development.

2.1 Spectral Analysis

One of the unresolved issues concerned the required dynamic range required when making our spectral measurements. That is, what the resolution of the analog to digital conversion needed to be when measuring spectral peaks, in order to differentiate between different concentration levels. The result of the calculations showed that a 16 bit analog to digital (A/D) should provide the necessary accuracy to resolve absorption's from 200K ppm (water) to 5-10 ppm of No_x. If we examine the range provided by a 16 bit A/D, we get 2^{16} bits available to represent a range from 200K (signal intensity (linear extrapolated) to 60 specs) to 5 ppm resolution (signal intensity (linear extrapolated) to 0.0009 specs).

$2^{16} = 65{,}536$

$60/65{,}536 = 0.000915$ Spec/ppm

$0.000915/0.00018$specs $= 5.08$ ppm-resolution

Where 0.00018 specs is the intensity for 1 ppm of No_x using MIDAC measurements and 0.000915 is the minimum resolution provided over a range from 0 to 60 for a 16 bit A/D with all 16 bits used to represent data. These calculations indicate that the minimum resolution of No_x will be 5.08 ppm.

2.2 Optical Front End Fabrication

As reported, we placed orders for the fabrication and processing of the silicon waveguides. Because of the uniqueness of the design, our vendors have had some difficulty in processing the parts. However the parts have now been machined to there desired shape and the diffraction gratings applied. The parts have been inspected and ship to the last vendor for AR and gold coating.

2.2.1 Silicon Waveguide Processing

Computer Optics was contracted to machine the silicon blanks to their final shape before the diffraction grating was applied. They were also tasked with developing a fixture that would facilitate polishing and handling, and also applying the diffraction grating to twenty blanks simultaneously. A picture of this fixture and the waveguides appears in Figure 2.1 Using this fixture, and scrap waveguide blanks, they refined the polishing process and delivered finished pieces in early October.

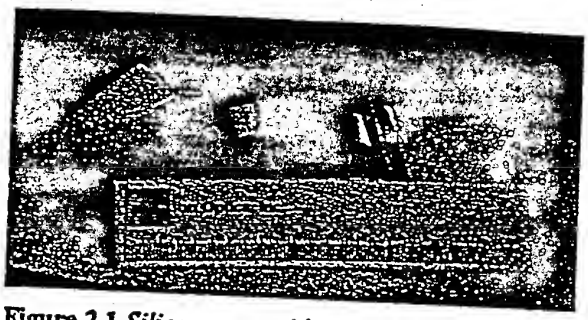

Figure 2.1 *Silicon waveguides mounted in polishing fixture.*

2..2.2 Grating Application

The fabrication of the gratings required three steps, spin coating the photoresist onto the blocked up benches, exposing the hologram into the resist, and then transferring the hologram into the silicon via ion beam etching. All three of these steps required very careful preparation, testing and finally execution.

The photoresist spin required the fabrication of a special spin rig to handle the heavy and cumbersome silicon block. The block was carefully cleaned to remove surface contaminant from the edges of the pieces. Special adaptations were made to the blocking fixture to allow for the differential expansion of the silicon and the aluminum block.

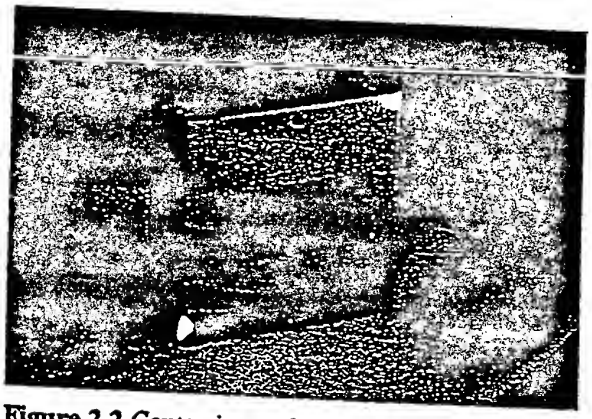

Figure 2.2 *Contaminants from the small spaces or "cracks" between adjacent waveguides destroyed the original grating mask.*

The hologram required extensive exposure testing and precise alignment on the optical table. Numerous test were made on trial pieces and ion etch rates determined. Finally the exposure was made and the hologram processed. The block was then baked to set the resist. At this point, contaminants that had been contained between the slab layers migrated from between the slabs and destroyed the hologram. It is hypothesized that the extra thirty degrees of baking temperature caused the appearance of these contaminants.

It was decided to remove the hologram, re-clean the surface and then re-coat and reprint the hologram. Because of the set up time required to re-shoot original holograms, the second hologram was done as a reprint from a master. This lowered its fidelity, therefore we expect a reduced efficiency in the grating, from 70% down to 45%.

The second hologram was successfully etched into the surface measured and delivered to Computer Optics for final coatings.

The finished pieces with the machined gratings appears in figure 2.3. It appears that at least 10 of the waveguides look very good and that there are another 6 or so that are usable. In order to minimize risk, we have decided to coat only 10 of the devices and hold the others in reserve. The coating process involves applying an anti-reflection coating to the flat surface to allow scattered light to easily escape, and to gold coat the diffraction grating and back cylindrical surface. We expect to received finished pieces before the end of the year.

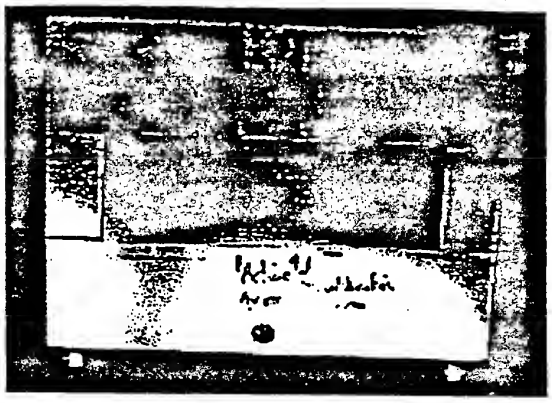

Figure 2.3 *Photograph of silicon waveguides with the diffraction grating applied. The grating can be seen in the center of the waveguides.*

2.3 Detectors

We've received the first PbSe detector array with the multiplexer. Although there were some minor mechanical alignment problems, these have been resolved. However we were not able to successfully test the finished assembly, it appears that the problem lies in the drive electronics. We have returned the assembly back to the vendor for additional testing.

We also received a 64 element micro-thermopile detector developed by JPL under another program. We plan to integrate this detector into our unit and evaluate its performance. There are many advantages to using the micro-thermopile: it is sensitive over a wide range of wavelengths, it does not suffer from 1/f noise and so does not require a chopper, and it does not have to be cooled. Conventional thermopiles are not as sensitive as a PbSe detector, however this device has a measured D* of 1.4 x 10^9. We are also investigating using a custom multiplexer/readout circuit being designed at Hypress (Stanford Conn.) for a micro-thermopile under development at Hypress. We have built a breadboard circuit and installed the micro-thermopile array in our optics h using. However at this time we are only using a small number of channels, for test purposes, until the multiplexer becomes available.

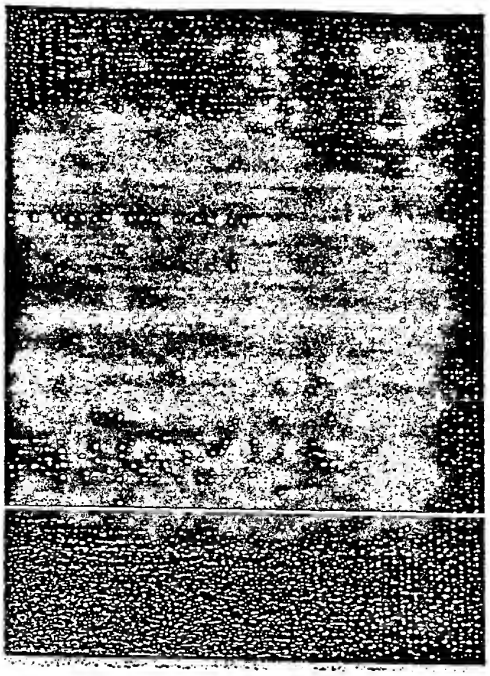

Figure 2.4 *This photograph shows a portion of the PbSe detector array. The long thin rectangular shape of each pixel is clearly visible.*

2.4 Processing

Significant progress has been made in the development of the signal processing software. As discussed last quarter, we plan to use digital signal processing (DSP) techniques in order to extract the modulated signal from each detector element. The neural network software being developed for determining chemical concentrations based on the spectral content is also most efficiently processed on a DSP. We are using an evaluation board for the Motorola DSP56L811 from Motorola as a development platform. This processor will perform the signal processing necessary for signal extraction and chemical detection and can also control a display and keypad: a serial interface will be used for communication with an external computer. This processor was only recently introduced; software development has been hampered because of the immaturity of the development tools. However, these problems have been addressed, and various algorithms implemented and tested.

2.5 Mechanical

The design of the optical housing and associated components has been finalized and the parts have been received. We are currently in the process of assembling an optics housing using a spare unpolished waveguide (see 2.5). The optical housing has a removable cover that will permit the components to be aligned prior to the cover being applied. The cover contains the entrance window with a replaceable cutoff filter. This filter can be replaced accommodating different spectral bands. The package also incorporates a mount to hold the input lens or a fiber optic input.

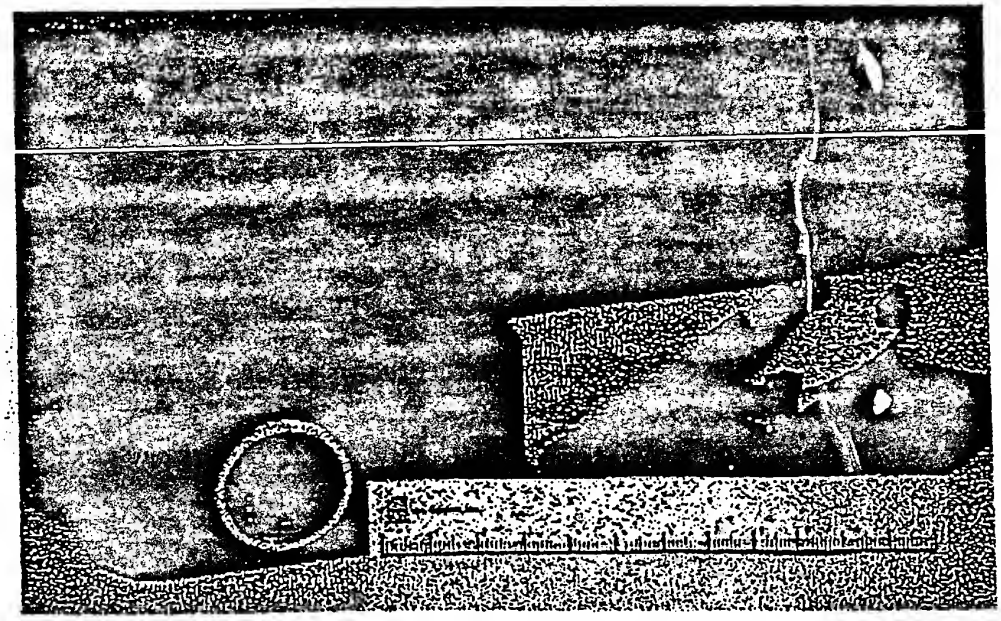

Figure 2.5 *Photograph of the completed optical housing and base. A silicon waveguide has been mounted to the base with the chopper and beam dump. The I/O connector is visible mounted to the base under the waveguide.*

2.6 Commercial Development Marketing

We have recently hired a consultant to assist in the marketing of our micro-spectrometer. We are researching who our potential customers may be (beyond those we have already identified) and what features they would like to see. We have also held discussions with a potential partner in the manufacture and marketing of a micro-spectrometer. Textron Systems, Wilmington Ma., has expressed considerable interest in our product. This partnership could be particularly significant in that Textron/Opto, a sister division, is a potential source for the PbSe detector array. This partnership may help us procure a detector/multiplexer assembly at a significantly reduced cost.

3. WORK PLANNED FOR NEXT QUARTER

3.1 Silicon Waveguide Fabrication

We expect to receive the finished silicon waveguides the last week in December. They will be characterized for spectral resolution, through-put, and scattered light.

3.2 Optical Chopper

We have received the chopper assembly. We shall be testing and integrating them shortly.

3.3 Detector Assembly

We have received the 64 element PbSe array and multiplexer from NEP however it was returned for repair. When the assembly arrives we will characterize the performance of the detector and readout electronics including D*, responsivity, pixel to pixel uniformity, and frequency response.

3.4 Assembly Test and Integration

We have started the assembly of the optical housing. As new components arrive, they will be integrated into the housing. We expect to have a fully assembled optical housing by the third week in January. At that time, data will be collected for data processing and system characterization.

1. Introduction

There is considerable topical interest in the content of Martian soils and sub-soil composition and particularly in establishing the presence or evidence of past water, carbonate minerals, or organic matter. Because of the problems of oxidation leaching in the near surface and the constant surface recovering by dust storms, it is extremely desirable to obtain composition and structure data at some depth below the surface. Typical procedures include sampling soil or core via drilling, extracting these samples and performing some sort of ex-situ analysis on the intact core samples. This requires specialized drills to extract the core samples, and even then, it is difficult to keep the core samples intact and to establish the sample orientation for measurement. We propose to enable downhole measurements which will extend the capability of these remote Martian probes with a tiny, rugged reflection analyzer instrument so small that it can make measurements from inside typical boreholes from soil and core sampling drills.

Phase I demonstrated the feasibility of a compact, rugged, lightweight spectrograph operating at room temperature in the 2-to-5 μm wavelength range. The critical innovation is the spectrometer's completely solid state construction -- it can be assembled entirely from micro-machined silicon components (even the MWIR detector arrays can be made of silicon). The resulting instrument has the advantages that it can be made very small and very light (about an inch in diameter and weighing a few grams), is permanently aligned for operation over a broad spectral range, and is extremely resistant to damage resulting from harsh environments (launch vibration, aggressive chemicals, radiation). The Phase II instrument will be approximately ¼ the size of the Phase I instrument with higher spectral resolution, lower noise , and more sophisticated signal processing and control.

We have continued to make good progress this quarter on the fabrication of the phase II instrument. Orders have been placed for the fabrication and processing of the micro-machined silicon waveguide, the detectors, the housings and mechanical mounting hardware. We have procured the computer processing board and software development is well under way. However the micro-machining of the silicon waveguide has proved more difficult than anticipated. Although our vendors are confident that these manufacturing difficulties can be overcome, it has caused a small slip in schedule.

2 System Design

From the analysis of the Phase I device and the results of our system models we have developed an improved design that will greatly increase the utility of the spectrometer. We previously completed the baseline silicon block spectrometer optic design. It uses a modified 'Ebert' layout fabricated from micro-machined silicon, with an F/1 input design (Figure 2.1)

In the 'D' shaped optic, IR light enters the entrance slit, a thin film deposited A/R coated area, and illuminates a cylinder mirror which collimates light. The high refractive index of silicon greatly reduces the angle of the cone of light, this permits the use of an F/1 lens at the entrance aperture. It also reduces the size of the cylinder mirror and permits the spectrograph to operate near the diffraction limit. The collimated beam is reflected off a gold coated diffraction grating.

The grating disperses the IR spectrum which is re-imaged after a second reflection off the cylinder mirror. The light exits the block through an AR coated surface and is imaged onto the detector plane. The detector plane is at a slight angle in order to flatten the field across the image. The air gap permits the detector plane location to be adjusted, allowing for manual focusing. As the rays exit the block, the large cone angle of the rays is restored, fully filling the acceptance angle of the detector.

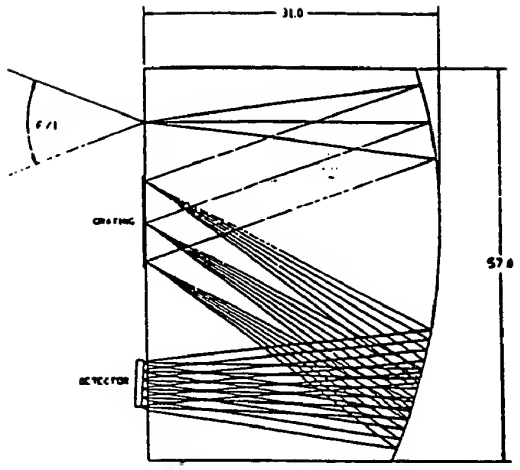

Figure 2.1 *Phase 2 optical bench raytrace. This layout has only two optical surfaces, greatly simplifying fabrication and increasing reliability by eliminating tolerance stack up inaccuracies. The flat grating design increases grating efficiency and makes the device easier to manufacture. Its F/1 design allows for twice the through put of the Phase 1 design, and its air gap at the detectors provide for focusing and permit the use of conventional AR coats.*

The grating produces a number of lower energy unwanted diffraction orders. In our earlier design these orders were trapped in the block and were scattered and added to unwanted background signal on the detector. The new design permits the exit of these unwanted orders out of the flat surface where they will be captured by a light trap. The components themselves incorporate a number of advanced design features. In particular the diffraction grating is made with a variable line density or "chirp" to flatten the Rowland circle and provide a flat focal plane for the array. The slab waveguide is formed to include mounting surfaces for other components and includes baffling and beam dumps. Since the silicon is opaque to photons above its bandgap, the slab excludes visible light from the detector. Silicon's high refractive index provides lossless reflections at the polished top and bottom faces of the device, waveguiding the radiation in the plane of the device. However, more important, because of the high index of the silicon, the cone of incident illumination is dramatically smaller inside the device. This provides better optical throughput than can be achieved with an open-air design. In addition, for measurements at longer wavelengths, the entire spectrograph can readily be cooled on a single cold-finger, in much the same way that focal plane arrays are now cooled in conventional instruments.

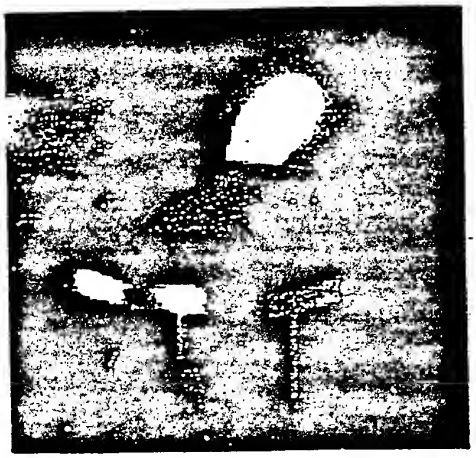

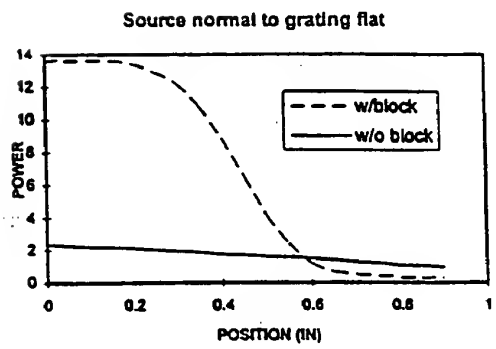

Figure 2.2 *The central innovation which makes the design of the instrument possible is the high-index slab waveguide. Refraction at the entrance slit sharpens the entrance cone and improved throughput, as shown in the thermal image and line scan data.*

3. Technical Accomplishments

This quarter, the major effort for the program shifted from the analysis and design of the instrument to the fabrication of the optical components and detectors and development of the signal processing and interface software. In parallel with this effort, our subcontractor NeuroDyne has continued with its efforts extracting chemical compositions from measured spectra. A detailed discussion of our accomplishments follow.

3.1 Spectral Analysis

The mid infrared waveband operating range of the phase 2 instrument should reveal the presence of many of the scientifically important CO_2 and H_2O along with Fe^{3+} minerals, distinguished by Cpx - Opx, and Olivine. Observations of the C-H stretch band at 3.4 micron wavelength and bound water in the 2.5-3.5 micron band should also confirm the likely presence of organic materials and/or hydrated minerals. The ability to resolve characteristic carbonate absorption bands in the 3.2-4.4 micron waveband and sulfates in the 1.3-3.6 micron region should provide the ability to distinguish various clays and micas. This is illustrated in 3.1 by an FTIR spectrum obtained in our laboratory from a calcite sample furnished by JPL.

Figure 3.1 *FTIR reflection spectrum of a representative calcite rock furnished by JPL. In this figure the high resolution spectra obtained from FTIR spectrograph indicate that the fundamental absorption bands are quite broad and may be resolved by the 64 channel spectrograph.*

For the instrument under development, a spectral range of 3.17 to 5.5 microns has been selected with a resolution of 0.034 microns. This range is acceptable for measuring hydrocarbons, CO, CO_2,and NO. Experimental spectral measurements have been made for NO, CO, and CO_2 at different concentration levels. These measurements were made independently and as such, the spectra had to be assembled to resemble measurements with all three constituents present. In the initial processing, the CO, CO_2, and NO data were added together uncorrelated and then treated independently. Thus NO could increase or decrease independent of CO or CO_2 levels.

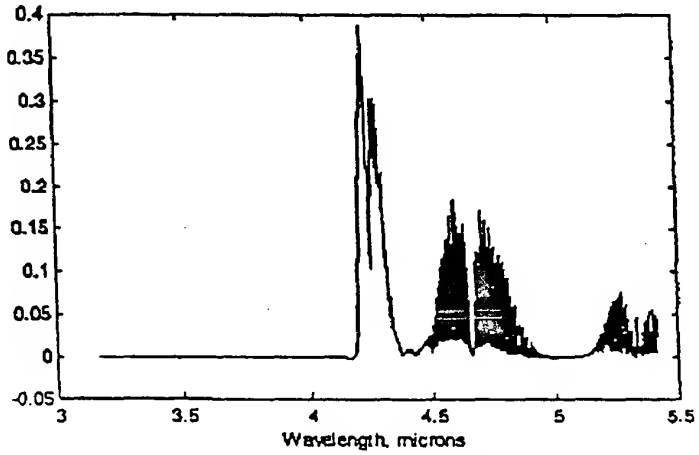

Figure 3.2 *Mean of spectral intensities over 4560 samples of absorption measurements. Note the characteristic peaks corresponding from left to right for CO_2, CO, and NO.*

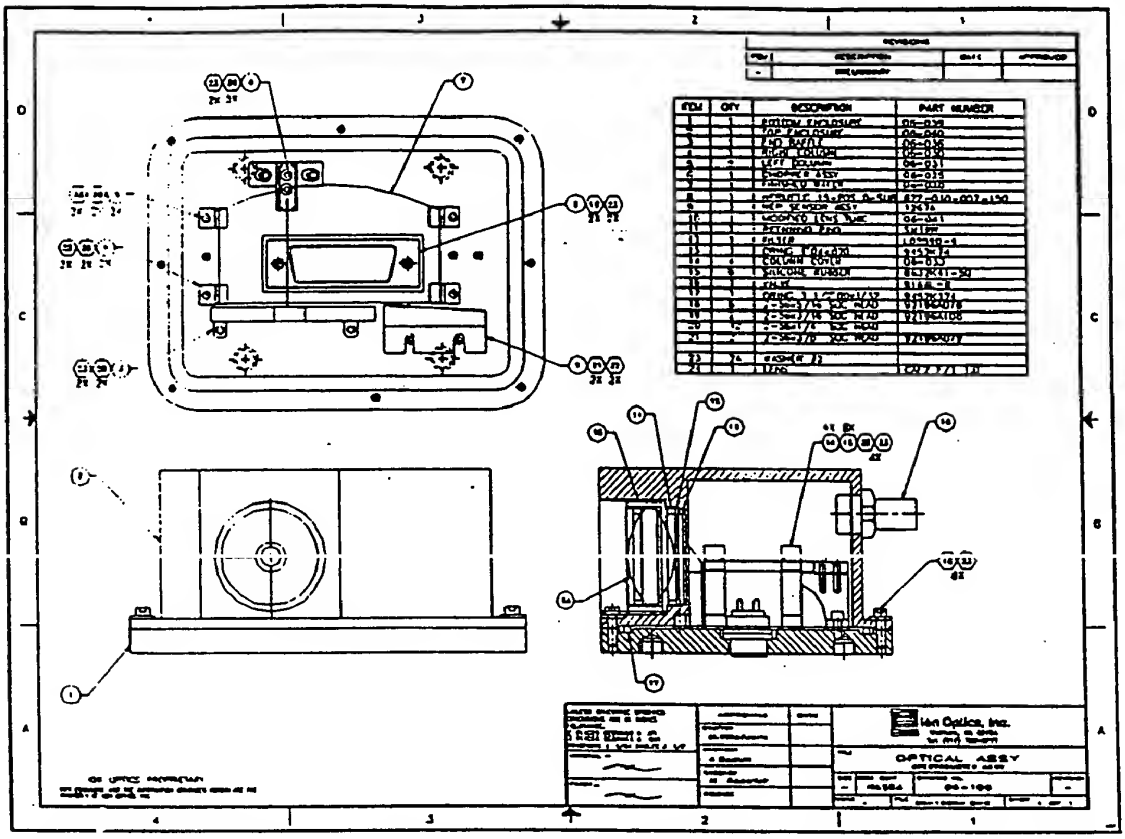

Figure 3.3 *The design of the optical housing and mounts is essentially complete. This drawing shows the assembly drawing for the optical housing.*

The design of the optical housing and associated components has been finalized and the parts sent out for quotation. We have also completed the detail design on most of the other mechanical components and have started to receive fabricated components. The spectrometer tree below details the components necessary to build the instrument and their relationship.

Now that a plan is in place for the detector readout electronics, the layout and packaging of these elements has been completed. Cooling the PbSe array and providing an interface to the readout electronics within a small volume complicates the mechanical design. Because we want to cool the detector assembly itself, not the readout electronics, we must mount the PbSe array directly on the TE cooler with the multiplexor circuit close by. The detector assembly must be adjusted relative to the optical waveguide in order to optimize the detection of the refracted radiation. While working closely with the detector vendor, we optimized the design for both optical and electrical performance while striving for a design that is easy to assemble and adjust while being small and cost effective.

Spectrometer Tree
Ion-Optics

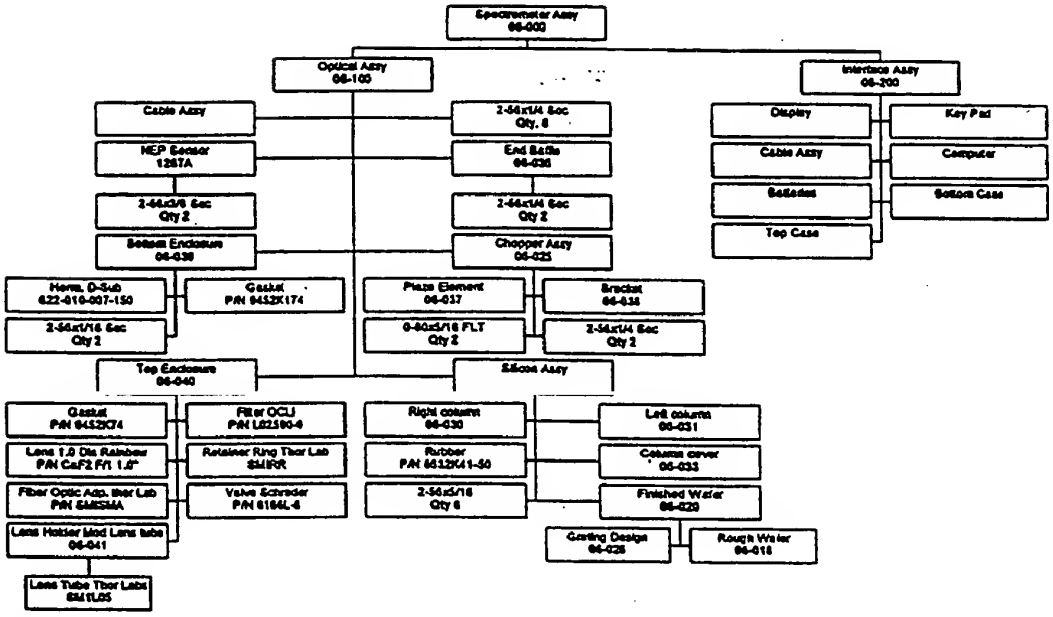

Figure 3.4 *The spectrometer tree identifies all the subassemblies of the miniatur spectrometer and their relationships.*

The optical housing has a removable cover that will permit the components to be aligned prior to the cover being applied. The cover contains the entrance window with a replaceable cutoff filter. This filter can be replaced accommodating different spectral bands. The package also incorporates a mount to hold the input lens or a fiber optic input.

3.4 Optical Chopper

The chopper consists of a two layer piezo-electric modulator. The deflection at the tip of the device depends on the bias voltage applied. By applying a time varying waveform to the device, a flag at the tip of the device alternately opens and blocks the entrance slit of the silicon waveguide. We have designed the device to operate from 200 to 350 Hz. A vendor has been selected and the element ordered. After fabrication it will be mounted on a base and tested.

3.5 Detectors/Readout Electronics

As discussed last quarter, we have selected a PbSe detector and selected a linear detector array vendor. However, we have spent considerable time evaluating a new custom multiplexor designed by our vendor. In order to optimize the performance of the PbSe detector it is customary to modulate or chop the optical signal in order to avoid 1/f noise in the detector. A

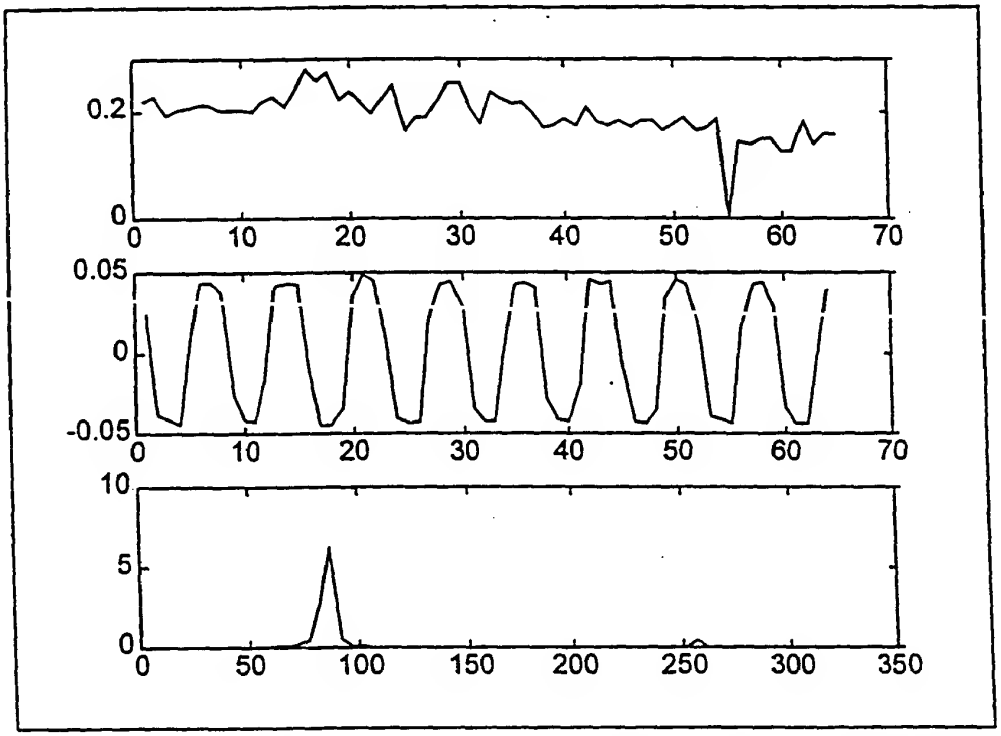

Figure 3.5 *The top trace shows the raw multiplexed data from all pixels during a single frame. The middle trace corresponds to the signal on a single pixels over many frames after the data has been unpacked. The modulated input signal is clearly evident. The bottom trace is the power spectral density for the modulated signal.*

lock-in amplifier is then used to recover the modulation and narrow band the signal. This process is greatly complicated by the use of the multiplexor. We proposed last quarter that we would use a digital detection scheme to accomplish the same result. This involves directly digitizing the multiplexor output and then using digital signal processing techniques to narrowband the signal. Figure 3 illustrates the process. Synchronizing the A/D clock with the pixel clock, the serial data output of the multiplexor is sampled. Consecutive samples in time for each pixel are assembled to form a sampled waveform for each and every pixel. The modulation signal can then be identified and measured using Fourier transform analysis techniques.

In performing our measurements, we found that we could not accurately calculate D* due to the limited performance of our data acquisition system. The noise contributed by the data acquisition system dominated the D* calculation. The calculated D* was only $5*10^{}$, orders of magnitude less than our expected value for an un-cooled PbSe detector. (In order to simplify the measurements, the initial tests were performed with an un-cooled array.) However, recognizing

the limitations of the data acquisition equipment, we were nonetheless encouraged enough by the performance of the multiplexed array to proceed with the procurement of the detector array with the custom multiplexor. We will work closely with the detector vendor in the design and layout of the multiplexor circuit and design data acquisition for the instrument compatible with its expected performance.

There is a large DC offset associated with each pixel due to dark current and background radiation. We will subtract this bias on a pixel by pixel basis, multiply the resulting signal by a fixed gain, and then digitize the signal. This will greatly reduce the dynamic range requirements on the A/D and allow the detection of low level signals in the presence of large background offsets.

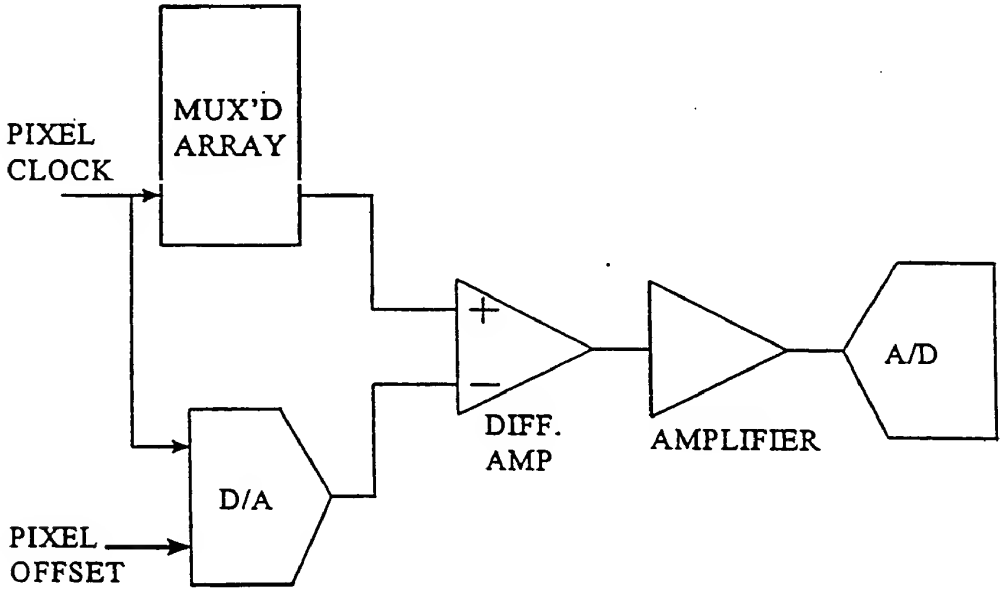

Figure 3.6 *Pixel to pixel offsets can be extracted and the signal amplified improving the dynamic range of the measurement.*

We continued to monitor the development of a 64 element micro-thermopile detector under development in a separate JPL-sponsored effort. There are many advantages to using the micro-thermopile: it is sensitive over a wide range of wavelengths, it does not suffer from 1/f noise and so does not require a chopper, and it does not have to be cooled. Conventional thermopiles are not as sensitive as a PbSe detector, however scientists at JPL believe that they can produce a micro machined thermopile, in the configuration we desire, with a D* of 10^9, equivalent to un-cooled PbSe. Although this device is experimental, we hope to incorporate this device into a prototype spectrometer and evaluate its performance. Although we believe we need the sensitivity of a PbSe detector at this time, the micro-thermopile is a very attractive alternative, that could be used in spectrographs that range from 1 - 20 μm (the full IR spectrum).

3.6 Processing

The continued growth of the digital signal processing market has resulted in a number of low cost DSP processors for embedded applications. After examining the requirements for the signal processing and concentration extraction algorithms, we have chosen the DSP56L811 from Motorola. This processor is a cost-effective solution that combines the prodigious number crunching of a digital signal processor with the versatile functionality of a microcontroller. This processor will perform the signal processing necessary for signal extraction and chemical detection and can also control a display and keypad; a serial interface will be used for communication with an external computer. An off-the-shelf development board has been acquired which will facilitate the rapid development of the spectrometer processing unit. A compiler has also been acquired for software development in 'C'. Benchmark tests performed on the processor at Ion Optics have verified the performance of the processor in our application.

4. WORK PLANNED FOR NEXT QUARTER

4.1 Silicon Waveguide Fabrication

We expect to receive the finished silicon waveguides by the end of Oct. They will be characterized for spectral resolution, through-put, and scattered light.

4.2 Optical Chopper

A vendor has been selected and the piezo-electric element ordered. We expect to receive and test the chopper assembly shortly.

4.3 Detector Assembly

We are awaiting delivery of the 64 element PbSe array and multiplexor from NEP which is due the end of September. At that point we can characterize the performance of the detector and readout electronics including D*, responsivity, pixel to pixel uniformity, and frequency response.

4.4 Assembly Test and Integration

With the delivery of the silicon waveguides, PbSe detectors, optical housing and mounts expected in October, the optical front end will be assembled and tested. Data will be collected for data processing and system characterization.

4.5 Phase III Product Evaluation

To investigate commercial markets for this spectrographs we have contacted several spectrograph vendors, and started a market survey of users. To assist in this we have produced a preliminary spec sheet showing two embodiments of the device. The first is the handheld spectrometer and the second is the OEM bench. In the coming months we hope to refine these specs by contacting various potential end users and OEM customers.

1. Introduction

NASA has a need for low-cost, low-power, low-mass, highly integrated spectral data acquisition instruments that enable space science observations from small and micro-spacecraft. Phase I demonstrated the feasibility of a compact, rugged, lightweight spectrograph operating at room temperature in the 2-to-5 μm wavelength range. The critical innovation is the spectrometer's completely solid state construction -- it can be assembled entirely from micro-machined silicon components (even the MWIR detector arrays can be made of silicon). The resulting instrument has the advantages that it can be made very small and very light (about an inch in diameter and weighing a few grams), is permanently aligned for operation over a broad spectral range, and is extremely resistant to damage resulting from harsh environments (launch vibration, aggressive chemicals, radiation).

This past quarter we have made considerable progress in the design and fabrication of the next generation instrument. This instrument is about ¼ the size of the device currently operating in our laboratory. A detailed system analysis has been performed and validated the basic design. In some cases we have modified our design based on this analysis and our experience fabricating the phase I instrument. We are now beginning to place orders for the optics, detectors, and other long lead items. We anticipate beginning test and integration of the next generation device early next quarter.

2. Technical Accomplishments

Significant progress has been made this quarter. System modeling and concept design for the new instrument have been completed. A detailed discussion of our accomplishments follow.

2.1 Reevaluation of Phase 1 Spectrometer

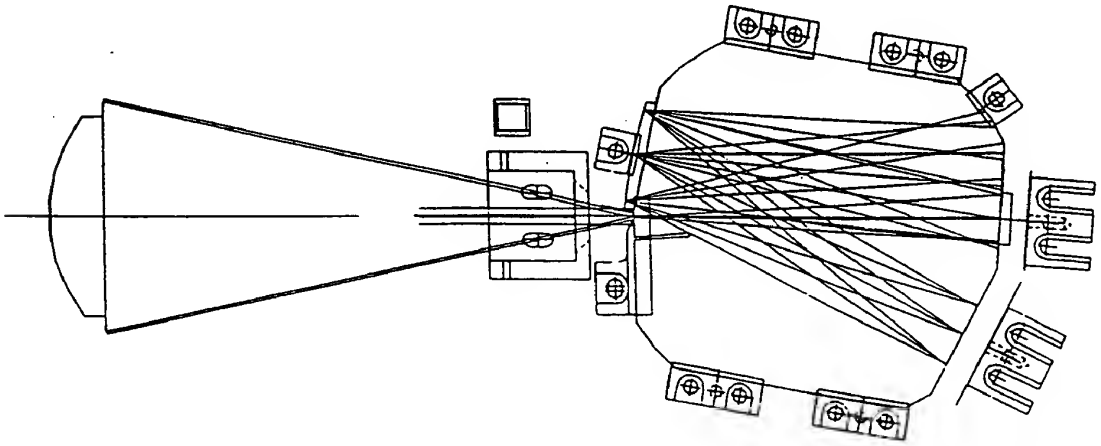

Figure 2.1 Phase one optical bench and lay out showing grating, detector plane, chopper, and filter.

D 2

The components themselves incorporate a number of advanced design features. In particular the diffraction grating is made with a variable line density or "chirp" to flatten the Rowland circle and provide a flat focal plane for the array. The slab waveguide is formed to include mounting surfaces for other components and includes baffling and beam dumps. Since the silicon is opaque to photons above its bandgap, the slab excludes visible light from the detector. Silicon's high refractive index provides lossless reflections at the polished top and bottom faces of the device, waveguiding the radiation in the plane of the device. However, more important, because of the high index of the silicon, the cone of incident illumination is dramatically smaller inside the device. This provides better optical throughput then can be achieved with an open-air design. In addition, for measurements at longer wavelengths, the entire spectrograph can readily be cooled on a single cold-finger, in much the same way that focal plane arrays are now cooled in conventional instruments.

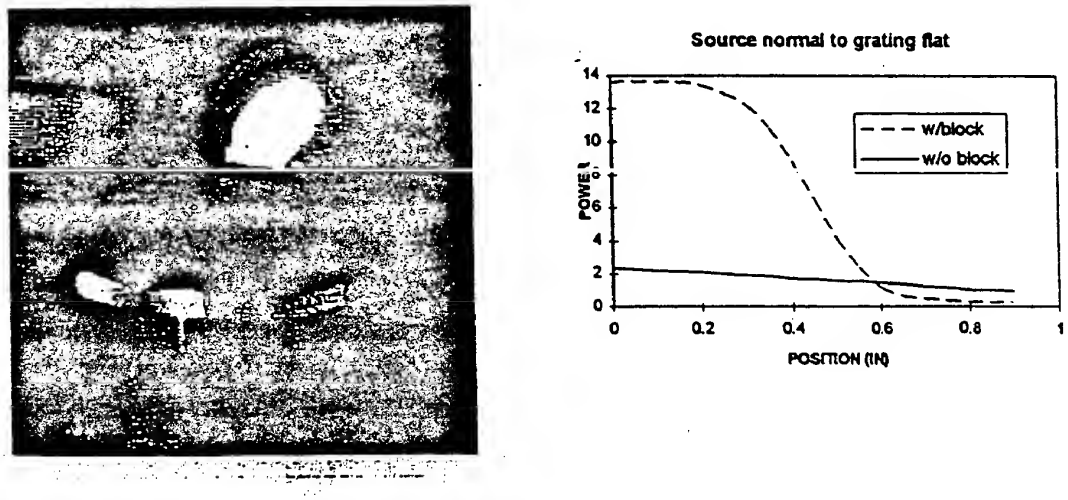

Figure 2.2 *The central innovation which makes this possible is the high-index slab waveguide. Refraction at the entrance slit sharpens the entrance cone and improved throughput, as shown in the thermal image and line scan data.*

The phase 1 block spectrograph was reevaluated to uncover the lessons learned and to find areas of improvement for the phase two miniaturization redesign. The following lists some of the key points:

•*Size* - The Phase 1 design is too large, does not provide an advantage over more conventional designs, and is relatively complex and expensive to manufacture.

•*Facets* - The Phase 1 block had 4 active facets, which were at precise odd angles to one another, two of which require AR coating.

•*Fabrication* - The Phase 1 design called for the grating to be fabricated onto a cylindrical surface whose radius was smaller than the block. This proved impossible to fabricate, since it would require acute inside corners in the silicon block. In the Phase 1 design we solved this problem by applying the curvature to an external piece and contact coupling it to the block. This functioned correctly but proved to be lossy and provided reflection ghosts in the system.

•*Grating Design* - The design utilized a chirped grating to flatten the image field of the Rowland circle optical design. This required an expensive holographic setup. The curvature of the grating substrate made it difficult to etch the grating into the silicon uniformly, resulting in uneven optical efficiency across the grating.

•*Readout Electronics* - The 16 channel lock-in amplifier of the Phase 1 device was superior in performance to the digital lock-in initially used. However it required two 4" x 6" PC boards, much too bulky for the Phase 2 miniature device.

•*Chopper Design* - The tuning fork chopper used in the Phase 1 device has magnetic coil drivers, which radiate EM interference. This interference is at the chopping frequency and can not be filtered from the signal. This is an intrinsic short coming of the tuning fork design.

•*Light baffle* - The internal baffle cut in the block proved to be a tremendous scattering sight, greatly increasing the background radiation reaching the detector and reducing the optical signal discrimination.

•*Entrance Slit* - The entrance slit, built from a separate piece of machined aluminum, caused scattering from its edges, contributing to the background noise.

•*AR Coatings* - The system requires anti reflection coatings on its entrance and exit facets, this will reduce the losses by 50%. However since the facets are at odd angles this could be difficult and expensive to accomplish. Since the detectors are contact coupled to the silicon, special matching AR coatings must be devised to match the detector to the silicon index. This is a development task of its own.

These factors along with the discoveries we made from the system model were used to design a new spectrometer lay out and detection system.

2.2 System Modeling

A system model was created to determine the detectivity of the system. The basic question to be answered was how much radiance must the target provide in order to be detected by the spectrographic system. The intuitive answer is to make the system with the highest detectivity. However within the limitation of the detectors and spectrometer throughput what can we reasonably expect to see, and is that sufficient to make measurements to detect the chemicals of interest. Two aspects of this question have been explored, the first is to determine what temperature of the target (a measure of radiance) is required to get a signal to noise of 1 out of the detectors at each wavelength. This assumes that the sample radiates like a black body. The second aspect is what spectral features are we looking for in the sample gasses, what resolution is required to resolve them, and are they within our spectral sensitivity.

We developed a system model that took into account temperature of the target, spectral throughput of the lens and optical bench, efficiency of the grating, spectral separation, and detectivity of the detector array. The model produced the following results

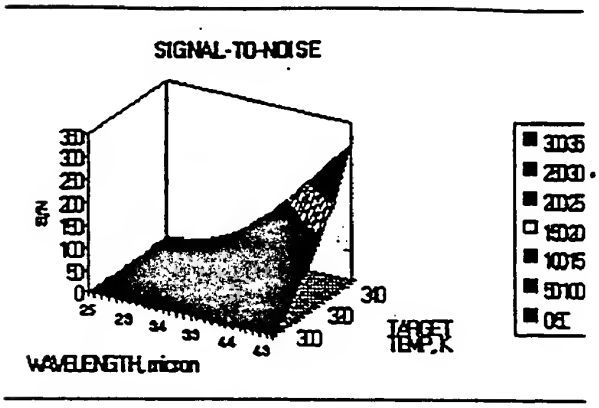

FIGURE 2.3 *This figure shows the detectivity of the spectrometer system, as modeled. The horizontal axes indicate the spectral band and the thermal temperature (radiant intensity) the vertical axis indicates the signal to noise ratio. Not surprisingly, this analysis shows that at longer wavelengths the signal to noise is higher (system will detect better).*

2.3 Spectral Analysis

There is considerable topical interest in the content of Martian soils and sub-soil composition and particularly in establishing the presence or evidence of past water, carbonate minerals, or organic matter. Because of the problems of oxidation leaching in the near surface and the constant surface recovering by dust storms, it is extremely desirable to obtain composition and structure data at some depth below the surface. Typical procedures include sampling soil or core via drilling, extracting these samples and performing some sort of ex-situ analysis on the intact core samples. This requires specialized drills to extract the core samples, and even then, it is difficult to keep the core samples intact and to establish the sample orientation for measurement. We propose to enable downhole measurements which will extend the capability of these remote Martian probes with a tiny, rugged reflection analyzer instrument so small that it can make measurements from inside typical boreholes from soil and core sampling drills.

The mid infrared waveband operating range of the phase 2 instrument should reveal the presence of many of the scientifically important CO_2 and H_2O along with Fe^{3+} minerals, distinguished by Cpx - Opx, and Olivine. Observations of the C-H stretch band at 3.4 micron wavelength and bound water in the 2.5-3.5 micron band should also confirm the likely presence of organic materials and/or hydrated minerals. The ability to resolve characteristic carbonate absorption bands in the 3.2-4.4 micron waveband and sulfates in the 1.3-3.6 micron region should provide the ability to distinguish various clays and micas. This is illustrated in Figure 2.4 by an FTIR spectrum obtained in our laboratory from a calcite sample furnished by JPL.

Figure 2.4 *FTIR reflection spectrum of a representative calcite rock furnished by JPL. In this figure the high resolution spectra obtained from FTIR spectrograph indicate that the fundamental absorption bands are quite broad and may be resolved by the 64 channel spectrograph.*

2.4 Optical Front End Design

From the analysis of the phase 1 device and the results of our system models we have developed an improved design that will greatly increase the utility of the spectrometer. We have completed the baseline silicon block spectrometer optic design. It uses a modified 'Ebert' layout fabricated from micro-machined silicon, with an F/1 input design (Figure 2.5)

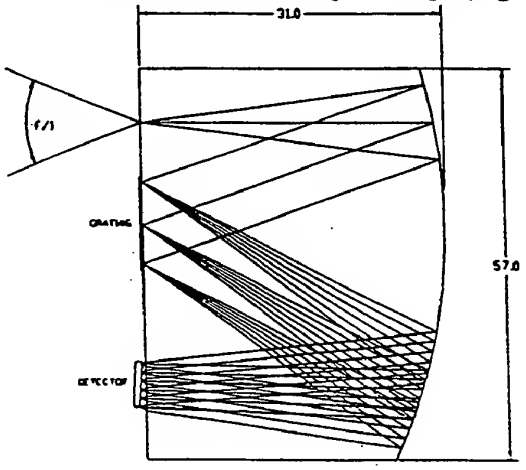

Figure 2.5 *Phase 2 optical bench raytrace. This layout has only two optical surfaces, greatly simplifying fabrication and increasing reliability by eliminating tolerance stack up inaccuracies. The flat grating design increases grating efficiency and makes the device easier to manufacture. Its F/1 design allows for twice the through put of the Phase 1 design, and its air gap at the detectors provide for focusing and permit the use of conventional AR coats.*

In the 'D' shaped optic, IR light enters the entrance slit, a thin film deposited A/R coated area, and illuminates a cylinder mirror which collimates light. The high refractive index of silicon greatly reduces the angle of the cone of light, this permits the use of an F/1 lens at the entrance apearature. It also reduces the size of the cylinder mirror and permits the spectrograph to operate near the diffraction limit. The collimated beam is reflected off a gold coated diffraction grating. The grating disperses the IR spectrum which is re-imaged after a second reflection off the cylinder mirror. The light exits the block through an AR coated surface and is imaged onto the detector plane. The detector plane is at a slight angle in order to flatten the field across the image. The airgap permits the detector plane location to be adjusted, allowing for manual focusing. As the rays exit the block, the large cone angle of the rays is restored, fully filling the acceptance angle of the detector.

The grating produces a number of lower energy unwanted diffraction orders. In our earlier design these orders were trapped in the block and were scatterred and added to unwanted background signal on the detector. The new design permits the exit of these unwanted orders out of the flat surface where they will be captured by a light trap. The following table addresses all the pros and cons of this new "D" shaped design.

Requirement	Phase 1Design	Phase 2 Design	Pro / Con
[illegible]	3" dia. x .25" thk 1.75 cu. in.	1" x 1.5" x .040" thk 0.06 cu .in.	Provides a 30x decrease in optical bench weight
Number of Facets	6 - 4 on block and 2 on contact coupled grating	2 - each facet used multple times	4 reflection design significantly decreases size
Grating	Chirped grating on seperate curved surface	Conventional flat grating	Easier to manufacture, and maintain uniform efficiency, etched into block prohibits the exchange of gratings
Chopper	Tuning fork	PZT bimorph	No radiated fields, chopper not required with micro thermopile detector
Scattering	No exit for higher diffracted order, no beam dump, scattering internal baffle	AR coated exit for higher orders, external beam dumps, no internal baffles,	Decreases signal noise by eliminating scattered light to detector
AR coating	AR coating on two odd angle surfaces	AR coating on 1 surface	Cheaper to manufacture
Spectral band	2.5 - 5 um	3.13 - 5.5	Better spetral features, but requires TE cooling of the PbSe detecotr
Spectral Resolution	0.15 um	0.039 um	Higher resolution required for gas identification
Detector	PbSe 16 element	TE cooled PbSe 64 element or micro thermopile	Required to find spectral features, PbSe cooling improves SNR
Read out electronics	16 channel lock-in amplifier	64 Channel muttiplexed w/ digital lock-in; or w/ 64 hybrid lock-in amplifiers	Greatly reduces space, Hybrid has fewer noise sources in system but is more bulky
Filter	External	Used as window on vacuum package	Dual use saves components
Package	Open air, large	Sealed, for dry gas or vacuum	Needed to keep condensate of TE cooled detector, more expnsive
Detector/block interface	Contact coupled	Air gap	Provides for focusing, eases exchange of detectors.
Slit	Free standing to provide focus	Deposited on block	Deposited slit is finer, less scattering and ghosts

Proprietary

2.5 Optical Front End Fabrication

Due to to the uniqueness of the design we have worked closely with our vendors to develop a fabrication plan that is consistent with the inexpensive mass production of the front end. This consists of the following:

Optical blanks. "D" shaped optical blanks are purchased from VA Optical, a silicon supplier. Their main business is to produce substrates for the micro-chip industry. For this reason they can produce superior flat polish on both sides of the optic. The near net shape will include all the polished flats but not the cylindrical surface.

Cylinder. The blanks will be sent to Digital Optics Corporation who will stack twenty parts into a monolithic block than shape the block into a cylinder lens. They possessed the interferometric equipment necessary to measure and produce the necessary surface on the cylinder mirror. They will gold coat the mirror and AR coat the flat.

Grating. The gratings will be built by Diffraction Limited. They will produce a grating in photoresist on the surface and etch it into the silicon. They will also work with the elements assembled in a stack. Once the grating is made they will add gold reflector overcoat and deposit the entrance slit.

Assembly. The part will be returned to Ion Optics where its performance will be measured. This is done by feeding the block with a lab spectrometer and measuring the quality of the output image with an IR camera. Once its performance is verified the device will be integrated into the housing with the detector and focused.

2.6 Mechanical

The design requires the precise alignment of the optical bench, the chopper, the detector array, and the filter. This is all accomplished with a precision sealed package. The package holds the chopper, filter and detector in position and provides for a vacuum seal.

The miniature chopper we developed consists of a piezo-electric (PZT) bi-morph strip with a flag on the end. The bi-morph strip is a sandwich of PZT and stainless steel bonded together. The bi-morph curls like a bi-metallic as a voltage is applied across the PZT causing it to change length. This provides very fast chopping of the optical beam within a minimum volume and with less EMI.

The electronic read-out will fit into the vacuum package so the signals are amplified and multiplexed before leaving the package. This provides for the minimum number of electrical feed throughs. It also provides a modularity of the design so the spectrometer optics package can be traded out with little effort.

The detector mount will hold the backside of the TE cooler to which the detector array is bonded. The mount will allow the detector to be precisely positioned with micrometer screw adjusts and then locked into place. Heat from the TE cooler will be conducted through the mount and into the base of the package.

The package will have a removable cover that will permit the components to be aligned prior to the cover being applied. The cover will contain the entrance window that will be coated to act as a cutoff filter in the system. The package will also incorporate a mount to hold the input lens or a fiber optic input.

2.7 Detectors

When it comes to determining system performance, no other component will have as much effect perhaps than the detector. For this reason, we have extensively researched detectors applicable for our requirements. However criteria other than performance must be considered when evaluating detector systems for our portable, handheld spectrometer. These include cost, size, complexity and flexibility. For example, photoconductive devices typically suffer from low frequency or 1/f noise which can be reduced by chopping the input signal and AC coupling the output from the detector. However this adds a level of complexity to the optical system and the read out electronics.

After considering the wide range of detector arrays available, we have narrowed our options to two choices: a PbSe photoconductive array and a micro-thermopile linear array. A thermoelectrically cooled PbSe array provides the best performance with moderate cooling requirements in our region of interest. When cooled to approximately 145 to 250 K, low NEP performance extends well beyond 5.5 micrometers. Thermoelectric coolers are rugged low cost devices that can provide adequate cooling for the PbSe device. We anticipate a requirement for a two stage TE cooler.

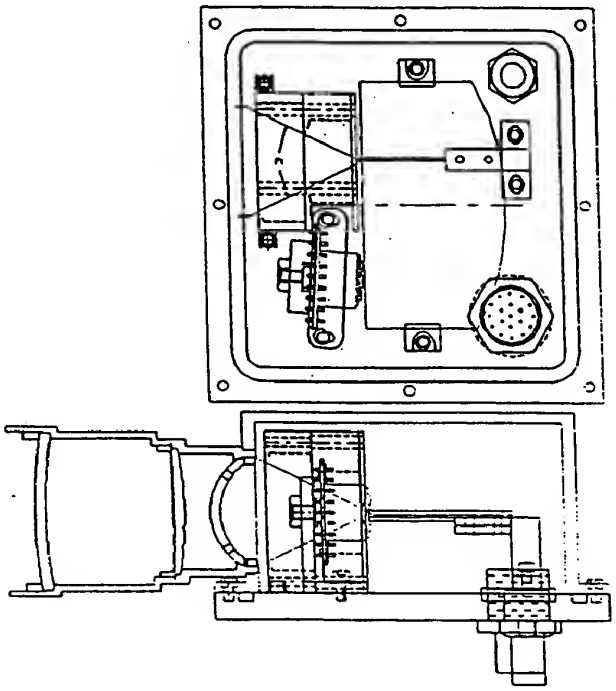

Figure 2.7 *This is the package design that utilized the Optoelectronics/Textron integrated multiplexer and PbSe detector array.*

We have completed an extensive survey and contacted all the PbSe array detector vendors in the U.S. Out of this survey we located only one, Optoelectronics Texton, with an operating multiplexed PbSe array. We spent several months in good faith effort, developing an array design operating parameters, and package. However when it came time to formalize our Purchase Order, Opto provided a price 3 times that of the ball park figures we had been working to (approaching $100k). This cost is well outside our budget, and the episode has been a major schedule set back to the program. We have now developed an alternative detector plan, and have begun to carry it out

After investigating a number of other PbSe detector array sources, we have selected New England Photoconductor (NEP) as the detector array vendor. NEP is a local manufacturer of photoconductive arrays that supplied the array used in the phase I system. Their performance under that contract was very favorable. NEP quoted the lowest price for a custom 64 element linear array and will integrate their array with a newly developed custom integrated multiplexor circuit. We are in the process of evaluating the technical risk and system performance of this developmental multiplexor and its possible impact on system performance. Its major disadvantage is that it adds significant technical and schedule risk. However an integrated multiplexor will significantly reduce the size, cost, and complexity of the readout electronics.

We have also investigated the use of a 64 element micro-thermopile detector under development in a separate JPL-sponsored effort. There are many advantages to using the micro-thermopile: it is sensitive over a wide range of wavelengths, it does not suffer from 1/f noise and so does not require a chopper, and it does not have to be cooled. Conventional thermopiles are not as sensitive as a PbSe detector, however scientists at JPL believe that they can produce a micro machined thermopile, in the configuration we desire with a D* of 10^9, equivalent to uncooled PbSe. Although this device is experimental, we hope to incorporate this device into a prototype spectrometer and evaluate its performance. Although we believe we need the sensitivity of a PbSe detector at this time, the micro-thermopile is a very attractive alternative, that could be used in spectrographs that range from 1 - 20 um (the full IR spectrum).

2.8 Readout Electronics

Typically, a modulated or chopped detector signal is recovered using a lock-in amplifier or synchronous detection scheme. The large number of pixels and the use of a multiplexor complicates the extraction of the modulated signal from our PbSe detector. We are currently investigating extracting the modulated output digitally. The serial output of the multiplexor will be digitized with a high speed, high resolution A/D converter. The sampled outputs from each pixel will be collected from multiple scans and processed digitally. For example, by performing a Fast Fourier Transform (FFT) on the data collected for each one pixel, the energy content at the modulation frequency can be determined. The FFT acts as a narrowband filter at the modulation frequency. This energy can be averaged over time to further increase signal to noise. We plan to evaluate this approach using an off-the-shelf A/D board and a standard analysis package running on a personal computer. This allows us to rapidly prototype and test different processing techniques.

In order to reduce our technical risk, we have also specified and received a proposal for a hybrid multi-channel lock-in amplifier. This device will replace the multiplexor. It is assembled from un-packaged die and mounted on a thick film circuit; an eight channel device occupies 2.56 square inches. Although this approach is fairly large and costly, it has a low technical risk and guaranties maximum performance.

2.9 Processing

The continued growth of the digital signal processing market has resulted in a number of low cost DSP processors for embedded applications. We are currently investigating several processors for our application. In particular, we are evaluating the DSP56L811 from Motorola. This processor is a cost-effective solution that combines the prodigious number crunching of a digital signal processor with the versatile functionality of a microcontroller. This processor could perform the signal processing necessary for signal extraction and chemical detection and also control a display and keypad; a serial interface will be used for communication with an external computer. An off-the-shelf development board will facilitate the rapid prototyping of the final spectrometer unit.

3. WORK PLANNED FOR NEXT QUARTER

3.1 Fabrication of the Silicon Spectrometer Optic.

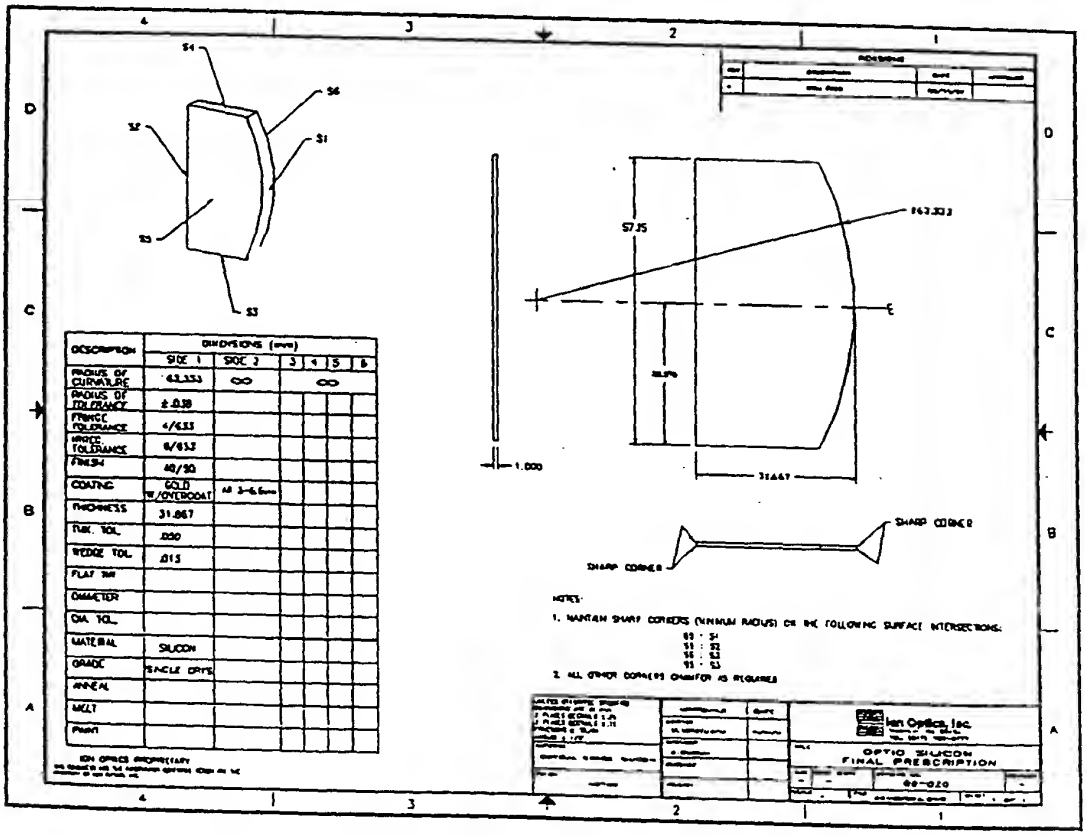

Figure 31 *Detailed drawing of optical bench ready for fabrication.*

The drawing package has been sent out for quotation. We intend to contract three vendors to build the assembly in stages.

1.) The silicon wafer and optical substrate fabricator will produce the silicon optic without the cylindrical optical surface and optical coatings.
2.) The lens fabricator will finish the cylindrical surface and AR coat the opposite flat.
3.) The grating fabricator will etch and gold coat the grating

At this point the Silicon Spectrometer Slab is complete and will be characterized for spectral resolution, through-put, and scattered light.

The goal of these three steps is to define a manufacturing process to maximize yield and operating characteristics.

3.2 Optical Chopper

A vendor has been selected and a quote obtained for five chopper assemblies based on the proof of concept prototype. The purchase order will be executed as soon as the final drawing package for the optical bench is released. This is anticipated to occur in June, 1997.

3.3 Detector Assembly

We have ordered a 64 element PbSe array from NEP and are currently evaluating the multiplexor. The characterization will be completed shortly. We can then place the order for the multiplexor and complete the packaging design. At that point, we will also begin the design of the data acquisition and signal processing circuitry. Delivery of the array will be in about 8-10 weeks.

3.4 Packing

The next major mechanical design task will be the case for the instrument. Particular emphasis will be placed on designing a low cost package that is easy to assemble.

3.5 Phase III Product Evaluation

To investigate commercial markets for this spectrographs we have contacted several spectrograph vendors, and started a market survey of users. To assist in this we have produced a preliminary spec sheet showing two embodiments of the device. The first is the handheld spectrometer and the second is the OEM bench. In the coming months we hope to refine these specs by contacting various potential end users and OEM customers.

4. CUMULATIVE COSTS

The cumulative costs for this PHASE 2 project is shown in the accompanying graph. Current expenditures are in line with projected cost to complete.

3.2 Optical Front End Fabrication

Due to the uniqueness of the design we have worked closely with our vendors to develop a fabrication plan that is consistent with the inexpensive mass production of the front end. This process was discussed in the last report. A brief summary follows:

Optical blanks. "D" shaped optical blanks are purchased from VA Optical, a silicon supplier. The near net shape will include all the polished flats but not the cylindrical surface.

Cylinder. The blanks will be sent to Digital Optics Corporation who will stack twenty parts into a monolithic block then shape the block into a cylinder lens. They possessed the interferometric equipment necessary to measure and produce the necessary surface on the cylinder mirror. They will gold coat the mirror and AR coat the flat.

Grating. The gratings will be built by Diffraction Limited. They will produce a grating in photoresist on the surface and etch it into the silicon. They will also work with the elements assembled in a stack. Once the grating is made they will add gold reflector overcoat and deposit the entrance slit.

Assembly. The part will be returned to Ion Optics where its performance will be measured. This is done by feeding the block with a lab spectrometer and measuring the quality of the output image with an IR camera. Once its performance is verified the device will be integrated into the housing with the detector and focused.

We have now placed orders with all three vendors. Although we had to rejected the first optical blanks supplied by VA optical due to surface defects, they have now delivered new devices that are much higher quality. Any remaining defects will be removed during the polishing phase of the processing. Computer Optics has fabricated a jig for holding the devices during processing. Using this jig, and scrap waveguide blanks, they are refining the polishing process. In the meantime, Diffraction Limited has been modeling the grating design and testing their etch process, again using scrap waveguide components. Successful processing of these the optical waveguide requires a close coordination between Ion Optics, Computer Optics, and Diffraction Limited. Communication between Diffraction Limited and Computer Optics has been hampered because of Diffraction's location in Waitsfield Vt. We are closely monitoring the progress of both vendors and have facilitated communication between them. However this issue, and problems Computer Optics has had in refining the machining process has caused a delay in the delivery date of the machined waveguides. While communicating frequently with our vendors, we have been working to both reduce the delay in the delivery of these components and its effect on the program.

3.3 Mechanical

The spectrometer design requires the precise alignment of the optical bench, the chopper, the detector array, filter, and input lens. This is all accomplished with a precision sealed package. The package holds the chopper, filter and detector in position and provides for a vacuum seal.

Introduction

Phase I demonstrated the feasibility of a compact, rugged, lightweight spectrograph operating at room temperature in the 2-to-5 μm wavelength range. The critical innovation is the spectrometer's completely solid state construction -- it can be assembled entirely from micromachined silicon components (even the MWIR detector arrays can be made of silicon). The resulting instrument has the advantages that it can be made very small and very light (about an inch in diameter and weighing a few grams), is permanently aligned for operation over a broad spectral range, and is extremely resistant to damage resulting from harsh environments (launch vibration, aggressive chemicals, radiation).

All critical spectrometer components were designed, built, and integrated into a working spectrograph in Phase I, producing an instrument which exceeded efficiency projections and confirmed the resolution predicted by ray-tracing models. Phase II's objective is to extrapolate this prototype to a rugged, lightweight, uncooled MWIR spectrograph applicable to ongoing and upcoming NASA/JPL program needs. These needs include remote sensing from airborne and satellite platforms, and planetary programs to measure water vapor (H_2O) and carbon dioxide (CO_2) in clouds, sulfur dioxide (SO_2) and hydrogen sulfide (H_2S) in volcano plumes, and frozen gases and organic compounds in borehole cores. The Phase II focus will be upon (1) improving the Phase I spectrometer design for better resolution, sensitivity, manufacturability, and smaller size, and (2) extensive testing and evaluation in cooperation with scientists at JPL, yielding a miniature, mass-producible device with better resolution and lower noise than its Phase I parent. Beyond its usefulness to NASA, the fully developed spectrometer is expected to excite extensive commercial interest for applications requiring a low-cost, compact chemical sensor.

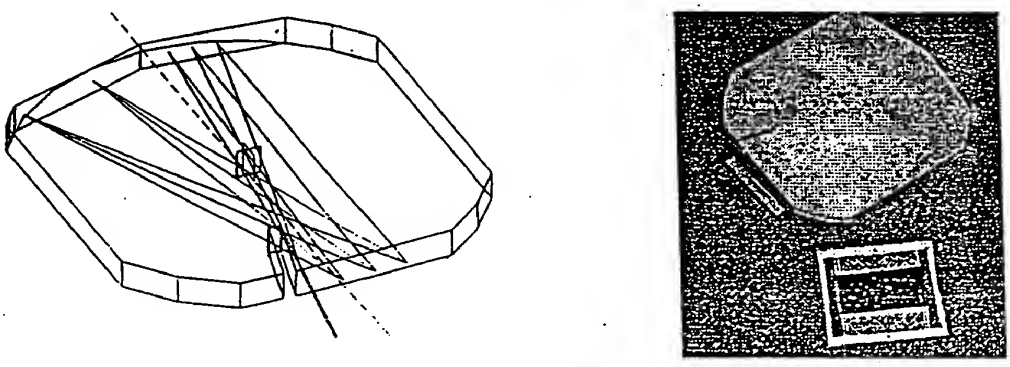

Figure 1 *In the Phase I proof-of-concept device, light enters the block, reflects off a flat fold mirror and is dispersed (and focused) onto the detector plane by a diffraction grating. The holographic grating (lying next to the block in this picture) is built on the surface of a silicon plano-convex lens. It has a variable line density, or chirp, to overcome the Rowland circle problem and flatten the focal plane.*

E 2

AMENDED SHEET

The silicon micro-spectrograph is a slab of high purity, optical grade silicon, with a holographic IR grating and linear detector array. This system will be lightweight, compact, rugged, alignment-free, calibration-free, and low-cost. During the third quarter of this project, we completed integration and test of a 3" prototype device with a 16-channel PbSe linear detector array. We were able to demonstrate clear resolution of molecular absorption/emission bands in the mid infrared.

Efforts to integrate the spectrometer test bed into a single package are underway. The package includes an optical bench, detector array, chopper and chopper driver, input optics and filter, 16 channel lock-in amplifier, high voltage drive batteries, and stand alone bar graph display. Detector output, previously fed into a PC via an A/D card, the digitally demodulated and displayed, is now demodulated via a dedicated 16 channel analog lock-in circuit and viewed on a stand alone bar graph display. The total spectrograph runs on two batteries and occupies the volume of a shoe box. Its compactness allows it to be easily carried and used in the field. This is emphasized by Ion Optics' recent demonstration of the spectrometer for Exxon/Chemical in Houston Texas, and its exhibition at the Boston SPIE conference.

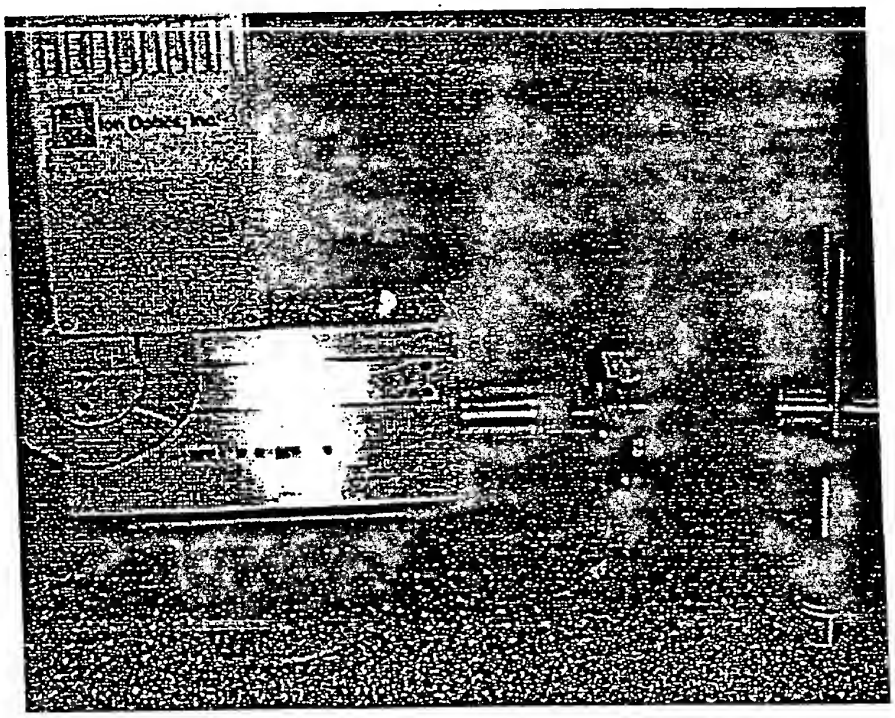

Figure 9 *A major internal milestone for the phase 2 program is an optimized 3" system to address stray-light and throughput issues identified in the phase I test results. In the 3rd quarter, we built a room temperature benchtop demonstration with an integrated 16 channel linear detector array, signal processing electronics, and an LED bar graph display.*

Already at this stage of integration, we have shown that a micromachined silicon device can achieve resolution and throughput comparable to off-the-shelf 1/8 meter monochromators which are

several times larger and heavier. Work this quarter has concentrated on design and component fabrication for the next generation prototype, about 1/4 the size of the device currently operating in our laboratory. An additional major activity this quarter has been the identification and quantitative evaluation of NASA mission requirements for a potential MARS rover instrument based on our infrared spectrograph.

2. Technical Accomplishments

We have completed the baseline one inch microspectrograph design and we are presently involved in detailed negotiations with vendors for specifications and deliveries of components required for this. We expect to place orders for these components during April and begin integration and test of the final phase 2 deliverable spectrograph. This superior design uses only two milled facets, with reduced size electronics and detectors.

The heart of the system is the all solid-state spectrometer-on-a-chip. (Figure 2) It uses a modified "Ebert" layout , fabricated entirely from micromachined silicon. It consists of a roughly "D" shaped silicon die with an entrance slit defined by thin film coatings. IR light crosses the slab (with the silicon acting as a waveguide) and is focused toward a diffraction grating by the cylindrical edge of the die. The chirped (variable line spacing), grating disperses the spectrum and images the source onto a flat focal plane where it is detected by a linear infrared detector array.

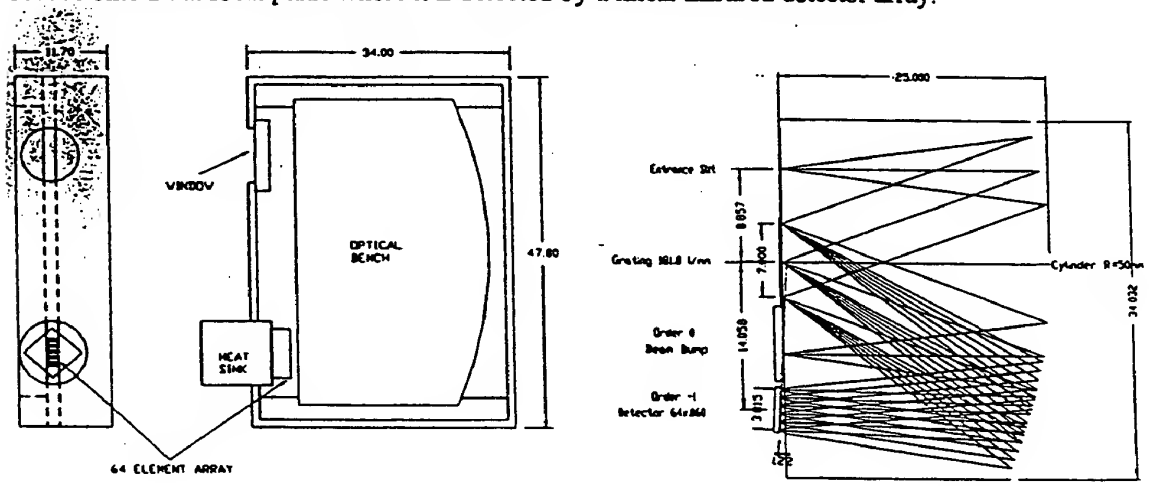

Figure 3 *Mechanical layout (left) and (CODE-V) ray trace (right) illustrate the operation of the miniature solid state optical bench. The entire assembly will be small enough to fit in a standard microprocessor chip carrier. The new design has fewer milled facets and incorporates built-in beam dumps for disposal of unwanted diffraction orders. The importance of these beam dumps was confirmed by our test results with the 3" prototype. They are implemented as AR-coated exit windows on the flat spectrometer entrance/exit facet. Dimensions are in mm.*

Applications for Mars Exploration

There is considerable topical interest in the content of Martian soils and sub-soil composition and particularly in establishing the presence or evidence of past water, carbonate minerals, or organic matter. Because of the problems of oxidation leaching in the near surface and the constant surface recovering by dust storms, it is extremely desirable to obtain composition and structure data at some depth below the surface. Typical procedures include sampling soil or core via drilling, extracting these samples and performing some sort of ex-situ analysis on the intact core samples. This requires specialized drills to extract the core samples, and even then, it is difficult to keep the core samples intact and to establish the sample orientation for measurement. We propose to enable downhole measurements which will extend the capability of these remote Martian probes with a tiny, rugged reflection analyzer instrument so small that it can make measurements from inside typical boreholes from soil and core sampling drills. The mid infrared waveband operating range of the phase 2 instrument should reveal the presence of many of the scientifically important CO_2 and H_2O along with Fe^{3+} minerals. This should also confirm the likely presence of hydrated minerals, anhydrites, and carbonates.

There are two critical innovations – a tiny (cm size) all solid state optical bench, and an electronically controlled, self stabilized blackbody radiator. (Figure 1) This instrument will provide complete spectral characterization of the surrounding soil media by allowing stratigraphic traces of specific infrared lines as a function of depth down the borehole. The combination of a pulsed blackbody source with the spectrometer has the advantage that, in addition to making reflection mode measurements of contaminant composition and concentration, it can also be used to measure thermal inertia of the surrounding media. Thermal inertia, the rate of heating and cooling following a measured thermal pulse, provides an important measure of the density of the surrounding media

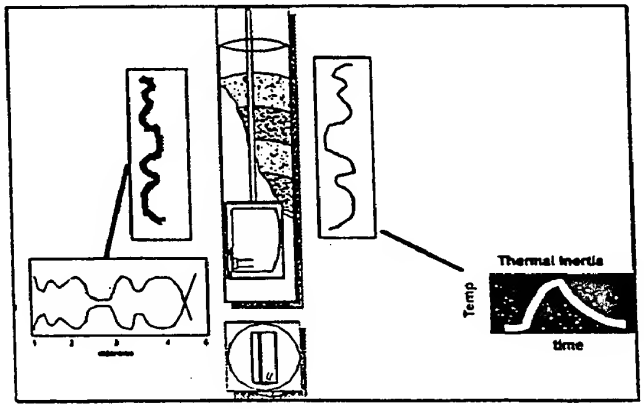

Figure 1 *Schematic of tiny infrared micro spectrophotometer arrangement for contaminant monitoring in boreholes. The miniature solid-state FTIR and pulsed infrared source allows spectroscopic measurement of spectral lines from specific contaminants as well as local measurements of thermal inertia and soil density.*

3. Layout and Component Selection for Final Phase II Deliverable Instrument

The manufacturing technique for the 1 inch spectrograph is being developed to facilitate quantity production. We are working with three vendors to develop a simultaneous multi element fabrication technique. Under this approach each vendor's contribution is optimized to effectively utilize their capital equipment, thus reducing fabrication cost. Under this approach, the raw silicon is purchased as silicon wafers from an electronic chip supplier; the advantage is that their standard electronic product is to a much higher surface finish then is normally available from optical manufacturers. Special optical grade silicon is used to meet our requirements (micro chip grade silicon is opaque in our wavebands). They will slice the wafers to near net shape with all the flat sides polished to the required finish. The wafers are shipped to the lens grinder, (who owns a cylinder generating machine). There they are stacked and clamped into a single monolithic block, to be shaped as if it were a solid lens. This finishes the entire block of 15 wafers at once. The gold coats and AR coats are applied and the block is forwarded to the gating vendor. The grating is etched into the monolithic block using a holographic transfer process. Finally the slit is applied, and the grating gold coated. The block is returned to Ion Optics for separation and integration with the detector array in the optics package.

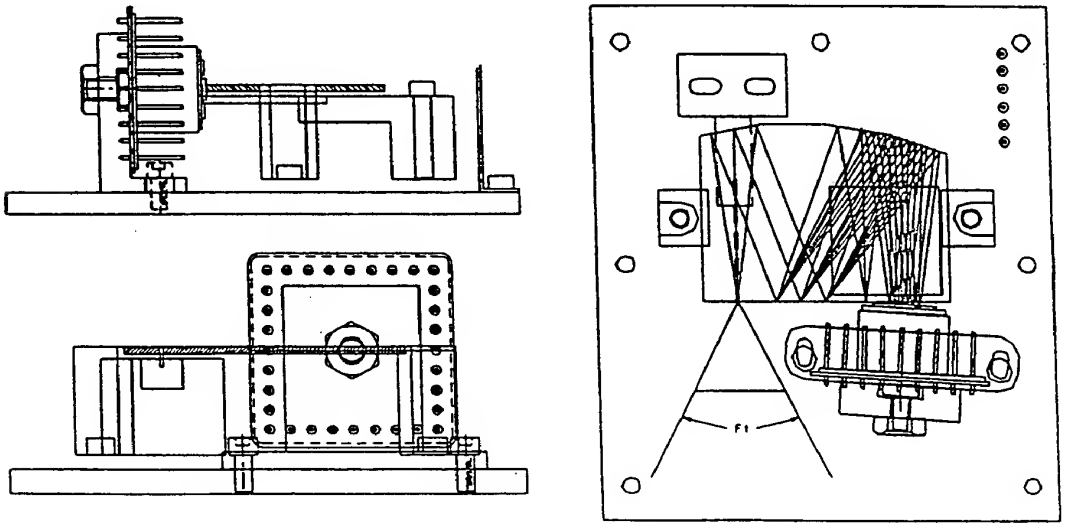

Figure 4 *Baseline mechanical layout for 1" spectrometer demo including focus, alignment and preliminary package and hermetic sealing details..*

4. Results of the Phase 1 project

We are developing a hand-held infrared spectrometer to measure the spectral emission of rocket plumes during test firings. This rugged, uncooled, field-instrument will fill an important need by providing laboratory-quality data on rocket plumes in the infrared emission bands. It will be useful not only as a diagnostic tool for engine performance but also for assessing the environmental impact (compliance) of new engine designs or different operating conditions. By measuring a complete spectrum and using neural net processing to reduce the data in real time, the finished instrument will be able to measure the concentration of NO_x constituents in a plume, despite the presence of water emission in the same spectral band. In Phase 1 we demonstrated the concept and showed that the optical measurement works. In phase 2 we will develop signal processing, analysis, and packaging required to build our sensor into a fieldable instrument. We expect that it will become a standard tool for propulsion research, not only for rockets but for high performance aircraft engines and for industrial process monitoring.

The new instrument will be about the size of a video palmcorder, containing a miniature infrared spectrograph, simple sighting and focusing optics, a control panel, and a flat panel display. A visible spotting scope boresighted with the spectrograph is used to train light from the plume onto the entrance window of the block spectrograph. The spectrum is dispersed onto a linear detector array covering the mid infrared gas emission band (2.5 - 5 μm wavelength). Signals from the array are preamplified, conditioned, and digitized so that a microprocessor with embedded data reduction software can convert the signal into a spectrum and extract concentrations of compounds in the plume. The result is then displayed on the instrument's LCD flat panel display.

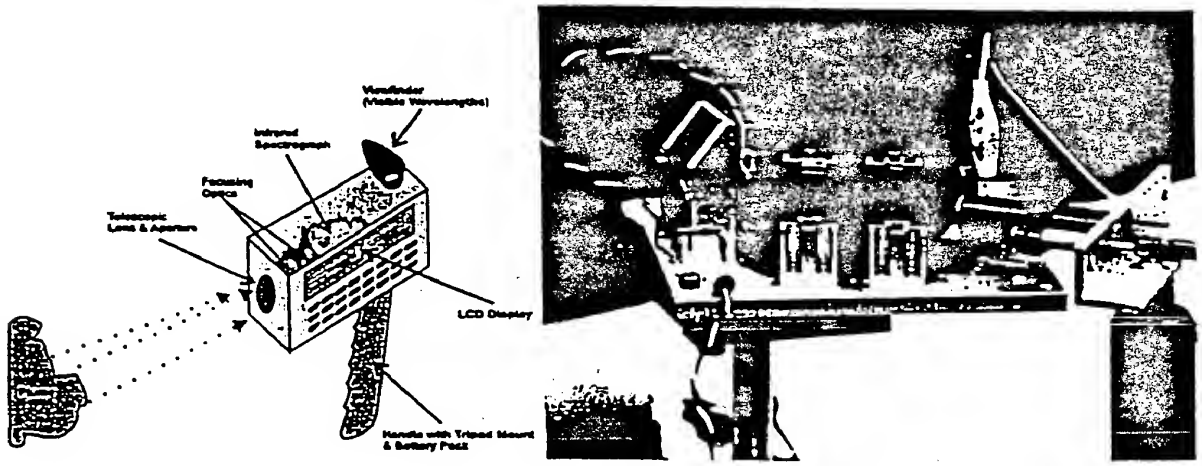

Figure 1 *Schematic illustration of compact, IR plume spectrometer (left). The phase 1 breadboard device (right) exceeded our performance predictions and successfully measured spectral lines from a 1 cm flame in our laboratory testing.*

F 4

As described in the phase 1 project summary, performance of the breadboard prototype has met or exceeded our design expectations and successfully measured spectral emission from test flames in our laboratory. The phase 2 brassboard prototype will, itself, be a useful diagnostic tool for engine work at SSC. It will also lead to a revolutionary new product for propulsion research and for on-line monitoring of industrial combustion and chemical processes.

At the heart of the system is the solid-state block spectrograph, fabricated entirely from micromachined silicon, which we demonstrated in Phase 1. It consists of a roughly square silicon slab. The entrance slit is defined by the gold coated grating and a baffle slot. IR light crosses the slab (with the silicon acting as a waveguide) and is reflected toward a diffraction grating by a flat-fold mirror. The chirped (variable line spacing), concave diffraction grating disperses the spectrum and images the source onto a flat focal plane where it is detected by a room temperature linear infrared detector array. Each component of the spectrometer: the slab waveguide, the fold mirror, and the reflective diffraction grating are made out of silicon and fabricated separately using standard microelectronics processing methods.

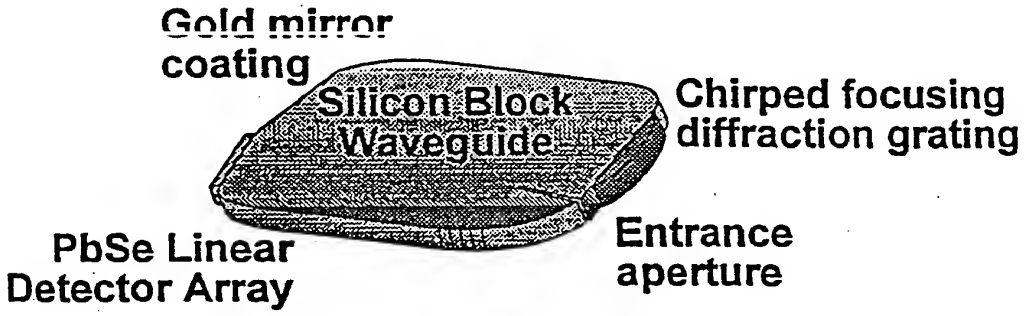

Figure 4.2 *Modular fabrication allows straightforward adaptation of this simple design to different wavebands and resolution requirements. The resulting sensor is rugged, permanently aligned, all solid-state; opaque to visible light and other interferences.*

The components themselves incorporate a number of advanced design features. In particular the diffraction grating is made with a variable line density or "chirp" to flatten the Rowland circle and provide a flat focal plane for the array. The slab waveguide is formed to include mounting surfaces for other components and includes baffling and beam dumps. Since the silicon is opaque to photons above its bandgap, the slab excludes visible light from the detector. Silicon's high refractive index provides lossless reflections at the polished top and bottom faces of the device, waveguiding the radiation in the plane of the device. However, more important, because of the high index of the silicon, the cone of incident illumination is dramatically smaller inside the device. This provides better optical throughput then can be achieved with an open-air design. In addition, for measurements at longer wavelengths, the entire spectrograph can readily be cooled on a single cold-finger, in much the same way that focal plane arrays are now cooled in conventional instruments.

F 5

AMENDED SHEET

PCT/US 99/17338
IPEA/US 29 FEB 2000
PCT/US99/07781

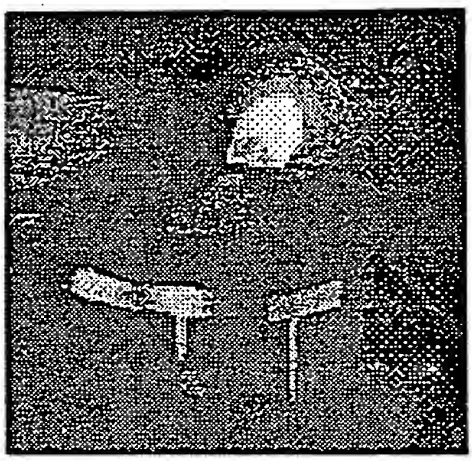

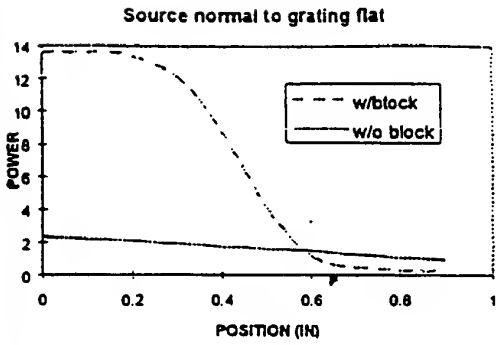

Figure 4.2 *The central innovation which makes this possible is the high-index slab waveguide. Refraction at the entrance slit sharpens the entrance cone and improved throuput, as shown in the thermal image and line scan data.*

4.1 Importance of this development for NASA

This instrument fills a gap in available field instrumentation for plume measurements -- a hand-held spectrometer capable of measuring the concentration of chemical species (CO_2, hydrocarbons, NO_2, N_2O, and HCl) present in rocket engine exhaust plumes. This is important to assure environmental compliance during test firings (for example, the Space Shuttle Main Engine (SSME)). Because the combustible mixtures in rocket engines are typically fuel rich, most of the active IR signature is caused by afterburning of the plume in the atmosphere.

In an era of increasing environmental consciousness, reducing greenhouse gas emissions and combustion by-products is an important part of engine design and optimization. In particular nitrogen oxides (NOx -- N_2O, NO_2, NO) are a natural by-product of high temperature combustion in rockets and in high performance jet engines. These compounds can be harmful to the ozone layer, so minimizing their presence in engine exhausts is a concern in the design of new engines for high altitude aircraft. The nitrogen oxides have strong infrared emission lines, but unfortunately, these are coincident with other prominent infrared emission bands, notably water and hydrocarbons.

F 6

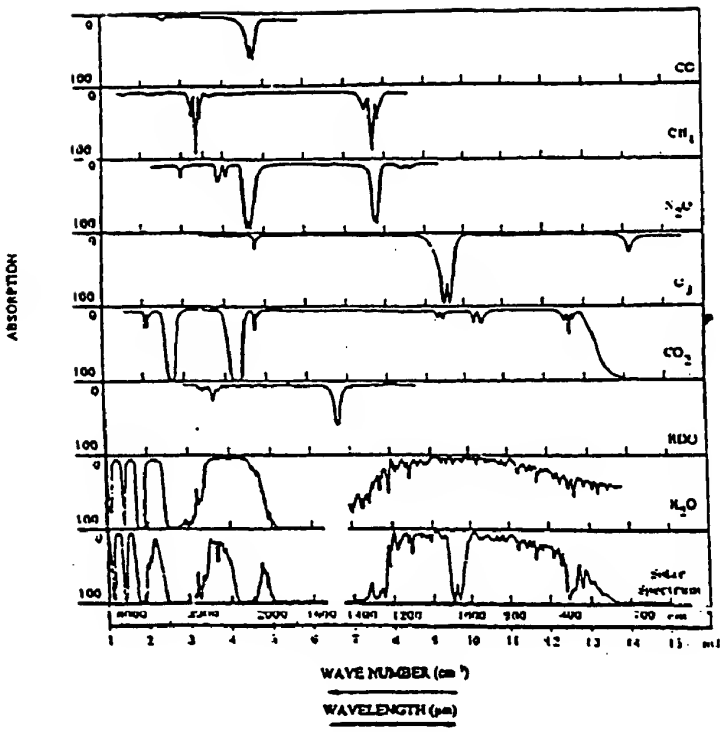

Figure 4.4 *The N_2O absorption/emission band, centered around 4.5μm, is near the edge of a water band. The harmonic band at 7.8μm is near a hydrocarbon line.*

The spectrometer will also be useful for engine performance testing (and environmental monitoring) of liquid propellant engines and hybrid motors burning hydrocarbon fuels. Typical fuel/oxidizer combinations of interest to SSC include RP1-JP/liquid oxygen (LOX) and polybutadiene hybrid engines. The resulting exhaust plumes have blackbody-like characteristics and contain CH_x, CO_x, and NO_x. These species are readily detectable by emission spectroscopy in the 2 to 8 micron range, thus the proposed spectrometer will function as a performance diagnostic for next-generation engines and motors employed on NASA's orbital and interplanetary flight vehicles, and perhaps for high performance air-breathing aircraft as well.

4.2 Phase 1 achievements and current project status

The phase I project consisted of three major related activities -- spectrograph optimization, spectrograph modeling/performance predictions, and breadboard device integration and test. Because of the possibility of detecting nitrogen oxides in the presence of interferences from other engine plume constituents, we have paid special attention to the stray light and optical signal-to-noise performance of the spectrograph in Phase 1. Stray light analysis and testing is important because a critical design feature of the plume spectrometer is its reliability and accuracy. To quantify the likely errors and evaluate potential self-referencing schemes, it is vital to understand the stray light performance of the instrument itself. To study the light budget,

Table 1 summarizes the results of stray light calculations. To realize a signal-to-noise (S/N) ratio of eighty, all the improvements indicated must be made to our basic spectrometer block. By far the most important, however, is adding a beam dump to reduce scattered background and zero-order light diffracted from the block. Ray tracing suggested that beveling and polishing the block between the mirror and detector facets will accomplish this without major rework of the basic design.

Table 1. *Summary of signal-to-noise ratio calculations*

Block Configuration	S/N ratio	Improvement in S/N ratio
Basic block configuration of phase 1 proposal	0.03	——
Polish and clad top and bottom surfaces, resulting in efficient total internal reflection and eliminating surface scattering	0.38	0.35
Blaze the grating	1.24	0.86
Apply antireflection coatings to eliminate reflections at the spectrometer input and detector facets	3.42	2.18
Add a zero order beam dump	78.41	76.23

In addition to projecting signal-to-noise ratios, ray traces were performed to study zero order diffraction and to locate the system focus. Paraxial calculation and ray tracing indicates a need to increase the optical power of the dispersing grating/mirror to improve system throughput.

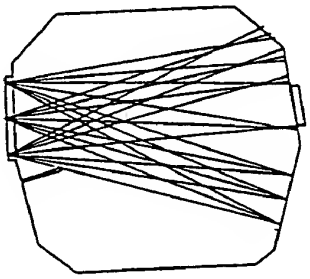

Figure 4.5 *One of the improvements suggested by the paraxial ray trace exercise was the addition of beam dumps. The sinusoidal grating diffracts unwanted orders into the top half of the block and are absorbed to eliminate scatter.*

F 8

AMENDED SHEET

An analysis was completed to determine the magnitude of the signal to noise ratio (SNR) for the PbSe detector for various temperture sources (where the noise refers to the intrinsic electronic noise of the detector). The signal analysis considered the source as a black body with temperature ranging from 300K to 350K. This was multiplied by the NA of the spectrometer, after conversion to effective FOV, and then by the smaller of the line width of the emissions of interest or the detector element size, to determine the spectral power available to the detector. We assumed a detector $D^*(\lambda)$ which is linear with wavelength (λ), and peaks at λ_{cutoff} of D^*_{max}. We used a λ_{cutoff} of 5μm, a chop frequency of 1 khz, and a D^*_{max} of $1x10^9$ cm-√hz / watt. From this, Noise Equivalent Power (NEP) is computed for the 2π field-of-view (FOV) and 300K background for which the D* is valid. Then SNR is the ratio of the signal computed in the first analysis to the NEP. A "correction" term is then applied to account for the transmittances of the optics and the fact that internal scattering and stray light from the entire range of wavelengths to which the detector is sensitive will also be impinging on the detector.

Finally, the SNR is plotted on a 3-D surface plot to show SNR as a function of both wavelength and source temperature, and the projection of the surface on the temperature wavelength plane, with color used to show the regions within the SNR is within specific bounds.

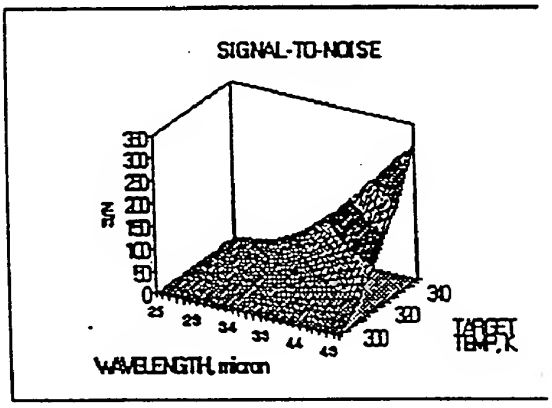

Figure 4.6 *Computed signal-to-noise achievable with the phase I breadboard device.*

Flame temperatures and corresponding emitted energy in the region of 4.45 μm are shown in the following plot. As may be seen, relative energy (at 4.45 μm) rises with flame temperature faster than as the square of the temperature (energy rise 2 orders of magnitude as temperature rises less than 1 order of magnitude), and faster still at the "lower" temperatures. At 3.5 μm, the rate of rise will be greater still. Hence, to get the equivalent signal from a 1-cm thick flame as from a black body of 315K, the flame temperature need be no higher than 1000-1200K. This is certainly on the low side of typical flame temperatures, and sufficient energy should be available for detecting the No_X emissions from a test flame.

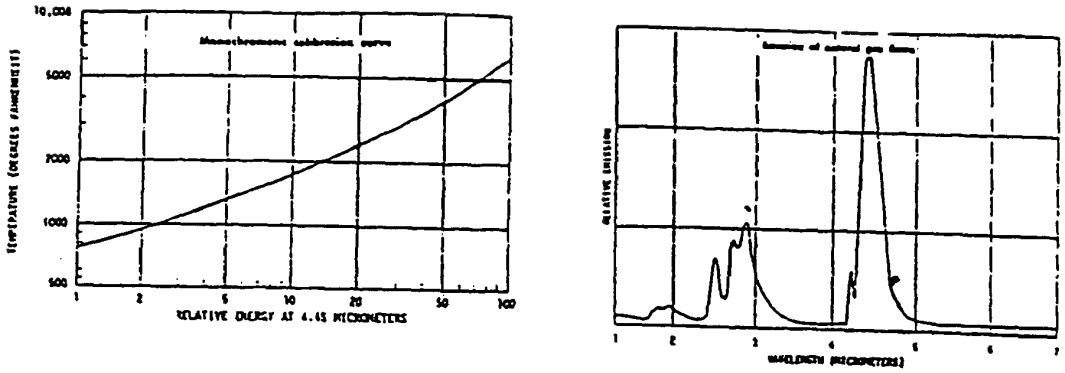

Figure 4.7 *Dependence of emission on flame temperature, and a representative spectrum. (From Bernard, Burton, abc's of Infrared, 1970, p.123)*

After building the solid state spectrograph components according to designs suggested by the ray-tracing and stray light analysis, we tested each of the components individually. The plot of transmitted power through the silicon slab (Figure 4.3) is an example of these measurements made to ring out individual components. In particular, we used an Agema ThermaVision camera to verify grating performance before the gratings were mounted on the spectrograph. The basic test setup is illustrated in Figure 4.8.

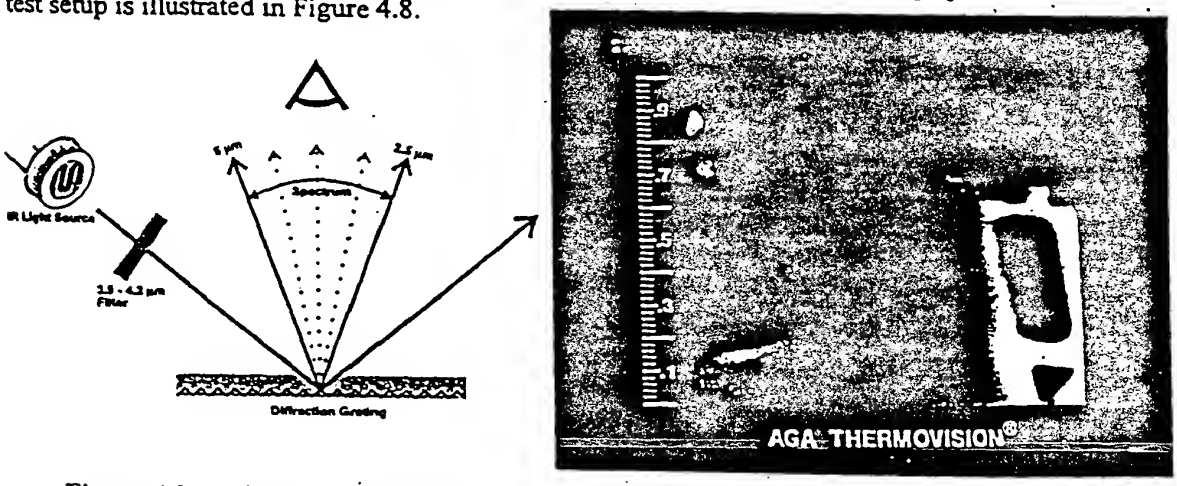

Figure 4.8 *A thermal imaging camera was used to check out the gratings under back illumination.*

For maximum sensitivity, a PbSe detector array was chosen. For initial testing before delivery of the PbSe array, thermal images of the detector plane were capturedand as well as manually scanned single pixel PbSe traces. The single pixel detector used a a micrometer drive and a single channel prototype of the final readout electronics. To extract maximum sensitivity from the PbSe detectors, both DC illumination from blackbody sources, and test flames from a

F 10

torches were collected through an external optical train with a 400 Hz tuning fork chopper. Preamplified signals were brought off the device on a ribbon cable to a computer A/D card. A simple synchronous detection scheme in software, for direct digital lock-in analysis of the PbSe signals was developed. Data acquisition software will command the board to sample each channel at roughly 20 kHz (depending on the number of channels configured for a given measurement.) Monitoring the trigger signal from the tuning fork chopper (which, itself, has a programmable phase delay), the software computes the HI and LOW integrals at pre-set delay times and average these over a pre-set integration time (currently baselined as 1 sec).

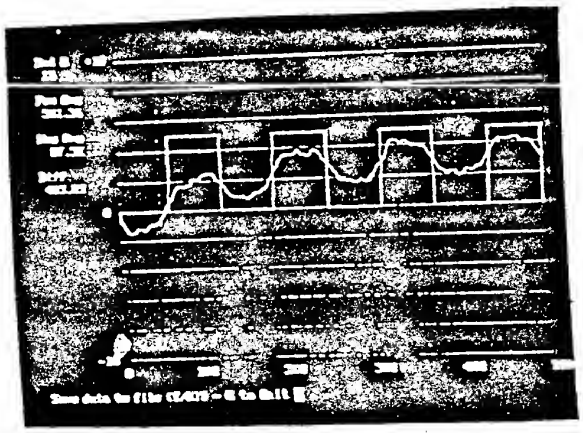

Figure 4.9 *Computer screen shows a typical image and signal-to-noise acheived from the digital lock-in program. Notice that the digital lock-in technique is rejecting both low-frequency (60 Hz pickup) and high frequency (1.5 kHz ringing) noise from the 400 Hz chopped signal.*

To facilitate stray light and efficiency measurements, individual modular components were mechanically clamped into position in the phase 1 test bed. A particular concern was the ability to move the mirror surface in order to avoid reflecting either the zero order or the -1 order beam from the diffraction grating. Actual integration of the optical components was done using laser alignment and infrared imaging techniques. Radiation was launched from a pulsIR black body source through the objective lens, chopper, filter and entrance aperture.

F 11

spectrograph itself and imaged into the spectrometer. Test 8 shows imagery of the output on the IR camera. In addition, we quantified these measurements with a single element PbSe detector positioned at the output plane. The 5 mm square detector was slid across the detector plane and the output amplified and fed into the A/D converter. Coherent detection was used to isolate the chopped frequency. Plots were created of a hot nichrome filament (black body), the same filament filtered through a 4 um peak filter, and a 2.7 um filter.

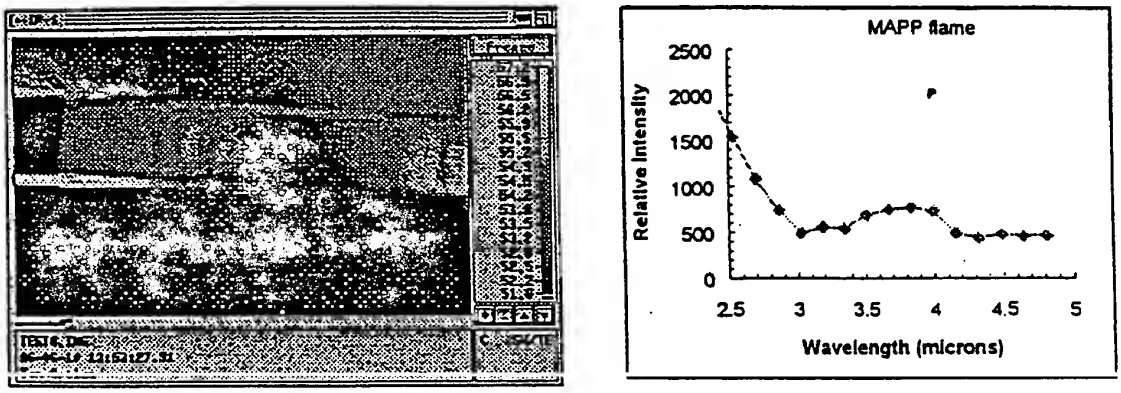

Figure 4.11 *Thermal image from IR camera shows a flame spectrum dispersed across the focal plane (left) and a micrometer scan from our PbSe detector (right). Two bright dots in the image correspond to the broad peaks in the discrete detector scan. At this resolution, water and hydrocarbon bands are clearly resolved.*

This test demonstrates that the phase 1 breadboard device met its signal to noise and spectral resolution goals. This clearly illustrates that the basic optical measurement design works and that this spectrograph can be the basis of a practical plume monitoring instrument for NASA. We believe it is also the basis of an exciting new commercial product.

5. Phase 2 Project Description

5.1 Technical Objectives

The goal of the phase 2 project is to make the successful phase 1 sensor into a successful plume monitoring instrument and ultimately into Ion Optics' next commercial product.

- Develop and test an "actual size" prototype spectrometer of approximately 1".
- Incorporate advanced neural network signal processing capability.
- Conduct extensive calibration and field tests in cooperation with SSC.
- Develop a marketing plan and commercialization strategy for the instrument.

5.2 Technical Approach

Ion Optics' approach to the Phase II program is ambitious but straightforward. We must address three major areas: miniaturization, spectral deconvolution, and field demonstrations. The phase I effort demonstrated that the basic optical measurement works. In phase 2, we must add signal processing and analysis to make useful plume measurements with this innovative device.

As described earlier, nitrogen oxides: N_2O, NO, NO_2 have absorption peaks which may overlap those of water vapor, carbon dioxide, and hydrocarbons. Water vapor in particular presents problems because its absorption peaks are broad and because it dominates the composition of the exhaust plume from the SSME. However since the spectrum for each of these compounds is known, we can use digital processing to deconvolute the spectrum by fitting the measured absorption spectrum with an iterative superposition of the individual spectra for each specie. We can increase accuracy by performing the fit for both the fundamental and first overtone absorptions. The spectrum we calculate from this superposition (of known spectra) method will give the best fit when the ratio of constituents is nearly identical to the actual composition in the plume. In order to perform the fit and subtract out the interfering spectra of water, CO_2 and hydrocarbons, we will team with experienced neural net processing experts at Neurodyne and at the MIT artificial intelligence laboratory.

For example, both NO and NO_2 have strong multiple absorptions in the range 1200-1800 cm^{-1}, a region of strong water vapor absorption. Each also has a weak overtone absorption in the 2900 cm^{-1} region where water vapor has no absorption. By fitting water vapor's known spectrum to the measured plume spectrum and adjusting the concentration and absorption strength to obtain the best fit, we can subtract out the water and fit the NO and NO_2 spectra to what remains of the measured spectrum. Because of water vapor's strong absorption in the 1200-1800 cm^{-1} range, there will be relatively little signal left after removing water and the fit may have much more uncertainty here than at 2900 cm^{-1}, even though the 2900 cm^{-1} absorption peak is relatively weak. In the phase 2 project, we will approach this problem with a combination of design improvements to improve the optical signal-to-noise performance and advanced signal processing to extract useful emission lines in the presence of interferences from other compounds.

5.3 Work Plan

5.3.1 Miniaturization

Compactness and light weight are, of course desirable in a hand-held field instrument. The phase 2 project will explore the practical lower limit of size for the silicon block waveguide spectrograph. The first consideration is the size of the detector array or, more accurately, the size of the detector pixels. We have seen that a typical lower limit on pixel size is 50 μm for the silicon microthermopile arrays. If we want to spread the wavelengths 3-5 μm over the detector array with a resolution of 0.01 μm, (10 nm) then we need 200 array elements. At 50 μm per element, the array would be at least 1 cm long. If instead of the silicon microthermopile array we were to use PbSe or InSb, then we might imagine a minimum pixel size of 5-10 μm, in which case the length of the detector array could be as little as 2 mm. This represents the minimal length of the detector plane facet of the block. So if we were to specify that the detector array occupy no

more than one quadrant of the block, then the block diameter must be at least 1.4 times the length of the detector array; which is just over $\frac{1}{2}$ -inch for a 1 cm long array.

The limits on the size of the focusing grating depend very much on the method of light injection into the waveguide. If we use a typical IR fiber as in the original design, then the fiber has a diameter of 250-400 μm, with a numerical aperture NA of ~0.2. This means that light exiting the fiber and entering the waveguide diverges very slowly, expanding from 250 μm to about 1 mm in a distance of ~6.4 mm. The grating should be large enough to intercept the entire beam at whatever distance from the fiber it is placed. For example, if the block is reduced to one-inch diameter and we maintain the 2:1 entrance path length to exit path length ratio, then the beam will expand to approximately 6 mm and the grating must be at least this large. However, we should remember that the focusing power of the grating is limited to ×2 by aberration and that therefore the focused spot size for a 250 μm fiber will be ~130 μm, covering several pixels and limiting resolution to about 0.03 μm for 3-5 μm spread over 200 pixels.

If light is coupled into the block waveguide using, then we can make the entrance slit any size suitable to our needs. Keeping in mind the 2:1 focusing power and the 50 μm pixel size, this would suggest an entrance slit of 100 μm in order to achieve 0.01 μm resolution for 3-5 μm with a 1 cm long, 200 pixel array.

We must also keep in mind the question of total internal reflection at the exit facet (detector plane) since this represents lost photons. If we use PbSe or InSb deposited directly on the silicon, then this is not an issue. If however we use the silicon microthermopile array, then the angle for total internal reflection is about 17°. This creates a relation between the length of the grating l_g, the length of the detector array l_d and the distance between the two d that is given by:

$$l_g \approx l_d < 2d \tan(17°)$$

For example, if the grating and detector array are both 1 cm long, then the distance between them must be at least 1.6 cm or about $\frac{5}{8}$ -inch to avoid total internal reflection at the detector facet. If the grating is larger or smaller (in length) than the detector, then the distance increases.

Flat Grating

We have used a cylindrical grating in our design to focus as well as diffract the light into its component wavelengths. The shorter the focal length, the more curved (the shorter the radius of curvature of) the cylindrical surface. This presents a challenge of processing if the grating is to be defined by lithography since it is nearly impossible to obtain a uniform photoresist thickness on a curved surface. For this reason it is desirable to develop a focusing grating on a flat surface. Ideally, we would use a holographic grating but such gratings are exceedingly difficult to design and fabricate. However we may be able to both focus and diffract the light with a flat grating similar to a Fresnel zone plate.[i] The question is, would we be able to fabricate the grating lines if

we reduce the size of the spectrograph? In the initial 3" prototype, the grating line widths were about 5 μm.

The radii for the zone plate are given by

$$\frac{m\lambda}{2} = \frac{r_m^2}{2}\left(\frac{1}{a} + \frac{1}{b}\right)$$

where r_m are the radii, λ is the wavelength of the light in the medium, a is the distance from grating to source, b is the distance from grating to detector, and m is an integer. If we assume a waveguide dimension of one-inch and maintain the 2:1 entrance path length to exit path length ratio, then the equation reduces to

$$r_m^2 = 1.69 \cdot m\frac{\lambda}{n}$$

in centimeters, where n is the index of refraction of the waveguide (n_{Si} = 3.4). For a one inch waveguide, the grating length (maximum r_m) could be no more than 1 cm. Then for a wavelength of 4 μm, m = 5029. This means the line spacing at its finest would be $r_{5028} - r_{5029} \approx 1.0$ μm. Though challenging, this is well within the capability of state-of-the-art lithography. Therefore, it is clear that we can reduce the size of the spectrograph to at least one-inch, possibly ¾-inch diameter when using a detector with 50 μm pixels. Shrinking the spectrograph further will mean making the detector pixels proportionately smaller (very possible) but should relax the lithography requirement since m is proportional to grating length squared.

5.3.2 Deconvolution

For a single species, it is straightforward to determine the concentration of gas in a plume by measuring either emission (or equivalently absorption over some known path). We demonstrated that our phase 1 optical breadboard can do this, without any additional signal processing. In phase 2 we will address the real-life situation with multiple species and the consequent need to both recognize which species are present and then determine the absolute concentration of each species. This is also a general problem faced by IR spectroscopists and instrument designers working with multiple sensor or transducer inputs. Following earlier work in the literature, References [Hashem, 1994; Lewis, 1995], we will team with the neural network experts at Neurodyne to apply neural network processing to solve the deconvolution problem.

The ability to extract concentrations from emission spectra is severely constrained by both chemical and instrumental factors when either a narrow spectral region, or only a few wavelengths are used for the measurement. The intent is to avoid or mitigate the influence of these problems by acquiring high resolution, detailed spectra with good signal-to-noise.

Spectral information can be very useful for characterizing multi-species environments. However this information is usually buried in thousands of variables captured over a wide range of wavelength. Chemometric methods attempt to separate the useful information from noise and redundancy by determining relevant correlations in the data. There are two fundamental steps in these approaches. The first is the compression of data and the second is the extraction of interesting characteristics.

F 16

Data Compression - *Principal component analysis* (PCA) addresses the compression of data and removal of noise. Using eigenfunction decomposition, a set of mutually orthonormal vectors (also know as factors or loading vectors) that span the spectral data are determined. These vectors can then be ordered according to the amount of variance captured. A subset of these vectors which capture a desired amount of variance is retained. By projecting the original data set upon this subset, the dimensionality of the data can be reduced while capturing a significant amount of the variance.

The feature extraction methods vary from simple linear regression [Wold, et al., 1987; Lorber, et al., 1987] (e.g. PCR, ridge regression) to nonlinear function approximation [Qin and McAvoy, 1992; White, 1995; Sanger, 1989] (e.g. neural networks). Our plan is to investigate three basic approaches; PCR, PLS and neural network based learning algorithms. A mathematical description of PCA and related methods can be found in [Jackson, 1981; Jolliffe, 1986; Wold, et al., 1987; MacGregor, 1989].

As shown in Figure 5.1, coordinates x_1 and x_2 indicate two zero-centered measurement variables with sampled data represented by the black points. The projections of the standard deviation of the data, σ_1 and σ_2 onto vectors v_1 and v_2 provide information regarding the natural coordinates of the data. By rotating the original axes x_1 and x_2 onto the more natural coordinates v_1 and v_2, an orthogonal space is found where the primary axes align along the directions of maximum variance. In the shaded example, the experimental data indicates a linear relationship between the two measured variables x_1 and x_2. By rotating the coordinate system along the direction of maximum variance in the data, the two measured variables could be well-represented by one variable v_1. PCA provides the direction of the maximum variance in the data and compresses the dimensionality of the data from 2 to 1.

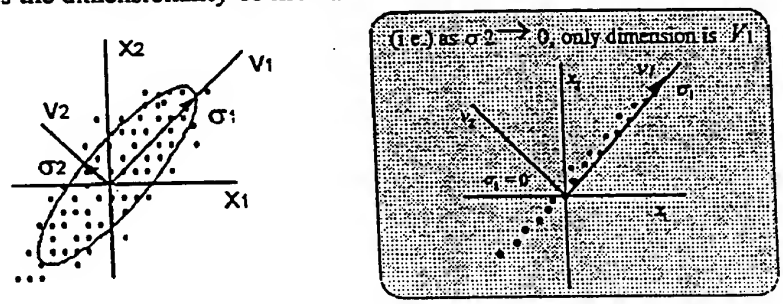

Figure 5.1 *Principal Components Analysis*

Once the principal components are determined, subsequent measurements can be projected onto the natural coordinates or principal components to reduce dimensionality. Once these projections are complete, the components can be plotted to determine linear correlations in the data or indicate variables which may be truncated.

An example of such a correlation using a polysilicon etch in a plasma reactor is provided in Figure 5.2. Each point represents a particular operating condition from a design of

PCT/US 99/17338
IPEA/US 29 FEB 2000
PCT/US99/07781

experiments. PCA was performed on the data and the first few components were found to account for 96% of the variation in the data. Projections of the optical emission spectral measurements onto the first two principal components indicates clustering along %HBr feedgas ratios labeled next to each point. In Figure 5.3, a secondary ordering is shown along magnetic field orientation. This is an example to indicate the ability of PCA in spectral data analysis. There are a number of more advanced methods which combine linear regression and neural networks to extract useful data from complex spectral measurements.

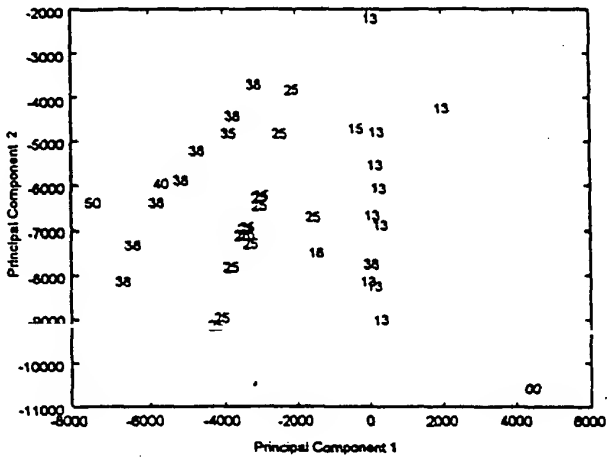

Figure 5.2 *Optical Emssion Spectral Projections by Gas Flow*

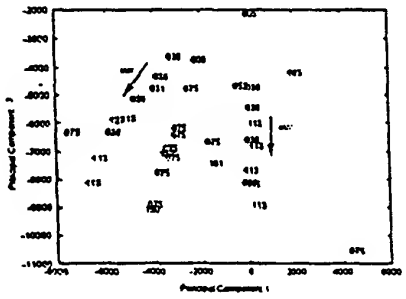

Figure 5.3 *Optical Emission Spectral Projections by Magnetic Field Orientation*

In most applications of PCA [7, 15, 9], it is desired to reduce the dimensionality and complexity of n-dimensional space to that which enables easier classification of the data. This is done by effectively rotating the $r \times n$ data matrix M onto the new orthogonal basis spanned by n eigenvectors of the $n \times n$ covariance matrix C=cov(M). Finally the eigenvector matrix of C, also referred to as principal components, is shown to transform the matrix M to an orthogonal matrix T of scores which have no cross-correlation and reduce the dimensionality of M.

F 18

In general, the $r \times n$ matrix of raw data L is formatted such that each element L_{ij} is the jth measurement over n total variables measured during the ith run over r total runs. The $r \times n$ raw data matrix L is mean-centered to produce the $r \times n$ data matrix M where the elements

$$M_{ij} = (L_{ij} - \bar{L}_j) \text{ for } 1 \le i \le r \text{ and } 1 \le j \le n \tag{1}$$

are mean-centered using the sample mean $\bar{L}_j$ of each column (or channel) j over the total number of experimental runs (r). The $n \times n$ sample covariance matrix C measures the dependence between variables of mean-centered matrix M can be written as

$$C = \left(\frac{1}{r-1}\right) \cdot M^T M \tag{2}$$

The eigenvectors of the covariance matrix are linear combinations of the original variables that represent orthogonal components of the variance in the data and are referred to as principal components. The right eigenvectors of the covariance matrix C can be calculated by solving the equation:

$$CV = V\Lambda \tag{3}$$

where $V = [v_1 \quad \cdots \quad v_n]$ is the $n \times n$ matrix containing n eigenvectors and Λ is an $n \times n$ diagonal matrix of eigenvalues. In equation (3), each n dimensional eigenvector v_j corresponds to the jth eigenvalue λ_j. Once calculated, the associated eigenvalues and eigenvectors are ordered in a descending manner such that $\lambda_1 \ge \lambda_2 \ge \ldots \ge \lambda_n$. Therefore the eigenvector v_1 associated with the largest eigenvalue λ_1 of C indicates the direction of maximum variance and the eigenvector associated with the smallest eigenvalue indicates the direction of minimum variance. The variance in any direction v_j may be measured by dividing the associated eigenvalue λ_j by the sum of the n eigenvalues or the trace of covariance matrix C.

$$\% \text{ variation in eigenvector } (v_j) = \frac{\lambda_j}{\sum_j \lambda_j} \cdot (100) = \frac{\lambda_j}{trace(C)} \cdot (100) \tag{4}$$

$$Mv_j = t_j \text{ for } 1 \le j \le n \tag{5}$$

If we project M onto the eigenvector v_j of the covariance matrix C we obtain an r-dimensional vector called a score t_j. If we project M onto the eigenvector matrix V, we obtain an $r \times n$ matrix T composed of n such column vectors. This transformation produces a new representation of the data. By projecting M onto the basis vectors in V, the new matrix T has orthogonal columns and retains all of the variance Λ in M:

$$MV = T \tag{6}$$

F 19

$$(MV)^T MV = T^T T \tag{7}$$

$$V^T M^T MV = T^T T \tag{8}$$

$$(r-1)V^T CV = T^T T \tag{9}$$

$$V^T V\Lambda = \left(\frac{1}{r-1}\right)T^T T \tag{10}$$

$$\Lambda = \left(\frac{1}{r-1}\right)T^T T \tag{11}$$

Since the principal components or eigenvectors of C are ordered along directions of maximum to minimum variance, the column dimension n of matrix V can be reduced to a more manageable number while capturing as much variance as possible. For example if the y most significant principal components or eigenvectors (e.g. y=4) capture 99% of the variation in the data we could reduce the n x n eigenvector matrix V to an n x y matrix $\hat{V}$. Data matrix M can then be projected onto these principal components reducing the measured data from an r x n matrix T to the r x y matrix, $\hat{T} = [t_1, t_2, \ldots, t_y]$.

$$M\hat{V} = \hat{T} \tag{12}$$

As with matrix M, the rows of $\hat{T}$ correspond to experimental runs 1 through r. The vectors of scores 1 through y represent the majority of variance in the data while reducing the column dimension by (n-y).

Feature Extraction - The feature extraction methods vary from simple linear regression [Wold, Kowalski] (e.g. PCR, ridge regression) to nonlinear function approximation [White, McAvoy] (e.g. neural networks). Our plan is to investigate three basic approaches; PCR, PLS and neural network based learning algorithms.

Principal Component Regression (PCR) and Partial Least Squares, (PLS) Methods Both PCR and PLS begin by using PCA to determine the orthonormal vectors that span the spectral data. The subset of these vectors are mapped to spectral characteristics (e.g. species concentrations) using regression. Using PCR, an ill-conditioned matrix of spectral data can be reduced to a subset of principal components and then fit to concentration or process variables. Partial Least Squares (PLS) generates a subset of orthogonal vectors for not only the spectral data but for the concentrations as well. PLS rotates the spectral and concentration factors in order to optimize the regression fit from the measured spectra to concentrations.

Both PCR and PLS utilize the decomposition of a matrix of input data X and the linear regression of output data matrix Y upon X.

$$Y = XB + e \tag{13}$$

In PCR, X is transformed by the orthogonal matrix of eigenvectors of $X^T X$ to a matrix of scores T (as shown in equation 6 above).

$$XV = T \tag{14}$$

The matrix output matrix Y is then regression upon the reduced subset of scores, $\hat{T}$. To accomodate the variance in Y, PLS weights the covariance matrix by the addition of positive definite matrix YY^T to $X^T X$, providing a new covariance matrix $X^T YY^T X$. In this new form, those elements of Y that are close to zero reduce the effect of associated rows of X and thus we do not try to predict noise [6]. The addition of Y containing elements that are close to zero (e.g. noise) results in the associated rows of X to not be used [6]. In this case, the weighted covariance matrix is decomposed into a matrix of eigenvectors, R and eigenvalues, D.

$$X^T YY^T X = RDR^T. \tag{15}$$

The matrix X is then transformed using the eigenvector matrix R to an orthogonal matrix of scores, T as described in (2) above. The output matrix Y is then regressed upon T, as performed in PCR.

In terms of the physical interpretation of PCA, PLS involves the rotation of the components of X and Y such that the resulting distance is minimized. This is accomplished by iteratively regressing on the selected components of X and Y and stopping when the components of X are no longer near those of Y.

Nonlinear Relationships Between Measurements and Concentrations There are often nonlinear relationships between spectral data and characteristics reflected in species concentrations, the influence of plume temperature noted above is a good example. In order to fit these relationships, a nonlinear function approximation method (e.g. locally weighted regression, polynomial networks, multi-layer perceptron networks) may be used. Often these methods are lumped into the general class of neural network or learning algorithms. Perhaps the most applicable learning algorithm to the application described herein are spatially localized learning algorithms. The most generic form of training a multilayer perceptron (MLP) network uses gradient descent where the weights are adjusted proportional to the derivative of error between the actual output and target values. This approach can best be visualized as a ball traveling along a bowl shaped surface along the steepest direction until the minimum is achieved.

Locally weighted regression is a function approximation method used with memory based learning [Cleveland and Delvin, 1988; Atkeson et al, 1995]. The training data for the learning algorithm is simply stored in memory. When a query is requested, locally weighted regression is done about the query point to make a prediction. For nonlinear modeling we assume that there is a locally linear model (holds in a spatial locality about the given query point). Global regression implicitly weights each data point equally in the regression. In local regression each data point is weighted according to its distance from the point being queried. Since only the points in the spatial neighborhood of the query point contribute strongly to its prediction, this method can accurately model globally nonlinear functions. Note that global regression is cheap because the

model parameters are solved once for all future queries where local regression is more expensive because new weights and a new solution for beta is required for each query. There are methods of making this computation efficient, however [Deng and Moore, 1995].

Multi-Layer Perceptron Neural Network - Although there exists several nonlinear function approximation approaches to select from, several neural network approaches have demonstrated benefits over traditional regression techniques in several semiconductor applications [3,5,9,14].

Often referred to as a neural network, this method uses a multilayer perceptron connectionist network with a backpropagation learning algorithm to fit multivariable data. Although basic knowledge regarding gradient descent based learning algorithms is necessary, the neural network offers an advantage over many nonlinear function approximation approaches in that one need not know much about the structure or order of the mapping. The most generic form of training a multilayer perceptron (MLP) network uses gradient descent where the weights are adjusted proportional to the derivative of error between the actual output and target values. This approach can best be visualized as a ball traveling along a rough bowl shaped surface along the steepest direction until a minimum is achieved.

There are many forms of backpropagation learning, most developed to speed convergence. In our approach, weight updates are achieved through Levenberg-Marquardt optimization [4] adapted for use with the MLP architecture. (A more thorough analysis of model based estimation and optimization using neural networks is provided in [14].) As with any learning algorithm, MLP networks can be overtrained thus reducing the generalization capabilities. To prevent this, leave-one-out cross validation can be used to achieve sufficient generalization.

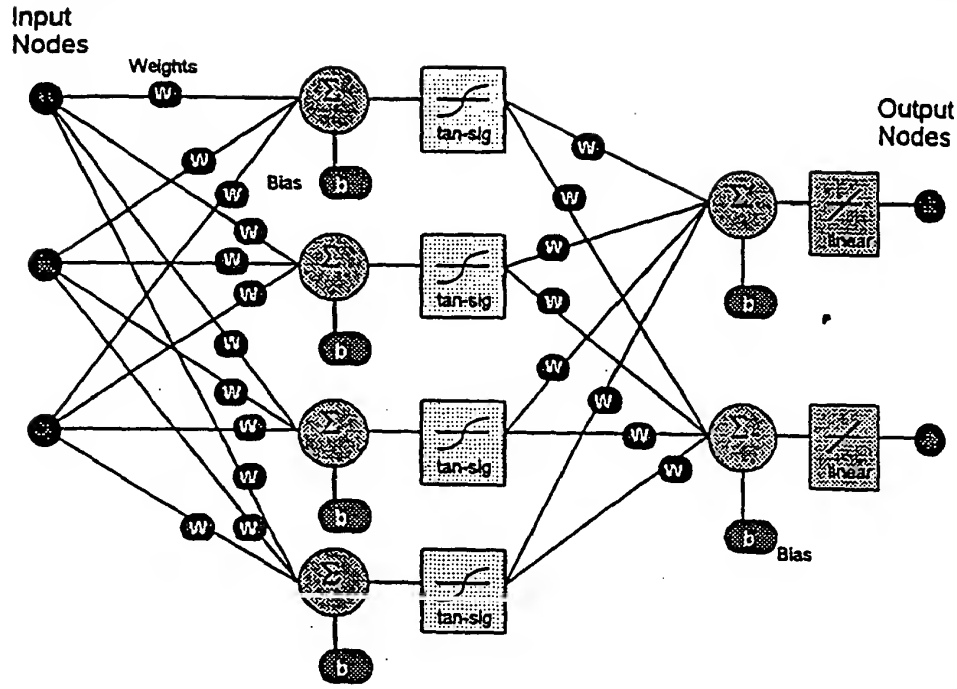

Figure 5.4 *Multilayer Perceptron Architecture*

5.3.3 Packaging and Instrumentation

The thrust of this Task will be to solidify system and sub-system designs and fabrication procedures with respect to producibility or adaptability to cost-effective production. While a large part of the design analysis will have been performed in previous tasks to optimize system performance, this task will re-evaluate the system with emphasis on how readily the design lends itself to high volume fabrication, manufacturing, and assembly. It is entirely possible that the best design from a performance standpoint will be compatible with volume manufacturing, while it is also possible that compromises will be required to make an effective and producible system. This evaluation will be carried out in conjunction with industrial partners, potential customers, and finally with the relevant outside vendors.

As an adjunct part of this activity, to be funded by the company, we will conduct market research, which we will expand and revise as the system becomes more fully developed and refined. At the time of the writing of this proposal the largest short-term commercial potential appears to be with the simple spectrograph which can be incorporated into many existing IR sensing systems. This has the appeal that there is an existing market of equipment manufacturing companies with established customer bases who have shown an interest based only on our

preliminary results. Ultimately we may choose to bring the complete instrument system to market, but in the short-term we will be more effective in providing them with this breakthrough spectrograph. Options for production-scale fabrication, marketing, and distribution will be investigated. Revenues from sales of the spectrograph, hopefully initiated before the end of Phase II, will solidify the Ion Optics business base, and support the aggressive development and commercialization of infrared sensors and instruments.

5.3.4 Calibration and Accuracy

Establishing NIST traceablity for the instrument will be a critical stage in the development and acceptance of our plume spectrometer. NIST's Radiometric Physics Division, in keeping with its charter to promote accurate and useful radiation measurement technology in the UV, visible, and infrared spectral regions, takes an active role in pyrometry and spectral radiance calibrations and the preparation of calibration protocols. We plan to utilize the Division's personnel and facilities to relate total and spectrally resolved *puls*IR output to those of a NIST reference blackbody, thus establishing traceablility to the source used to certify the secondary standards employed by instrument manufacturers and calibration laboratories.

To accomplish this, Ion Optics will coordinate with NIST to produce a calibration plan whose objective is to develop the pulsIR flat-pack as transfer standard. This will require working with personnel in the NIST laboratories, revising the plan to incorporate their recommendations, and finally resubmitting it to NIST for final review and approval. The approved certification plan will then be carried out in the appropriate facilities in the Physics Division's laboratories.

These facilities include a high accuracy cryogenic radiometer (HACR) whose intrinsic uncertainty is 0.01% or better (one sigma) over the range 0.2 to 11 μm; it serves as the basis for most of the calibrations offered by the Division. While the HACR is extremely accurate and widely employed to characterize the absolute spectral response, spatial uniformity, and linearity of photodetectors, the low background infrared (LBIR) facility (Figure 5.5) is likely to be the facility of choice. Using an absolute cryogenic radiometer capable of measuring irradiance at its aperture from a few nW/cm^2 to 10 $\mu W/cm^2$ with better than 1% uncertainty (two sigma), the LBIR provides accurate calibrations of IR sources, spectrophotometers, and low background detectors over the range from 0.2 to 25 μm.

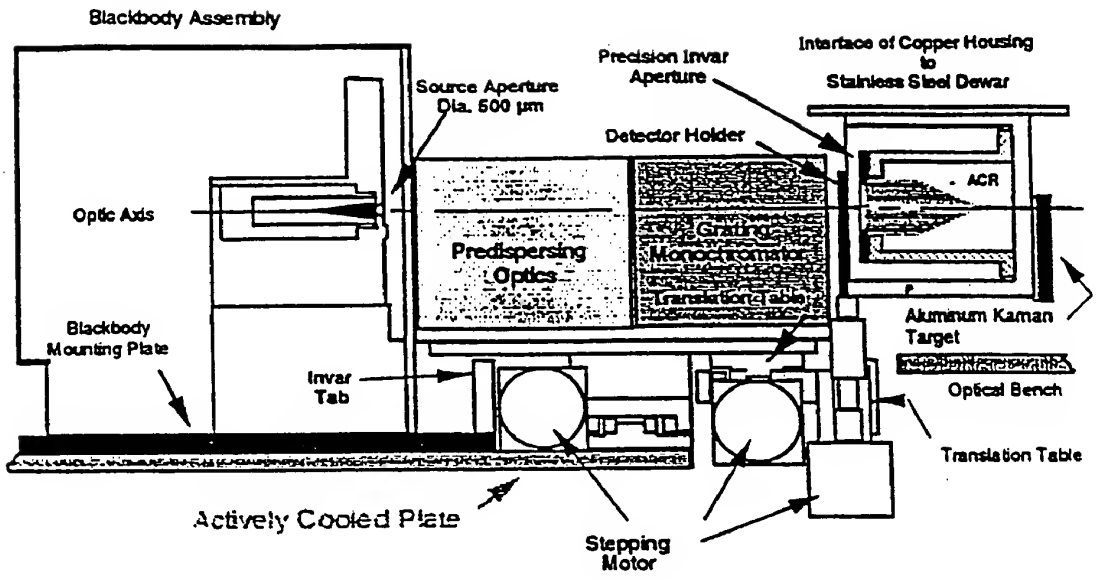

Figure 5.5 *A cross-sectional view of the low background infrared facility, its blackbody, and its absolute cryogenic radiometer.*

5.3.5 Brassboard Device Integration and Test

The assembled system will be subjected to a series of tests to validate its accuracy and reliability. To the extent possible, we will work with other organizations to achieve an absolute wavelength and intensity calibration of the system against secondary sources and NIST-traceable references. Stability tests will consist of measuring the system's response to known samples under controlled laboratory conditions and then subjecting the system to vibration, thermal cycling, and pressure changes. Throughout these environmental variations the systems response to the constant sample will be recorded and compared to the initial indication.

As an evaluation of the system's stability, these measurements will be performed continuously over a period of several weeks. Measurements performed under identical conditions will be compared to evaluate system stability. Based on the results of these evaluations, the design of the individual components, their assembly, and the packaging will be re-evaluated and modified as necessary.

After the iterative component and system analysis has been completed, the refined prototype system will be demonstrated in an actual field test. This test will consist of installing the instrument at SSC. By mounting the prototype system next to established monitoring equipment, we will be able to verify its reliability and accuracy for use as a sole source of information in plume testing on actual engines at SSC.

The most important part of the Phase II effort will be demonstration of the capabilities of the instrument, particularly in field trials. We will work with SSC and other potential customers to arrange for actual tests in the laboratory and in on-site tests. As illustrated by the attached

PCT/US 99/17338
IPEA/US 29 FEB 2000

1. Introducti n

NASA has a need for low-cost, low-power, low-mass, highly integrated spectral data acquisition instruments that enable data acquisition and feed back control from both ground based testing facilities and on spacecraft. We are building a novel, monolithically integrated, infrared micro-spectrograph. It is fabricated from silicon to address this need. This device will incorporate the silicon micro spectrograph, simple focusing optics, and an electrical interface for power input and remote readout. The silicon micro spectrograph is a slab of high purity, optical grade silicon, with a holographic diffraction grating and linear detector array monolithically integrated right on the surface. This system will be lightweight, compact, rugged, alignment-free, calibration-free, and low-cost. During the first quarter of this project, we have modeled and redesigned the 3" prototype device into a 1" device with improvements providing 4 times the resolution and sensitivity of the Phase I instrument. We have completed the design modifications and are preparing for the fabrication of the first test beds.

Already at this stage of integration, we have shown that a micro machined silicon device can achieve resolution and throughput comparable to off-the-shelf 1/8 meter monochromators which are ten times larger and heavier. Work for the next quarter will concentrate on fabrication of the next generation prototype, about 1/4 the size of the device currently operating in our laboratory.

2. Technical Overview

This past quarter has seen the re-evaluation of the Phase I design, determination of its week points and the development of an improved design. The process we followed to achieve this included: modeling the spectrometer system to determine minimum detectable signal strengths, determining the spectral bandwidth over which the system must operate, and determining minimum spectral resolution requirements. We have conceived and developed a new design for an easier to manufacture optical bench. After ray tracing and optimizing the optics, we have achieved a factor of 4 improvement in optical throughput. We have also finalized the selection of the detector array, developed a miniature integrated chopper design, and developed a fabrication plan with our vendors.

3. Technical Accomplishments

Significant progress has been made since the start of the program. System modeling, optical redesign, detector selection, fabrication procedures and preliminary mechanical housings have been developed. A detailed discussion of our accomplishments follow.

PCT/US99/07781
IPEA/US 29 FEB 2000

3.1 Reevaluation of Phase I Spectrometer

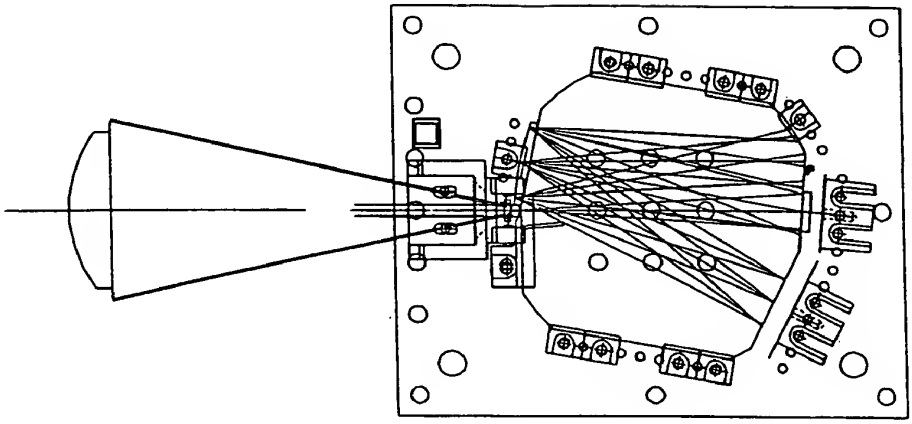

Figure 3.1 Phase I optical bench and lay out showing input lens, silicon slab, grating, detector plane, chopper, and filter.

The Phase I block spectrograph was reevaluated to uncover the lessons learned and to find areas of improvement for the Phase 2 miniaturization redesign. The following lists some of the key points:

•*Size* - The Phase I design is too large, does not provide an advantage over more conventional designs, and is relatively complex and expensive to manufacture.

•*Facets* - The Phase I block had 4 active facets, which were at precise odd angles to one another, two of which require AR coating.

•*Fabrication* - The Phase I design called for the grating to be fabricated onto a cylindrical surface whose radius was smaller than the block. This proved impossible to fabricate, since it would require acute inside corners in the silicon block. In the Phase I design we solved this problem by applying the curvature to an external piece and contact coupling it to the block. This functioned correctly but proved to be lossy and provided reflection ghosts in the system.

•*Grating Design* - The design utilized a chirped grating to flatten the image field of the Rowland circle optical design. This required an expensive holographic setup. The curvature of the grating substrate made it difficult to etch the grating into the silicon uniformly, resulting in uneven optical efficiency across the grating.

•*Readout Electronics* - The 16 channel lock-in amplifier of the Phase I device was superior in performance to the digital lock-in initially used. However it required two 4" x 6" PC boards, much too bulky for th Phase II miniature device.

•*Chopper Design* - The tuning fork chopper used in the Phase I device has magnetic coil drivers, which radiate EM interference. This interference is at the chopping frequency and can not be filtered from the signal. This is an intrinsic short coming of the tuning fork design.

•*Light baffle* - The internal baffle cut in the block proved to be a tremendous scattering sight, greatly increasing the background radiation reaching the detector and reducing the optical signal discrimination.

•*Entrance Slit* - The entrance slit, built from a separate piece of machined aluminum, caused scattering from its edges, contributing to the background noise.

•*AR Coatings* - The system requires anti reflection coatings on its entrance and exit facets, this will reduce the losses by 50%. However since the facets are at odd angles this could be difficult and expensive to accomplish. Since the detectors are contact coupled to the silicon, special matching AR coatings must be devised to match the detector to the silicon index. This is a development task of its own.

These factors along with the discoveries we made from the system model were used to design a new spectrometer lay out and detection system, whose advantages are discussed in section 3.5.

3.2 System Modeling

A system model was created to determine the detectivity of the system. The basic question to be answered was how much radiance must the target provide in order to be detected by the spectrographic system. The intuitive answer is to make the system with the highest detectivity. However within the limitation of the detectors and spectrometer throughput what can we reasonably expect to see, and is that sufficient to make measurements to detect the chemicals of interest. Two aspects of this question have been explored, the first is to determine what temperature of the target (a measure of radiance) is required to get a signal to noise of 1 out of the detectors at each wavelength. This assumes that the sample radiates like a black body. The second aspect is what spectral features are we looking for in the sample gasses, what resolution is required to resolve them, and are they within our spectral sensitivity.

We directed our consultant Dr. A. Tuchman of AVI to develop a system model that took into account temperature of the target, spectral throughput of the lens and optical

bench, efficiency of the grating, spectral separation, and detectivity of the detector array. The model produced the following results:

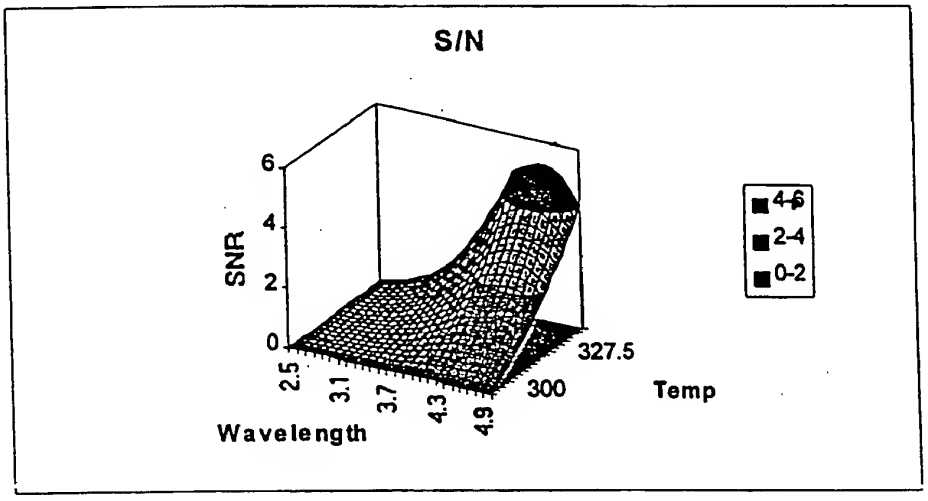

FIGURE 3.2 This figure shows the detectivity of the spectrometer system. The horizontal axis indicate the spectral band and the thermal temperature (radiant intensity), the vertical axis indicates the signal to noise ratio. It shows that at longer wavelengths and higher temperatures the signal to noise is higher (system will detect better).

The effort in the next quarter of Phase II will include estimates of S/N over the regions of interest and relative to the detectors being purchased under Phase II. This effort will be coupled with a determination as to what the spectral features are within the sample gasses, and what species are within our spectral sensitivity.

3.3 Spectral Analysis

We have subcontracted Neurodyne, Inc. (NDI) to develop gas identification software. The objective is to pick out the individual gas constituents from the compound spectral data. This is particularly difficult because the signals are overlapped, distorted, and vary rapidly with time. The neural net approach they will use will identify gas species not by their single prominent peaks alone, but will use all the spectral components in parallel. It is hoped that they will not only identify each species but also the concentration of each gas in the plume. An added benefit of this approach is that any non linearity in the system is accounted for in the calibration of the software, easing the design requirements.

The approach utilized data from a high resolution FTIR spectrograph. By averaging adjacent measurements, the resolution of the spectra was reduced to match that

obtained by our lower resolution device. The next step is to added these spectra together in various weights, and to test the software to see if they can id ntify the component spectra and the weights.

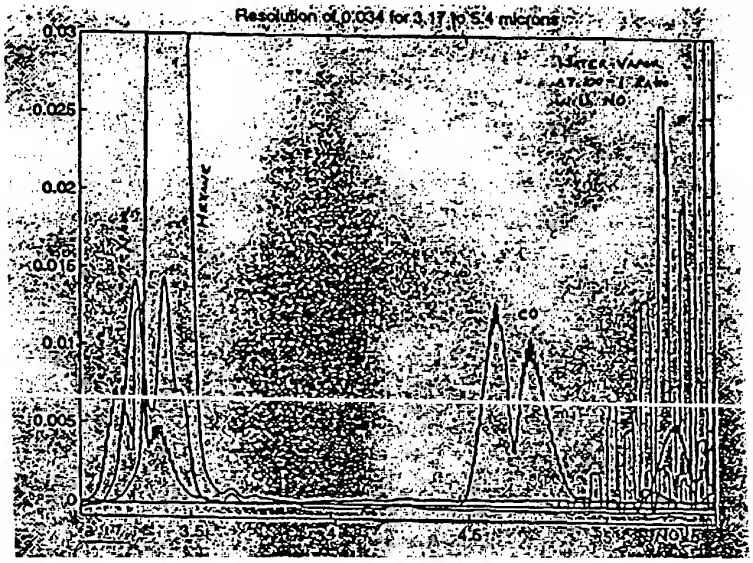

Figure 3.3 Chemical spectra selected are water vapor, carbon dioxide, carbon monoxide, sulfur dioxide, hydrogen sulfide, ammonia, methane, and ethane. In this figure the high resolution spectra obtained from FTIR spectrograph have been blurred to simulate the lower resolution of the 64 channel micro spectrograph.

The results of their analysis indicates that the spectral resolution is sufficient, but the spectral range needs to be translated slightly. A wavelength range of 3.17 to 5.42 um at a resolution of 0.034 um is acceptable for measuring hydrocarbons, CO, CO_2, and NO. This range will allow us to see the hydrocarbon major peaks from 3.2 to 3.6 microns, the CO_2 peaks from 4.2 to 4..4 microns, the CO peaks from 4.5 to 4.8 microns and the NO peaks from 5.1 to 5.4 microns.

Our initial design called for 2.5 to 5 um spectral range, this allowed us to use un-cooled PbSe detectors. However after the NDI analysis, it is apparent that important spectral feature exist out to 5.5 um, and that there are no significant features below 3.17 um. Therefore we have varied our optical design to operate from 3.17 to 5.5 um. This has also required the change of the detection scheme, requiring us to utilize TE cooled PbSe detectors. By cooling the detectors the spectral sensitive cut-off moves from 5 um to 5.5 um, with the added benefit that the D* improves by a factor of 2. However

the cooling will require a more complex housing to seal out moisture, a driver for the TE cooler with thermal feed back control, and a heat sink.

To develop a plume gas data base, NDI has utilized auto exhaust emissions. These emission contain similar gasses to that of the plume, are readily available, and can be provided in measured mixture by NDI's engine lab facility in West Virginia. Emission samples were taken from a diesel engine operated over a number of engine load conditions. The samples were evaluated using a MIDAC FTIR system. Macros were written to pull out key peaks in various ranges which would help deconvolve NO_x from water vapor. From their preliminary analysis, the water vapor is the most difficult problem, overlapping and masking the other gas constituents. They have been examining combustion equations to look for correlations that can be exploited in analyzing the spectra. One solution would be to correlate the CO_2 line with water vapor since their production is strongly associated within the combustion process.

NDI has requested information on rocket plume spectral data. We are in the process of trying to collect that data from sources such as NASA and the Air Force. We plan to submit a formal request for that data shortly.

3.4 Optical Front End

From the analysis of the Phase I device and the results of our system models we have developed an improved design that will greatly increase the utility of the spectrometer. We have completed the baseline silicon block spectrometer optic design. It uses a modified 'Ebert' layout fabricated from a single piece of machined silicon.

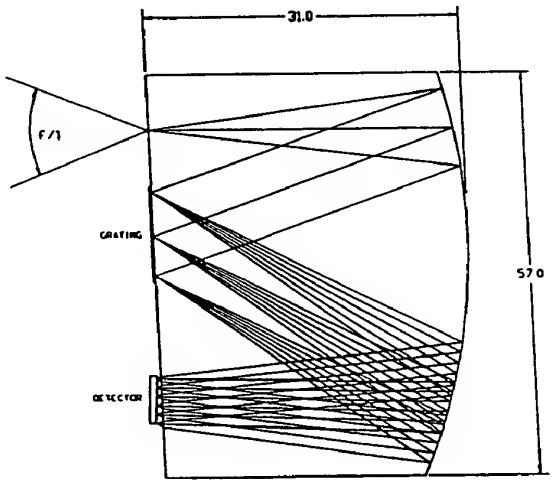

Figure 3.4 Phase II optical bench raytrace. This layout has only two optical surfaces, greatly simplifying fabrication and increasing reliability by eliminating tolerance stack up inaccuracies. The flat grating design increases the grating's efficiency and makes the device easier to manufacture. Its F/1 design allows for twice the throughput of the Phase I design, and its air gap at the detectors provide for focusing and permits the use of conventional AR coats. Dimensions are in mm.

In the 'D' shaped optic IR light enters the entrance slit, an AR coated area defined by thin film deposited layer. The radiation illuminates a cylinder mirror which collimates the light. The high refractive index of silicon greatly reduces the angle of the cone of light, this permits the use of an F/1 lens at the entrance aperture. It also reduces the size of the cylinder mirror, and permits the spectrograph to operate near the diffraction limit. The collimated beam is reflected off a gold coated diffraction grating. The grating disperses the IR spectrum, which is re-imaged after a second reflection off the cylinder mirror. The light exits the block through an AR coated surface and is imaged onto the detector plane. The detector plane is at a slight angle in order to flatten the field across the image. The air gap permits the detector plane location to be adjusted, allowing for manual focusing. As the rays exit the block the large cone angle of the rays is restored, more fully filling the acceptance angle of the detector.

The grating produces a number of lower energy unwanted diffraction orders. In our earlier design these orders were trapped in the block and were scattered and added to unwanted background signal on the detector. The new design permits the exit of these unwanted orders out of the flat surface where they will be captured by a light trap.

The following table addresses all the pros and cons of this new "D" shaped design.

Requirement	Phase 1D sign	Phas 2 D sign	Pro / Con
Size/weight/volume	3" dia. x .25" thk 1.75 cu. In.	1" x 1.5" x .040" thk 0.06 cu .in.	Provides a 30x decrease in optical bench weight
Number of Facets	6 - 4 on block and 2 on contact coupled grating	2 - each facet used multiple times	4 reflection design significantly decreases size
Grating	Chirped grating on separate curved surface	Conventional flat grating	Easier to manufacture, and maintain uniform efficiency, etched into block prohibits the exchange of gratings
Chopper	Tuning fork	PZT bimorph	No radiated fields, chopper not required with micro thermopile detector
Scattering	No exit for higher diffracted order, no beam dump, scattering internal baffle	AR coated exit for higher orders, external beam dumps, no internal baffles,	Decreases signal noise by eliminating scattered light to detector
AR coating	AR coating on two odd angle surfaces	AR coating on 1 surface	Cheaper to manufacture
Spectral band	2.5 - 5 um	3.13 - 5.5	Better spectral features, but requires TE cooling of the PbSe detecotr
Spectral Resolution	0.15 um	0.039 um	Higher resolution required for gas identification
Detector	PbSe 16 element	T : cooled PbSe 64 element or micro thermopile	Required to find spectral features, PbSe cooling improves SNR
Read out electronics	16 channel lock-in amplifier	64 Channel multiplexed w/ digital lock-in; or w/ 64 hybrid lock-in amplifiers	Greatly reduces space, Hybrid has fewer noise sources in system but is more bulky
Filter	External	Used as window on vacuum package	Dual use saves components
Package	Open air, large	Sealed, for dry gas or vacuum	Needed to keep condensate off TE cooled detector, more expensive
Detector/block interface	Contact coupled	Air gap	Provides for focusing, eases exchange of detectors.
Slit	Free standing to provide focus	Deposited on block	Deposited slit is finer, less scattering and ghosts

It was concluded that the new design was superior to the Phase I design, and the technical risk was small enough to make it worth pursuing.

3.5 Fabrication

Due to the uniqueness of the design we have worked closely with our vendors to develop a fabrication plan that is consistent with the inexpensive mass production of the front end. This consist of the following:

Optical blanks. "D" shaped optical blanks are purchase from VA Optical, a silicon supplier. Their main business is to produce substrates for the micro-chip industry. For this reason they can produce superior flat polish on both sides of the optic. The near net shape will include all the polished flats but not the cylinder surface.

Cylinder. The blanks will be sent to Digital Optics Corporation who will stack 20 parts into a monolithic block, then shape the block into a cylinder lens. They possess the interferometric equipment necessary to measure and produce the necessary surface on the cylinder mirror. They will gold coat the mirror and AR coat the flat.

Grating. The gratings will be built by Diffraction Limited. They will produce a grating in photoresist on the surface and etch it into the silicon. They will also work with the elements assembled in a stack. Once the grating is made they will add gold reflector overcoat and deposit the entrance slit.

Assembly. The part will be returned to Ion Optics where its performance will be measured. This is done by feeding the block with a lab spectrometer and measuring the quality of the output image with an IR camera. Once its performance is verified the device will be integrated into the housing with the detector and focused.

3.6 Mechanical

The design requires the precise alignment of the optical bench, the chopper, the detector array and the filter. This is all accomplished with a precision sealed package. The package holds the chopper, filter and detector in position and provides for a vacuum seal.

The miniature chopper we developed consists of a piezo-electric (PZT) bimorph strip with a flag on the end. The bimorph strip is a sandwich of PZT and stainless steel bonded to together. The bimorph curls like a bimetallic, as a voltage is applied across the PZT causing it to change length. This provides very fast chopping of the optical beam with minimum volume and no EMI.

The electronic read out will be fit into the vacuum package so the signals are amplified and multiplexed before leaving the package. This provides for a minimum number of

lectrical feed through. It also provides a modularity of the design, so the spectrometer optics package can be traded out with little effort.

The detector mount will hold the back side of the TE cooler to which the detector array is bonded. The mount will allow the detector to be precisely positioned with micrometer screw adjusts and then locked into place. Heat from the TE cooler will be conducted through the mount and into the base of the package.

The package will have a removable cover that will permit the components to be aligned prior to the cover being applied. The cover will contain the entrance window that will be coated to act as a cut off filter in the system. The package will also incorporate a mount to hold the input lens or an input fiber optic.

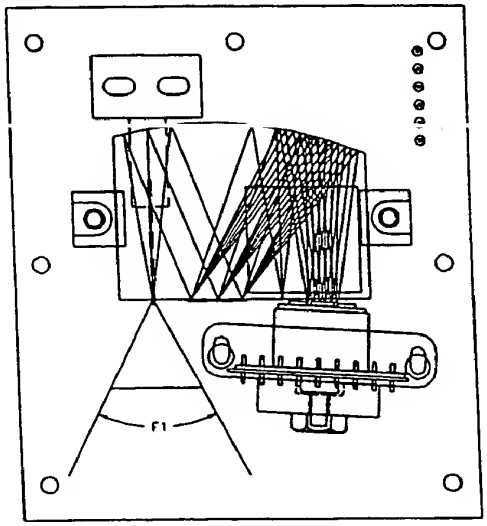

FIGURE 3.5 The preliminary design of housing, heat sinks, chopper, detector mount, and alignment fixtures have been completed. These will be further refined and detailed once the detector configuration has been finalized.

3.7 Detectors

When it comes to determining system performance, no other component will have as much effect perhaps than the detector. For this reason, we have extensively researched detectors applicable for our requirements. However criteria other than performance must be considered when evaluating detector systems for our portable, handheld spectrometer. These include cost, size, complexity and flexibility. For example, photoconductive devices typically suffer from low frequency or 1/f noise which can be reduced by chopping the input signal and AC coupling the output from the

detector. However this low noise detection scheme increase the level of complexity of the optical system and the read out electronics.

After considering the wide range of detector arrays available, we have narrowed our options to two choices: a PbSe photoconductive array and a micro-thermopile linear array. A thermoelectrically cooled PbSe array provides the best performance with moderate cooling requirements in our spectral region of interest. When cooled to between 145 and 250 K, low noise performance is obtained. We intend to use solid state thermoelectric coolers, which are rugged, low cost devices that can provide sufficient cooling for the PbSe device.

We have completed an extensive survey and contacted many of the PbSe array detector vendors in the U.S. Out of this survey we located only one, Optoelectronics Texton, with an operating multiplexed PbSe array. We spent several months in good faith effort, developing an array design, operating parameters, and package. However when it came time to formalize our purchase order, Opto provided a price three times that of the budgetary figures we had discussed (their quote approached $100K). This cost is well outside our budget, and the episode has been a major schedule set back to the program. We have now developed an alternative detector plan, and have begun to carry it out.

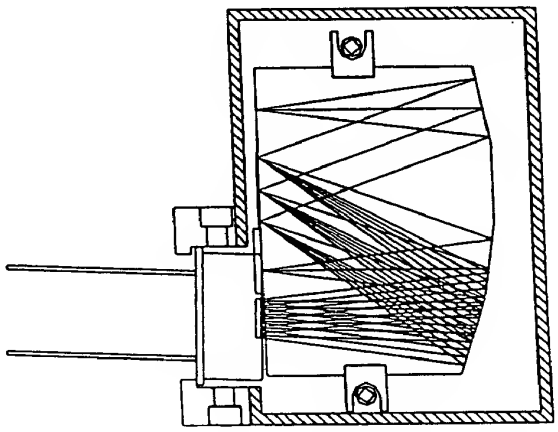

Figure 3.6 This is the package design that utilizes the Optoelectronics/Textron integrated multiplexor and PbSe detector array.

After investigating a number of other PbSe detector array sources, we have selected New England Photoconductor (NEP) as the detector array vendor. NEP is a local manufacturer of photoconductive arrays that supplied the array used in the Phase 1 system. Their performance under that contract was very favorable. NEP quoted the lowest price for a custom 64 element linear array and will integrate their array with a

newly developed custom integrated multiplexor circuit. We are in th process of evaluating the technical risk and system performance of this developmental multiplexor, and its possible impact on system p rformance. Its major advantage is that an integrated multiplexor will significantly reduce the size, cost, and complexity of the readout electronics.

We have also investigated the use of a 64 element micro-thermopile detector. There are many advantages to using the micro-thermopile: it is sensitive over a wide range of wavelengths, it does not suffer from 1/f noise and so does not require a chopper, and it does not have to be cooled. Conventional thermopiles are not as sensitive as a PbSe detector, however a source at JPL believes that they can produce a micro machined thermopile in the configuration we desire with a D* of 109, equivalent to PbSe. Although this device is experimental, we hope to incorporate this device into a prototype spectrometer and evaluate its performance. Although we believe we need the sensitivity of a PbSe detector at this time, the micro-thermopile is a very attractive alternative, that could be used in spectrographs that range from 1 - 20 um (the full IR spectrum).

3.8 Readout Electronics

Typically, a modulated or chopped detector signal is recovered using a lock-in amplifier or synchronous detection scheme. The large number of pixels and the use of a multiplexor complicates the extraction of the modulated signal from our PbSe detector. We are currently investigating extracting the modulated output digitally. The serial output of the multiplexor will be digitized with a high speed, high resolution A/D converter. The sampled outputs from each pixel will be collected from multiple scans and processed digitally. For example, by performing a Fast Fourier Transform (FFT) on the data collected for each one pixel, the energy content at the modulation frequency can be determined. The FFT acts as a narrowband filter at the modulation frequency. This energy can be averaged over time to further increase signal to noise. We plan to evaluate this approach using an off-the-shelf A/D board and a standard analysis package running on a personal computer. This allows us to rapidly prototype and test different processing techniques.

In order to reduce our technical risk, we have also specified and received a proposal for a hybrid multi-channel lock-in amplifier. This device will replace the multiplexor. It is assembled from un-packaged die and mounted on a thick film circuit; an eight channel device occupies 2.56 square inches. Although this approach is fairly large and costly, it has a low technical risk and guaranties maximum performance.

3.9 Processing

The continued growth of the digital signal processing market has resulted in a number of low cost DSP processors for embedded applications. We are currently investigating several processors for our application. In particular, we are evaluating the DSP56L811 from Motorola. This processor is a cost-effective solution that combines the prodigious number crunching of a digital signal processor with the versatile functionality of a microcontroller. This processor could perform the signal processing necessary for signal extraction and chemical detection and also control a display and keypad; a serial interface will be used for communication with an external computer. An off-the-shelf development board will facilitate the rapid prototyping of the final spectrometer unit.

4. Plans For Next Quarter

4.1 Fabrication of the Silicon Spectrometer Optic.

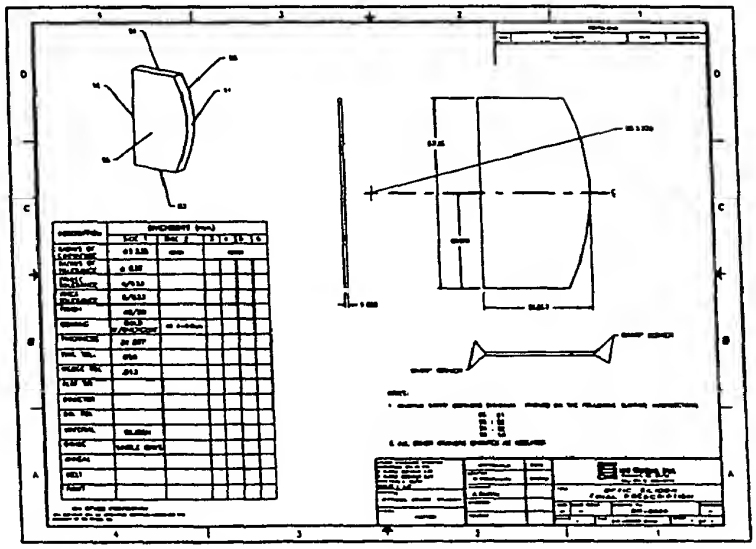

Figure 4.1 Detailed drawing of optical bench ready for fabrication.

The drawing package has been sent out for quotation. We intend to contract three vendors to build the assembly in stages.

1. The silicon wafer and optical substrate fabricator will produce the silicon optic without the cylindrical optical surface and optical coatings.
2. The lens fabricator will finish the cylindrical surface and AR coat the opposite flat.

3. The grating fabricator will etch and gold coat the grating

At this point the Silicon Spectrometer Slab is complete and will be charact rized for spectral resolution, through-put, and scattered light.

The goal of these three steps is to define a manufacturing process to maximize yield and operating characteristics.

4.2 Optical Chopper

A vendor has been selected and a quote obtained for five chopper assemblies based on the proof of concept prototype. The purchase order will be executed as soon as the final drawing package for the optical bench is released. This is anticipated to occur early June, 1997.

4.3 Detector Assembly

We are currently evaluating the multiplexed detector from NEP. The characterization will be completed shortly. We can then place the order for the multiplexed detector array. Delivery will be in about 8-10 weeks. At this point, the design of the data acquisition and signal processing circuitry will be initiated.

4.4 Packaging

The next major mechanical design task will be the case for the instrument. Particular emphasis will be placed on designing a low cost package that is easy to assemble.

5. Marketing

To investigate commercial markets for this spectrographs we have contacted several spectrograph vendors, and started a market survey of users. To assist in this we have produced a preliminary spec sheet showing two embodiments of the device. The first is the handheld spectrometer and the second is the OEM bench. In the coming months we hope to refine these specs by contacting various potential end users and OEM customers.

MICRO-SPEC®

The world's smallest IR spectrograph

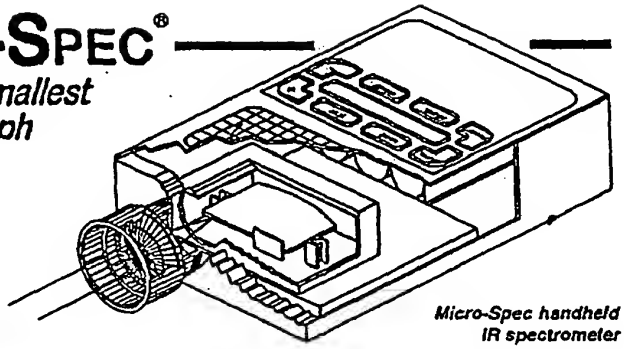

Micro-Spec handheld IR spectrometer

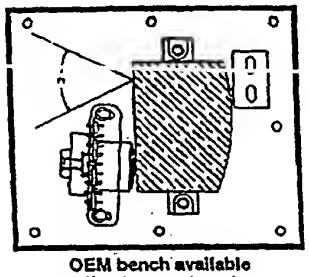

OEM bench available
1/4 meter monochrometer in a 3 inch package

The miniature Micro-Spec infrared spectrometer is the smallest, near/mid IR grating spectrometer available. The patent-pending design, developed for the space program, is now available for commercial users. It's unique waveguide construction provides four times the throughput of conventional designs. Monolithic construction provides vibration immunity and thermal stability. Designed for infrared gas detection (CH_4, CO, CO_2, NO, NO_2, H_2O), the system can be used for chemical identification in the field or on the loading dock.

PRELIMINARY SPECIFICATIONS
January 1, 1997

Input:	F/1 lens or fiber optic
Sensitivity:	3 - 5.5μm (1.5 - 3μm alt.)
Resolution:	0.04μm
Throughput:	F/1
Computer Output:	RS232
Grating:	Blazed Holographic
Slit:	0.07 x 1mm
Detector:	PbSe 64 element
Dimensions:	3" x 5.5" x 1.2"
Weight:	50oz
Display:	LCD Graphic
Power:	Battery (10W @ 12V)

Ion Optics, Inc.
Innovative Technology Building IR Products

411 Waverly Oaks Road, Suite 144, Waltham, MA 02154
Telephone (617) 788-8777 • Fax (617) 788-8811

Figure 5.1 Preliminary spec. sheet showing product concept.

PCT/US 99/17338
IPEA/US 29 FEB 2000
PCT/US99/07781

MICRO-SPEC

The world's smallest IR spectrograph

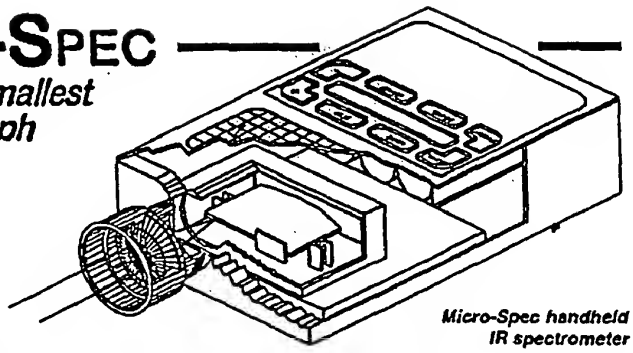

Micro-Spec handheld IR spectrometer

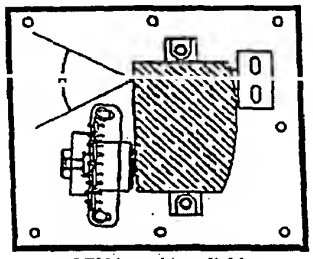

OEM bench available
1/4 meter monochrometer in a 3 inch package

The miniature Micro-Spec infrared spectrometer is the smallest, near/mid IR grating spectrometer available. The patent-pending design, developed for the space program, is now available for commercial users. It's unique waveguide construction provides four times the throughput of conventional designs. Monolithic construction provides vibration immunity and thermal stability. Designed for infrared gas detection (CH, CO, CO_2, NO, NO_2, H_2O), the system can be used for chemical identification in the field or on the loading dock.

PRELIMINARY SPECIFICATIONS
January 1, 1997

Input:	F/1 lens or fiber optic
Sensitivity:	3 - 5.5µm (1.5 - 3µm alt.)
Resolution:	0.04µm
Throughput:	F/1
Computer Output:	RS232
Grating:	Blazed Holographic
Slit:	0.07 x 1mm
Detector:	PbSe 64 element
Dimensions:	3" x 5.5" x 1.2"
Weight:	50oz
Display:	LCD Graphic
Power:	Battery (10W @ 12V)

Ion Optics, Inc.
Innovative Technology Building IR Products
411 Waverly Oaks Road, Suite 144, Waltham, MA 02154
Telephone (617) 788-8777 • Fax (617) 788-8811

Figure 5.1 Preliminary spec. sheet showing product concept.

6. Cumulative Costs

The cumulative costs for this PHASE II project are $197,346. Current expenditure is in line with the projected cost to complete.

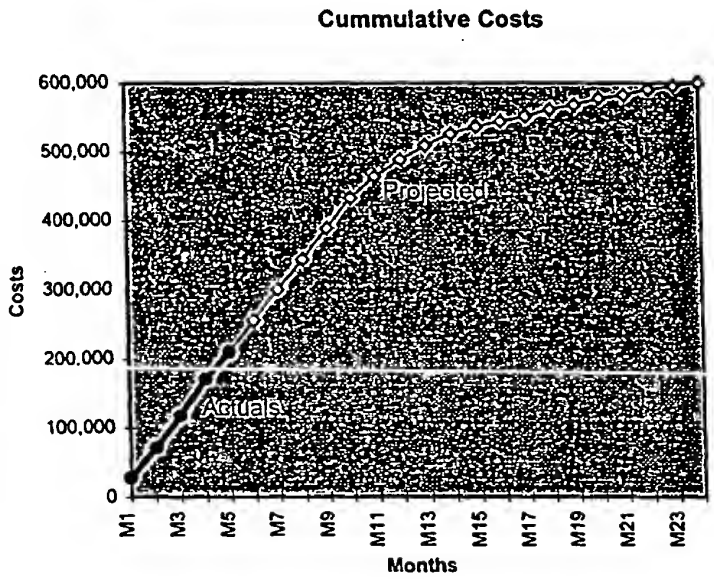

7. ESTIMATED PERCENT OF TECHNICAL EFFORT COMPLETE

The technical effort is estimated to be 35% complete.

What is claimed is:

1. A monolithic spectrometer system, comprising:

a slab waveguide having an input surface for accepting optical radiation and an exit surface;

a diffraction grating disposed with a third surface of the waveguide;

a detector array aligned adjacent to the second surface;

a first reflective mirror coated on the waveguide such that the radiation transmitted within the waveguide is reflected and collimated to the grating, wherein light energy diffracted from the grating is dispersed to the mirror for subsequent refocus through the second surface and onto the array.

2. A system according to claim 1, wherein the waveguide comprises silicon.

3. A system according to claim 1, wherein the detector array is selected from the group consisting essentially of microbolometers, PbSe, PbS, and CCD.

4. A system according to claim 1, further comprising input optics to focus optical radiation onto the first surface.

5. A system according to claim 1, further comprising an electronics subsystem for collecting signals from the array, for processing the signals, and for correlating the signals to reference data so that a chemical species of the radiation spectrum is determined.

APPENDIX -- PCT APPLICATION NO. PCT/US99/07781

Abstract

The invention includes a solid optical grade waveguide coupled to a line array of detectors. Light from a source (e.g., earth emissions transmitted through gases) is focussed at a first surface of the waveguide, reflected from an internal mirror to a diffractive surface, which diffracts the light to a second reflector. The reflector refocusses the diffracted light onto the array at a second surface of the waveguide. The detectors are preferably microbolometers or made from PbS or PbSe material. The waveguide is typically silicon to transmit IR radiation with relatively high index of refraction. Other materials can be used. Electronics, responsive to user input, processes detector signals and determines spectral characteristics of the light such as to indicate the presence of a chemical species.

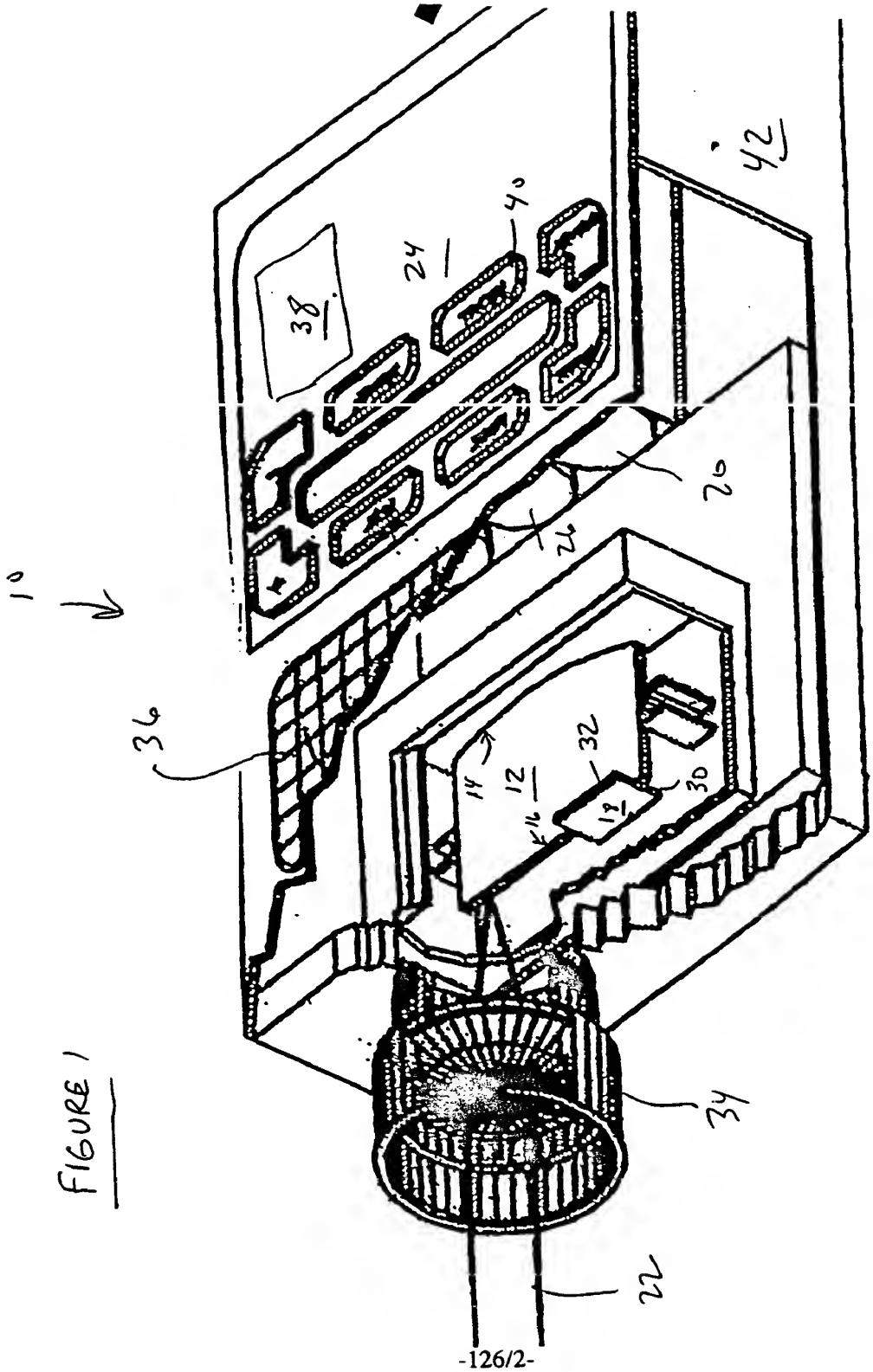

FIGURE 1

FIGURE 3

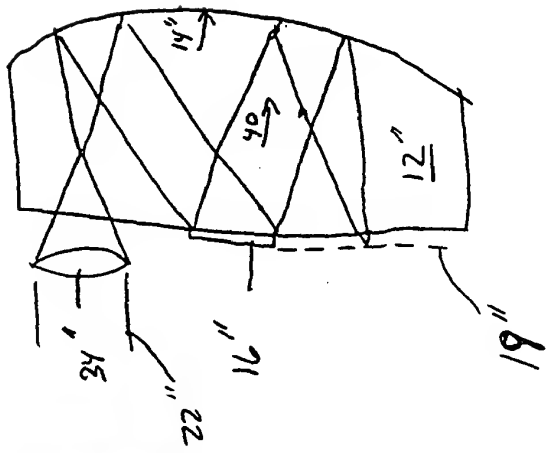

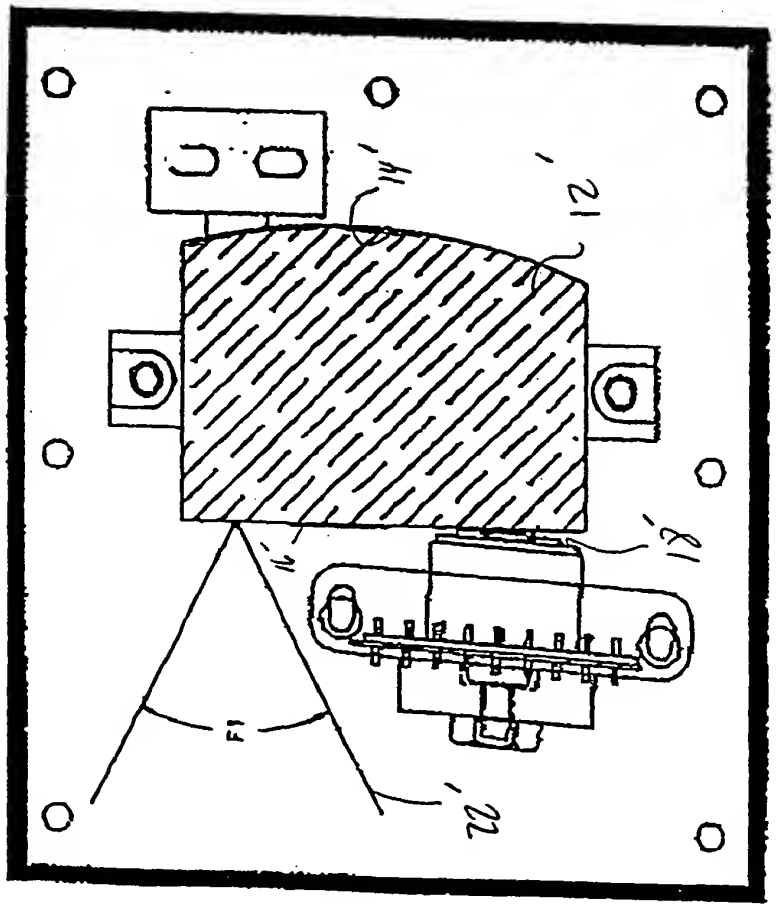

FIGURE 2

INTERNATIONAL SEARCH REPORT

International application No.
PCT/US99/17338

A. CLASSIFICATION OF SUBJECT MATTER

IPC(6) : H05B 3/26
US CL : 250/504R, 493.1, 495.1

According to International Patent Classification (IPC) or to both national classification and IPC

B. FIELDS SEARCHED

Minimum documentation searched (classification system followed by classification symbols)

U.S. : 250/504R, 493.1, 495.1

Documentation searched other than minimum documentation to the extent that such documents are included in the fields searched

NONE

Electronic data base consulted during the international search (name of data base and, where practicable, search terms used)

NONE

C. DOCUMENTS CONSIDERED TO BE RELEVANT

Category*	Citation of document, with indication, where appropriate, of the relevant passages	Relevant to claim No.
A	US 5,152,870 A (LEVINSON) 06 October 1992 (06/10/92), see entire document, especially fig. 2.	1-28
A	US 5,324,951 A (KOCACHE ET AL.) 28 June 1994 (28/06/94), see entire document, especially figs. 1 and 3.	1-28
A	US 5,838,016 A (JOHNSON) 17 November 1998 (17/11/98), see entire document, especially fig. 1.	1-28

☐ Further documents are listed in the continuation of Box C. ☐ See patent family annex.

* Special categories of cited documents:

"A" document defining the general state of the art which is not considered to be of particular relevance

"E" earlier document published on or after the international filing date

"L" document which may throw doubts on priority claim(s) or which is cited to establish the publication date of another citation or other special reason (as specified)

"O" document referring to an oral disclosure, use, exhibition or other means

"P" document published prior to the international filing date but later than the priority date claimed

"T" later document published after the international filing date or priority date and not in conflict with the application but cited to understand the principle or theory underlying the invention

"X" document of particular relevance; the claimed invention cannot be considered novel or cannot be considered to involve an inventive step when the document is taken alone

"Y" document of particular relevance; the claimed invention cannot be considered to involve an inventive step when the document is combined with one or more other such documents, such combination being obvious to a person skilled in the art

"&" document member of the same patent family

Date of the actual completion of the international search

29 SEPTEMBER 1999

Date of mailing of the international search report

28 OCT 1999

Name and mailing address of the ISA/US
Commissioner of Patents and Trademarks
Box PCT
Washington, D.C. 20231

Facsimile No. (703) 305-3230

Authorized officer

KIET T. NGUYEN

Telephone No. (703) 308-4825

Form PCT/ISA/210 (second sheet)(July 1992)★